

DOCTORAL THESIS

Co-pyrolysis of Estonian Oil Shale with Polymer Wastes

Olga Pihl

TALLINN UNIVERSITY OF TECHNOLOGY
DOCTORAL THESIS
36/2022

Co-pyrolysis of Estonian Oil Shale with Polymer Wastes

OLGA PIHL



TALLINN UNIVERSITY OF TECHNOLOGY

School of Engineering

Virumaa College

This dissertation was accepted for the defence of the degree 16/05/2022

Supervisor: Tenured Assistant Professor Allan Niidu
Virumaa College
School of Engineering
Tallinn University of Technology
Tallinn, Estonia

Co-supervisor: Professor Emeritus Andres Siirde
School of Engineering
Tallinn University of Technology
Tallinn, Estonia

Opponents: Professor Eric Suuberg
School of Engineering
Chemical and Biochemical Engineering Faculty
Brown University
Providence, RI, USA

Dr Indrek Aarna
Head of Development Department
Viru Keemia Grupp
Kohtla Järve, Estonia

Defence of the thesis: 30/06/2022

Declaration:

Hereby I declare that this doctoral thesis, my original investigation and achievement, submitted for the doctoral degree at Tallinn University of Technology, has not been previously submitted for doctoral or equivalent academic degree.

Olga Pihl

signature



European Union
European Regional
Development Fund



Investing
in your future

Copyright: Olga Pihl, 2022

ISSN 2585-6898 (publication)

ISBN 978-9949-83-853-0 (publication)

ISSN 2585-6901 (PDF)

ISBN 978-9949-83-854-7 (PDF)

Printed by Koopia Niini & Rauam

TALLINNA TEHNIKAÜLIKOOL
DOKTORITÖÖ
36/2022

Eesti põlevkivi ja polümeerjätmete koospürolüüs

OLGA PIHL



Contents

List of publications	7
Author's contribution to the publications	8
Introduction	9
Abbreviations	11
Terms	12
1 LITERATURE OVERVIEW	13
1.1 Oil shale.....	13
1.2 Polymer wastes	13
1.2.1 Plastic	13
1.2.2 Car tires	15
1.3 Pollution of the environment with polymer wastes	16
1.4 Types of plastics	17
1.5 Composition of ELTs.....	21
1.5.1 Natural rubber.....	21
1.5.2 Synthetic rubber	21
1.6 Polymer Recycling	22
1.6.1 Biological recycling	24
1.6.2 Mechanical recycling	24
1.6.3 Energy recovery.....	24
1.6.4 Chemical recycling.....	25
1.7 Pyrolysis of the most common plastics.....	26
1.7.1 Mechanism of pyrolysis.....	27
1.7.2 Pyrolysis process conditions.....	27
1.8 Tire pyrolysis	31
1.9 Theory of the study of kinetic parameters.....	31
2. EXPERIMENTAL.....	34
2.1 Sample characterization.....	34
2.2 Methods for the analysis of co-pyrolysis products	37
2.3 Thermogravimetric analysis	38
3. RESULTS AND DISCUSSION.....	40
3.1 Decomposition of Estonia oil shale, polymers and mixtures of polymer wastes with oil shale	40
3.2 Study of additivity based on the TG analysis.....	44
3.3 Kinetics of co-pyrolysis. Activation energy.....	45
3.4 Characteristics of the resulting co-pyrolysis products	49
3.5 Study of a possible synergistic effect in the output of co-pyrolysis products.....	49
3.6 Characteristics of liquid products of co-pyrolysis	50
3.7 Semi-coke and gas.....	52

3.8	Sulfur compounds balance.....	54
3.8.1	Sulfur compounds of the fraction up to 150 °C of oil obtained from tires and oil shale	55
3.9	Composition of co-pyrolysis oils.....	58
4.	CONCLUSION	62
	List of figures	64
	List of tables	65
	References	66
	List of other publications	74
	Acknowledgments.....	75
	Abstract.....	76
	Lühikokkuvõte.....	77
	Appendix 1	79
	Appendix 2	89
	Appendix 3	101
	Curriculum vitae.....	112
	Elulookirjeldus.....	113

List of publications

The list of author's publications, on the basis of which the thesis has been prepared:

- I O. Pihl, M. Tsepelevitsh, M. Burko, A. Siirde; Applying the correction for undecomposed carbonates to gross calorific values of oil shales from different deposits, *Oil Shale*, 36 (2), pp 250–256, 2019
- II O. Pihl, A. Niidu, N. Merkulova, M. Fomitsov, A. Siirde, M. Tsepelevitsh; Gas-chromatographic determination of sulfur compounds in the gasoline fractions of shale oil and oil obtained from used tires, *Oil Shale*, 36 (2), pp 188–196, 2019
- III O. Pihl, V. Khaskhachikh, J. Kravetskaja, A. Niidu, A. Siirde; Co-Pyrolysis of Estonian Oil Shale with Polymer Wastes, *ACS Omega*, 47, pp 31658–31666, 2021

Author's contribution to the publications

Contribution to the publications in this thesis are:

- I In Publication I, I was the main author, analyzed the results, prepared the figures and tables, and wrote the manuscript. The results were presented at the conference "Al Balqa Applied university, Second International Oil Shale Conference, Al-Salt Jordan".
- II In Publication II, I was the main author, analyzed the results, prepared the figures and tables, and wrote the manuscript. The results were presented at the conference "Al Balqa Applied university, Second International Oil Shale Conference, Al-Salt Jordan".
- III In Publication III, I was the main author, was responsible for planning and conducting the experiments, analyzed the results and wrote the manuscript.

Introduction

Oil shale is found in many areas of the world. About 600 deposits are distributed throughout the world, and these deposits vary in size and quality of oil shale [1]. The world's total shale oil resources are conservatively estimated at 4.8 trillion barrels [2].

Several years ago, shale oil production was concentrated in the following countries: Estonia, China and Brazil. These three countries produced 45,000 barrels of shale oil per day in 2015 [3]. Estonia is currently the leading oil shale processing country in the world. In 2019, the production of liquid fuels reached its highest level in history: 1.17 million tons [4]. The production of shale oil is based on the pyrolysis process.

According to the strategy "Estonia 2035", Estonia must strive to reach zero carbon emissions by 2050. To achieve this goal, the Estonian government announced two deadlines: an exit from the production of oil shale electricity no later than 2035 and the production of shale oil no later than 2040. During this period, it is planned to reduce the negative impact of oil shale production on the natural environment, and to use oil shale more efficiently [5].

The European Union has also set the goal of moving towards a circular economy with a high level of resource efficiency, according to which by 2025 the recycling of municipal waste (including plastic waste) should be increased to at least 55%, by 2030 to at least 60%, and by 2035 to at least 65% by weight [6].

Co-pyrolysis of oil shale with polymer wastes could be one of the alternative methods of transition to a circular economy and the reduction of CO₂ emissions by 2040. The pyrolysis of plastic waste components is one of the possible ways to recycle polymer wastes. A study of the environmental impact of the pyrolysis of mixed plastic wastes compared to conventional mechanical recycling and energy recovery showed that recycling via pyrolysis has about a 50% lower climate change impact [7].

This study is based on the need to reduce fossil fuel consumption and increase polymer waste recycling. There have been a large number of studies on obtaining oil by the pyrolysis of various plastics, including tires, but experiments on the pyrolysis of plastics have not gone far beyond laboratory research. In principle, it is known from autoclave experiments that the co-pyrolysis of Estonian oil shale and polyethylene or polyvinyl chloride is possible [8, 9]. However, the conditions of a closed autoclave system are not transferable to industry, so it is useful to simulate co-pyrolysis processes under conditions closer to today's shale oil production process. That is why additional applied research is needed to further the successful development of an industrial co-pyrolysis process for oil shale with polymer wastes.

The goal of this thesis is to prepare a theoretical and practical basis for the co-pyrolysis of Estonian oil shale and polymer wastes. To achieve this goal, in the course of the work, the following items were studied:

- the kinetics of the pyrolysis and co-pyrolysis of the studied samples;
- the thermal properties of the studied samples in mixtures when modeling the process of co-pyrolysis;
- the influence of mixture compositions on the yield of co-pyrolysis products;
- the influence of mixture compositions on the physical and chemical parameters of the obtained co-pyrolysis products;
- the distribution of co-pyrolysis products of sulfur compounds;

- the types of sulfur compounds in fraction up to 150 °C obtained from the studied samples containing sulfur;
- the group composition of fractions up to 150 °C and above.

This thesis is based on three published articles and is sub-divided into four chapters. The first chapter presents a review of the literature on the types and amounts of polymer waste generated, and the existing methods for their processing. The process of the pyrolysis of plastics and tires is described in detail, as well as the theoretical foundations for studying kinetic parameters. In the second chapter, the experimental methods and processes are described (Publication I). The third chapter of the dissertation is devoted to the results and their discussion. The thermogravimetric behaviors of the studied samples are shown, as is the possibility of calculating the mass loss during heating in an inert environment according to the additivity principle for mixtures consisting of various polymers. The synergistic effect of the oil of yield during the co-pyrolysis of Estonian oil shale with various polymer wastes is shown. The kinetics of the co-pyrolysis of Estonian oil shale and plastic wastes was studied (Publication III). The composition and characteristics of the products of co-pyrolysis were studied. It has been shown that the main sulfur compounds of the gasoline fraction of shale oil and oil obtained by the pyrolysis of tires are identical. (Publication II). Chapter 4 presents the results of the research.

Abbreviations

ABS	Acrylonitrile butadiene styrene
ASTM	American Society for Testing and Materials
BTX	Benzene Toluene Xylene
ELTs	End of Life Tyres
EOS	Estonian Oil Shale
EPS	Expanded Polystyrene
ETRMA	European Tyre and Rubber Manufacturers
EVS	Estonian Centre for Standardisation and Accreditation
FC	Fixed carbon
FTIR	Fourier-transform infrared spectroscopy
GOST	international technical standards maintained by a regional standards organization operating under the auspices of the Commonwealth of Independent States
ISO	International Organization for Standardization
MBS	Methyl butadiene-styrene
MF	Melamine-formaldehyde
NOX	Nitrogen oxides (nitric oxide and nitrogen dioxide)
PA	Polyamide
PAH	Polycyclic aromatic hydrocarbons
PC	Polycarbonate
PE-HD	High density polyethylene
PE-LD	Low density polyethylene
PE-LLD	Linear copolymers of PE-LD
PE-MD	Linear copolymers of PE-HD
PET	Polyethylene terephthalate
PMMA	Poly(methyl methacrylate)
PMP	Poly-4-methylpentene-1
PP	Polypropylene
PS	Polystyrene
PUR	Polyurethane
PVC	Polyvinyl chloride
SBR	Styrene-butadiene
SOX	Sulfur oxides
TG	Mass loss curve
TGA	Thermogravimetry analysis
UF	Urea-formaldehyde

Terms

A	Pre-exponential factor, sec^{-1}
C_{Total}	Total Carbon Content
E	Activation energy, kJ/mol
K	Rate constant of the decomposition reaction of the test substance
m_{τ}	Mass at time τ
m_0	Initial mass
m_f	Final mass
n	Reaction order
R	Molar gas constant, $\text{J}\cdot\text{K}^{-1}\cdot\text{mol}^{-1}$
S_{Total}	Total Sulfur Content
S_{Organic}	Organic Sulfur Content
T	Temperature of the test substance, K

Greek symbols

α	Conversion rate
τ	Thermal decomposition time, sec^{-1}

1 LITERATURE OVERVIEW

1.1 Oil shale

Oil shale does not have a specific chemical formula; it is a fine-grained sedimentary rock from which it is possible to obtain shale oil by pyrolysis [10]. The World Energy Council writes in its 2010 report: “Oil shale consists of organic (kerogen) and mineral matter. The organic matter in oil shale is composed chiefly of carbon, hydrogen, oxygen, and small amounts of sulphur and nitrogen. It forms a complex macromolecular structure that is insoluble in common organic solvents (e.g. carbon disulphide). The organic matter (OM) is mixed with varied amounts of mineral matter (MM) consisting of fine-grained silicate and carbonate minerals. The ratio of OM:MM for commercial grades of oil shale is about 0.75:5 to 1.5:5. Small amounts of bitumen that are soluble in organic solvents are present in some oil shales. Because of its insolubility, the organic matter must be retorted at temperatures of about 500oC to decompose it into shale oil and gas. Some organic carbon remains with the shale residue after retorting but can be burned to obtain additional energy. Oil shale differs from coal whereby the organic matter in coal has a lower atomic H:C ratio, and the OM:MM ratio of coal is usually greater than 4.75:5” [2].

1.2 Polymer wastes

1.2.1 Plastic

In recent years, the topic of the reuse of polymer wastes, including plastics and used car tires, has become increasingly important. According to Statista, more plastic has been produced in the past 15 years than in the 50 years prior to that. In the European Union alone the demand for plastics in 2020 amounted to 49.1 million tons [11]. Figure 1 shows data on the demand for plastics by country in the European Union.

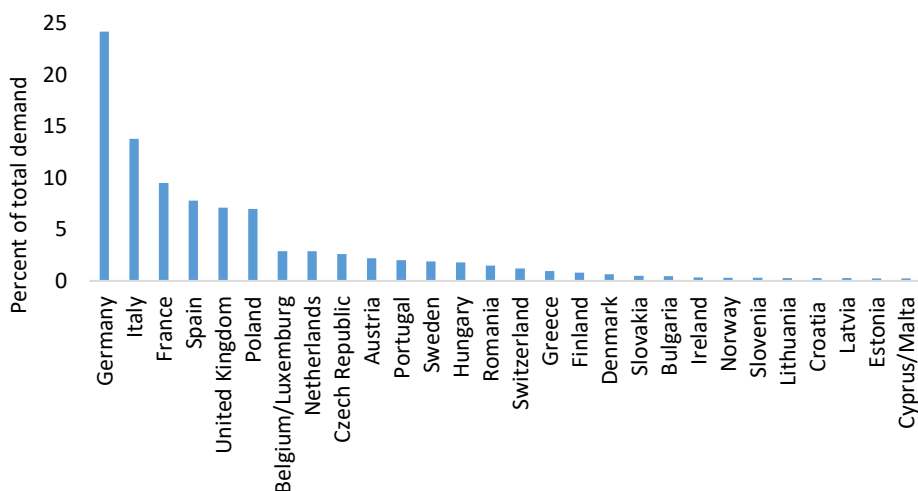


Figure 1. Plastics demand by country in the European Union in 2020.

Source: Plastics – the Facts 2021

More than 34 million tons of plastic were used in 2020 in Germany, Italy, France, Spain, the United Kingdom and Poland. This represents almost 70.0% of all plastic consumed in the European Union, with all other countries accounting for about 16 million tons of plastic. The largest use of plastics is packaging (40.5%), followed by building and construction (20.4%) [12]. The demand for plastics by segment is shown in Figure 2.

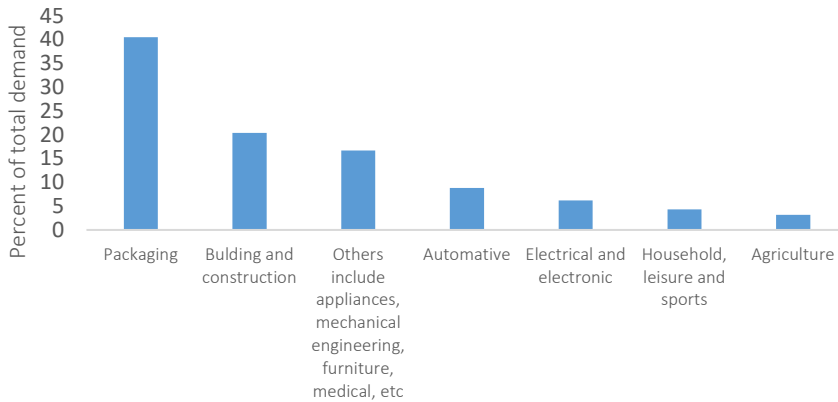


Figure 2. Distribution of plastics converters demand by segment in 2020.

Source: Plastics – the Facts 2021

Uses inFor appliances, mechanical engineering, furniture, medicine, etc. accounts for 16.7% of all plastics. A significant amount of plastics is used in the automotive industry (9.6%), followed by the electrical and electronic industries (6.2%), and for household use, leisure and sports are using (4.1%) and agriculture (3.4%).

The most common plastics used on a daily basis and universally applicable are polyethylene (PE-HD and PE-LD) and polypropylene (PP) [12]. These account for almost 50% of the total demand for plastic. The demand for plastics by type is presented in Figure 3.

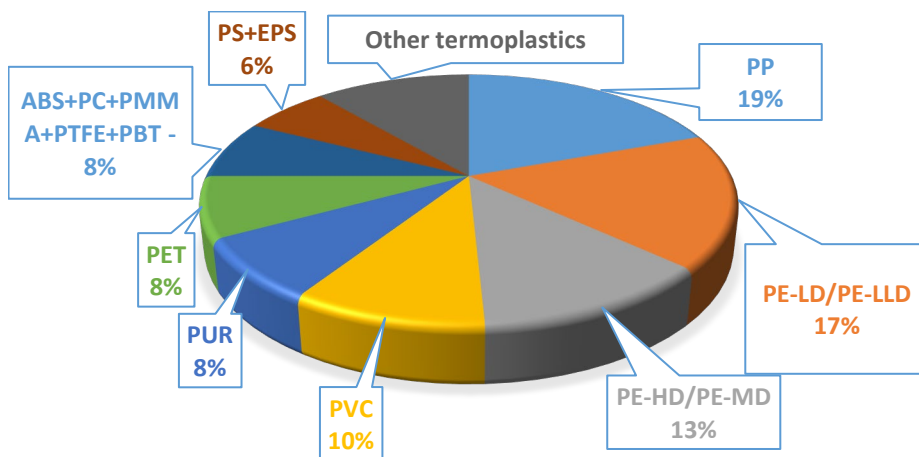


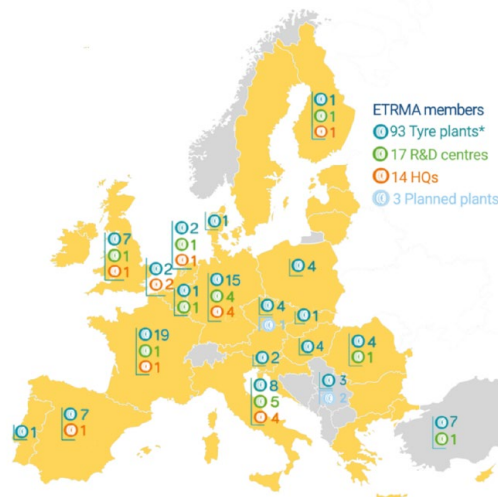
Figure 3. The demand for plastics by type.

Source: Plastics – the Facts 2021

The annual increase in the production of polymer/plastic materials inevitably leads to an increase in waste produced and requiring recycling. According to PlasticsEurope, in 2020 in Europe, of the collected 29.5 million tons of plastic waste, 42.0% went to energy recovery, 34.6% to recycling and 23.4% was buried at landfills, amounting to roughly 7 million tons [12].

1.2.2 Car tires

In the 2020 publication *The European tyre industry Facts and Figure*, the European Tyre and Rubber Manufacturers' Association (ETRMA) reported that 300 million passenger car tires and 18 million truck tires were produced in the European Union [13]. Industries related to the production and use of tires are dispersed throughout the European Union (Figure 4). The tire industry is constantly growing. China, Korea and Japan have invested in production facilities, which will lead to the opening of new tire plants in 2022 in the European Union [13].



*Including retreading facilities belonging to ETRMA members

Figure 4. A stronghold of European manufacturing.

Source: *The European Tyre Industry Facts and Figures - 2020 Edition*

The increase in the production of car tires will inevitably entail an increase in the number of used tires that must be disposed of. In September 2020, ETRMA reported [14] that in 2018, 32 countries (the EU28, Norway, Serbia, Switzerland and Turkey) collected 3.58 million tons of End of Life Tyres (ELTs), of which 193 thousand tons have not been reused. Thus, a fair amount of polymeric waste still needs to be incorporated into sustainable waste management and, as a result, into the circular economy. To this end, the European Union has prepared waste management plans [15]. A great deal of attention is paid, in the framework of the circular economy, to car tire recycling [16].

1.3 Pollution of the environment with polymer wastes

Polymers differ in chemical composition and application possibilities. The amount of consumed polymers increases every year, which has a significant impact on the environment.

About two-thirds of plastics are released into the environment, where they decompose slowly and at the same time affect the ecosystem. In the form of debris, plastics are found in oceans, air and soil. Nano plastics are added to some products, so plastic residues can be found in the human body and in sewage systems [17]. They can also emit greenhouse gases at all phases of their life cycle, from production to transportation and waste disposal.

The life cycle of plastics includes three phases as presented in Figure 5 [18].

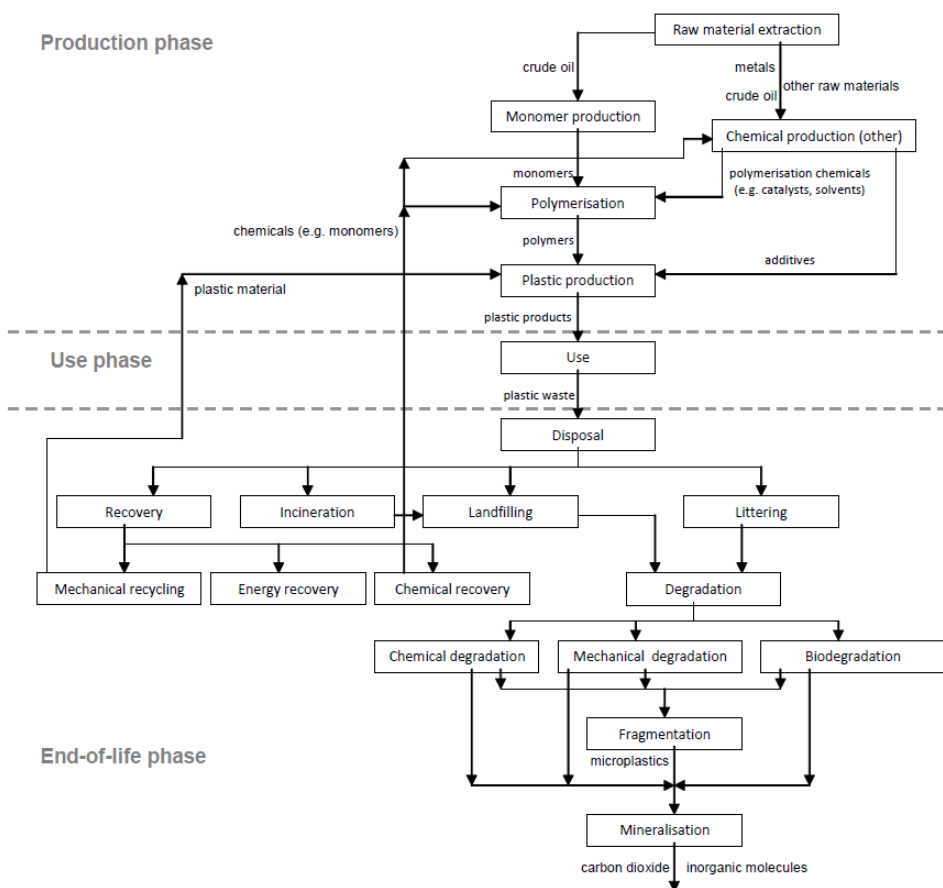


Figure 5. Life cycle of plastics.

The release of harmful substances into the environment occurs from the plastic production phase to the end of life phase. A study commissioned by the European Parliament's Citizens' Rights and Constitutional Policy Department at the request of the Petition Committee (PETI) indicates that the economic impact of plastic waste is enormous. Studies show that the economic damage to global marine ecosystems

exceeds € 11 billion. In Europe, € 630 million is spent annually on cleaning up plastic waste from coasts and beaches, and not recycling is costing the European economy € 105 billion annually [17].

Used car tires pose storage problems. Due to their flexibility, they cannot be compacted and therefore take up large amounts of storage area. The biggest problem with such storage of used car tires is the potential fire hazard. When a car tire burns, zinc oxides, dioxins and aromatic hydrocarbons are released into the atmosphere [19].

1.4 Types of plastics

In accordance with the international standard ISO 472 on terms and definitions, plastic is “material which contains as an essential ingredient a high polymer and which, at some stage in its processing into finished products, can be shaped by flow” [20]. The polymer macromolecule consists of compounds with low molecular weights [21]. According to the chemical structure of macromolecules, polymers are grouped into different classes. Figure 6 gives a hierarchical presentation of the classes of polymers plastics belong to [22].

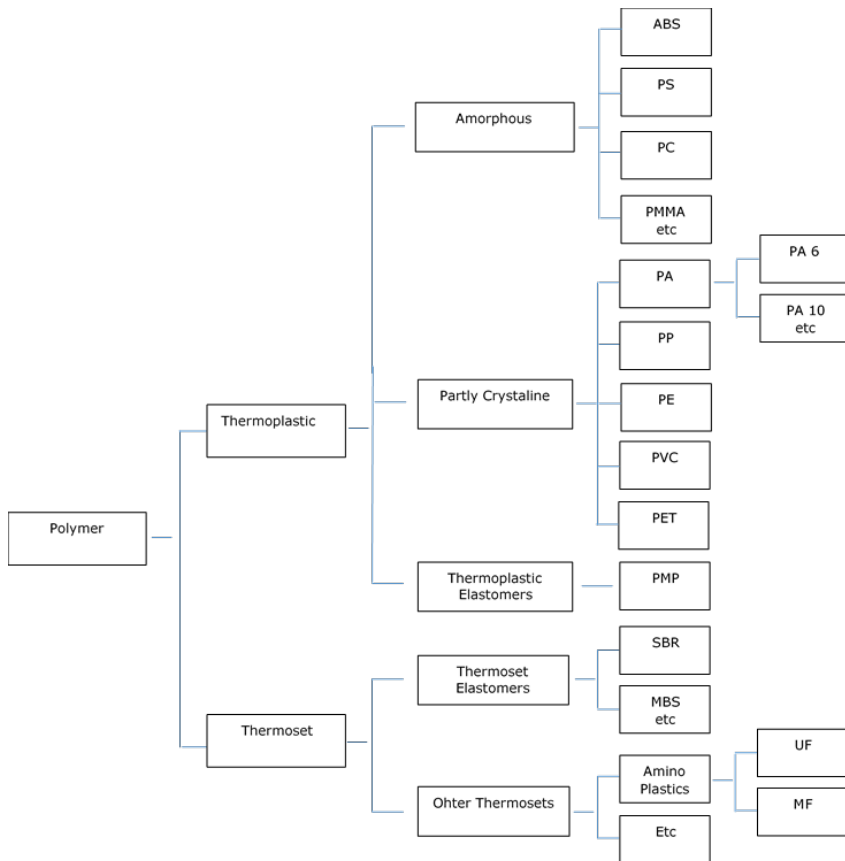


Figure 6. Classification of plastics.

Plastics are classified into two major groups: thermoplastic and thermosetting. A wide variety of additives are used in plastics to enhance their performance and increase their versatility. The additives mainly perform the following functions [23]:

- Calcium carbonate: Filler. Generally used for cost reduction, as it's much cheaper than polymer;
- Pigments: Give the plastic color. Generally for aesthetic purposes;
- Glass fiber: Increased strength and stiffness;
- Flame retardants: Increased fire resistance;
- Heat stabilizers: Increased resistance to heat exposure;
- Light stabilizers: Increased resistance to light exposure;
- Plasticizers: Process aid to reduce viscosity;
- Foaming agents: Lightness and stiffness.

The amounts of additives used are highly variable. PVC is the plastic type that requires by far the most additives. Of the world production of additives PVC alone accounts for 73% by volume, polypropylene and polyethylene account for 10 %, and styrenes account for 5% [24].

The difference between thermosetting plastics and thermoplastics is that thermoplastics can be remelted at low temperatures, while thermosetting plastics, after curing, remain in a permanent solid state and withstand high temperatures without losing hardness. The differences between the properties of different types of polymers are attributable to the varying functional groups within the molecular structures. These differences include mechanical, thermal and chemical resistance properties.

A thermoplastic polymer molecule consists of small molecules or monomers interconnected in long chains. They are usually pliable and flexible. When heated to high temperatures, these polymers soften and begin to flow, which allows them to be recycled. A thermosetting polymer molecule consists of long chains that are stitched together, forming three-dimensional network structures. Thermosetting polymers are tougher and stronger, but brittle. At the same time, they do not have a fixed melting point, so their recycling is difficult. Elastomers, including rubbers, have intermediate structures, in which some cross-linking of the chains is allowed. Elastomers can be elastically deformed without changing their shape [25]. Table 1 shows the chemical formulas of the most commonly used plastics.

Table 1. Chemical formulas of thermosetting and thermoplastic polymers.

Polymer name	Chemical formula
Thermoplastic	
Polyethylene (PE)	
Acrylonitrile butadiene styrene (ABS)	
Polyamide (PA)	
Polyethylene terephthalate (PET)	
Polypropylene (PP)	
Polystyrene (PS)	
Polycarbonate (PC)	
Polyvinyl chloride (PVC)	

1.5 Composition of ELTs

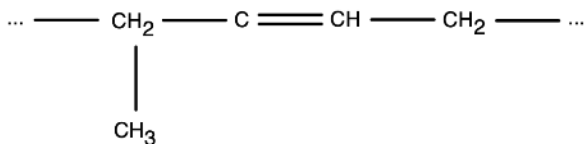
A car tire is a very complex engineering structure with many functions and tasks. In design, tires are not much different from each other; the main difference is in the composition. A car or passenger tire consists of 22–30% natural rubber, 15–23% synthetic rubber, 20–28% carbon black, 13–25% steel, 10–14% fabric, fillers, accelerators, etc., as shown in Table 2 [26].

Table 2. Typical materials used in tire manufacturing in Europe according to the percentage of the total weight.

Materials, m/m%	Passenger tire	Truck tire
Natural rubber	22	30
Synthetic rubber	23	15
Carbon black	28	20
Steel	13	25
Fabric, fillers, accelerators, etc.	14	10
Average weight	New 8,5 kg, Scrap 7kg	New 65 kg, Scrap 56 kg

1.5.1 Natural rubber

Natural rubber is obtained from the milky sap of rubber-bearing tropical plants. The sap is treated with acids and then the resulting product is rolled. The structure of natural rubber can be determined by its chemical properties: rubber adds bromine, hydrogen bromide and hydrogen, and when heated without access to air decomposes to form isoprene (2-methylbutadiene). This means that rubber is an unsaturated polymer, polyisoprene. A more detailed study of the structure of natural rubber revealed that rubber is a linear polymer, a product of a 1,4-polyaddition of isoprene [27]:



1.5.2 Synthetic rubber

Synthetic rubbers are obtained by the polymerization of unsaturated compounds. Depending on the type of starting material and the conditions of their processing, rubbers with different properties and durability are produced [28]. Table 3 shows the main types of synthetic rubbers.

Table 3. The main types of synthetic rubbers.

Industrial name of rubbers	Structural formula
Styrene-butadiene	$\left[\text{---CH}_2\text{---CH=CH---CH}_2\text{---} \right]_n \left[\text{---CH}_2\text{---CH---} \right]_m$ $\begin{array}{c} \text{C}_6\text{H}_5 \\ \\ \text{CH}_3 \\ \\ \text{C}_6\text{H}_5 \end{array}$
Butadiene methylstyrene	$\left[\text{---CH}_2\text{---CH=CH---CH}_2\text{---} \right]_n \left[\text{---CH}_2\text{---CH---} \right]_m$ $\begin{array}{c} \text{CH}_3 \\ \\ \text{C}_6\text{H}_5 \end{array}$
Butyl rubber	$\left[\text{---CH}_2\text{---C---} \right]_n \left[\text{---CH}_2\text{---C=CH---CH}_2\text{---} \right]_m$ $\begin{array}{c} \text{CH}_3 \\ \\ \text{C} \\ \\ \text{CH}_3 \end{array} \quad \begin{array}{c} \text{CH}_3 \\ \\ \text{C} \\ \\ \text{CH}_3 \end{array}$

1.6 Polymer Recycling

The recycling of polymers is extremely important as the disposal of plastic waste is a worldwide problem. Since the early 2000s, most of the plastic waste from European countries has been exported to developing countries (Figure 7) [29].

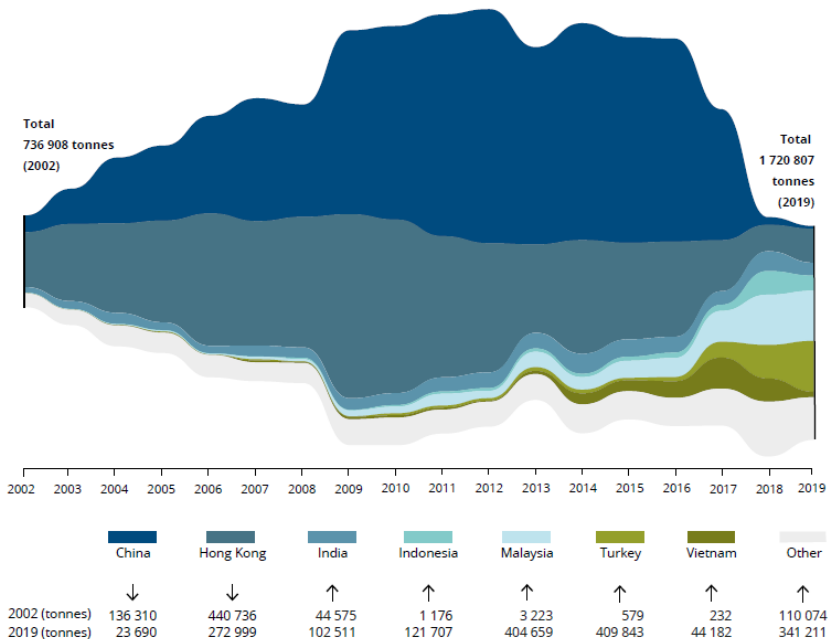


Figure 7. EU-28 plastic waste exports, 2002-2019.

Source: Based on data from UN Comtrade (2019b.)

The quantities of exported plastic waste changed following an initial temporary Chinese restriction in 2013. In 2017, China announced an unprecedented import ban on most plastic waste, resulting in a sharp decline in the global flow of the plastic waste trade and changes in how European countries need to dispose of plastic waste [30].

The circular economy has long been on the agenda of many states and large companies. In the context of the use of polymers, these principles are expressed, among other things, in the search for approaches to reduce the final volume of waste. Thus, in the European Union, the circular economy and waste reduction are the main tasks for the coming years with specific targets for the recycling of plastic waste [31].

There are four main types of recycling: primary recycling, secondary recycling, tertiary recycling, and quaternary recycling [32]. Common definitions of polymer recycling are presented in Table 4.

Table 4. Common definitions of polymer recycling.

Polymer recycling		Example
Biological recycling		Decomposition of polymers to compost or synthesis of useful compounds by biochemical transformation
ASTM D7209 definitions (withdrawn 2015) ^[33]	ISO 15270:2008 standard definitions ^[34]	
Primary recycling	Mechanical recycling	Bottle to bottle closed loop recycling
Secondary recycling	Mechanical recycling	Recycling into a new product lower value plastic (plastic bottles into polyester)
Tertiary recycling	Chemical recycling	Cracking (pyrolysis), gasification, depolymerization, solvent extraction
Quaternary recycling	Energy recovery	Direct incineration

Primary recycling includes the extrusion of virgin polymer or pure polymer streams. Secondary recycling requires sorting waste, crushing it, and then extrusion. If the polymer is not suitable for simple mechanical processing methods, then tertiary (chemical) recycling is used. Chemical recycling is the process of recycling a polymer to its monomer feed. Quaternary recycling processes plastics that are not suitable for the above-mentioned methods. These plastics are used for energy recovery through direct incineration [32].

Pyrolysis, depolymerization and the solvent extraction of polymeric waste make it possible to obtain fuels and chemical raw materials from polymeric waste. According to the company IDTechEx, which has been engaged in independent market research, new technologies and business analytics since 1999, in 2020 the range of polymer waste processing technologies significantly expanded [35].

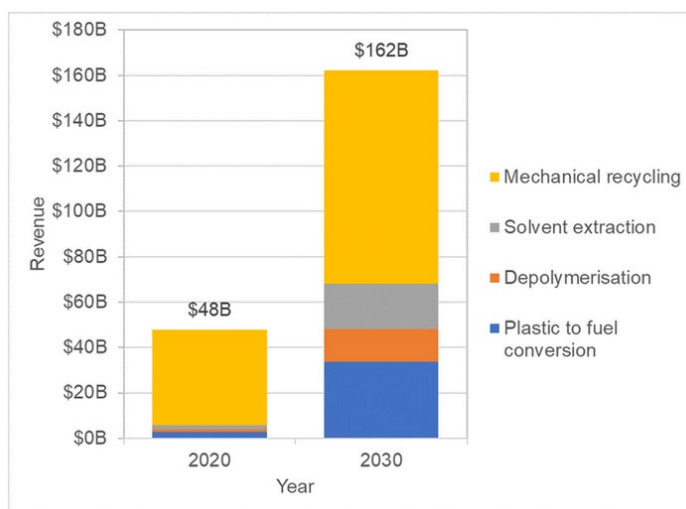


Figure 8. Global Revenues from Polymer Recycling by Process.

Source: ID TechEx

The report “Polymer Recycling Technologies 2020–2030. End of life options for plastic waste: tools, trends and markets” provides an assessment of the latest processing technologies. The SWOT analysis of mechanical and chemical methods for processing polymer wastes (Figure 8) shows a significant increase in revenues when using these methods for disposal [35].

1.6.1 Biological recycling

Biological recycling, recently developed, uses the help of living organisms or enzymes to decompose polymers. With this method of recycling, compost is formed or chemical compounds are synthesized through biochemical transformation [36].

1.6.2 Mechanical recycling

Mechanical recycling involves cutting, shredding and washing plastic waste by physical methods. This method makes it possible to separate contaminants from polymers by extrusion with melt filtration and then obtain polymer granules. After sorting, cleaning, drying and then directly processing waste into finished products or flakes, the size of the plastic waste is significantly reduced and it can be used to make other products. In the process of mechanical recycling, the main polymer does not change. However, due to the heterogeneity of solid waste, the properties of this polymer deteriorate at each cycle. In the presence of water and acids formed during the reaction of water and fillers, the molecular weight of the polymer decreases due to chain-breaking reactions. Thermosetting plastic cannot be melted or reprocessed, so mechanical recycling is not suitable for such plastics [37, 38].

1.6.3 Energy recovery

The direct incineration of polymers contained in municipal solid waste, resulting in significant air pollution, is common throughout the world, especially in developing and underdeveloped countries [40]. The direct incineration of high concentrations of

polyethylene, polypropylene and polystyrene produces carbon monoxide and other harmful emissions. The combustion of PVC leads to the formation of dioxins and aromatic compounds (pyrene and chrysene) [39, 40].

1.6.4 Chemical recycling

Depolymerization

During chemical recycling, polymers as a result of a chemical reaction are converted into monomers or partially depolymerized to oligomers. The monomers obtained by the chemical reaction are used for new polymerization reactions in order to obtain the original or a new polymer [41].

Gasification

Usually during gasification, materials that contain carbon will partially oxidize by reacting with air, oxygen, steam or mixtures thereof at temperatures from 700 °C to 1600 °C and in the pressure range from 10 to 90 bar. During the gasification of plastic waste, the resulting synthesis gas can be used to make new chemical products. The composition of the synthesis gas largely depends on the feed-stock from which it is obtained. If the feed-stock is not homogenous, then the resulting synthesis gas is of poor quality and expensive processes must be used to purify it [42].

Solvent extraction

Solvolysis is the most commonly used chemical recycling method and is implemented using a wide range of solvents, temperatures, pressures and catalysts. The general structure of plastic recycling by solvent extraction includes the removal of impurities, dissolution (homogeneous or heterogeneous dissolution), and re-precipitation or devolatilization. A polymer or polymer mixture is dissolved in a solvent or in several solvents, and then each polymer is selectively crystallized. The most successful variant is when the solvent can dissolve either the target polymer or all other polymers except the target one [43].

Pyrolysis

Pyrolysis is the thermal decomposition of organic compounds in an oxygen-free atmosphere to form gaseous, liquid and solid products [44]. The pyrolysis of plastics is carried out at a temperature range of 300–800 °C and, as a result, a product is formed of a wide range of hydrocarbons with practically no release of toxic or harmful gases, as is the case with waste incineration. In addition, waste water is not produced by the gas cleaning system [45]. The pyrolysis of plastics has been extensively studied. The first studies on the pyrolysis of plastics were published in the early 1960s. In this study, pyrolysis products were analyzed by gas chromatography to identify recycled polymers [46].

The advantage of the pyrolysis of polymer wastes is its versatility when recycling tires and plastics [47]. Pyrolysis has several advantages over other methods of disposing of plastic waste. The costs associated with sorting, washing and blending prior to the mechanical recycling of plastic waste are absent in the pyrolysis method [40].

1.7 Pyrolysis of the most common plastics

PVC pyrolysis

One of the most problematic materials for pyrolysis is PVC plastic, since it can contain up to 60% chlorine [49], leading to low yields of liquid products. The decomposition of PVC occurs in two stages. In the first stage, at a temperature of 200–380 °C, chlorine is removed in the form of HCl, and in the second stage, at a temperature of 380–550 °C, the decomposition of HCl-free plastic occurs [50]. As noted by the research groups that studied the pyrolysis of PVC [51, 54, 66], during the experiments up to 58.2% of very corrosive and toxic hydrogen chloride was obtained. The authors of the studies have also written that liquid pyrolysis products contain chlorinated compounds, such as chlorobenzene. One of the possible ways to obtain fuel with a low chlorine content in pyrolysis products is a fast pyrolysis method in combination with hydrothermal dechlorination. This combination of methods makes it possible to convert organic chlorine from condensable pyrolysis products to inorganic chlorine, which passes into gaseous products, thereby achieving a dechlorination efficiency of 99.9% [52]. Also known is a mechano-chemical method for reducing the chlorine content in PVCs. For this, PVCs are ground with CaO in a ball mill and then washed with water [53]. For the dechlorination stage, additional costs are required, which is a disadvantage of PVC pyrolysis.

PET pyrolysis

The thermal degradation of PET is observed at temperatures above 300 °C [54]. Certain difficulties arise during PET pyrolysis. Merve Sogancioglu et al. [55] noted that the thermal processing of PET at temperatures of 300, 400, 500, 600 or 700 °C produces an oligomer, not a liquid pyrolysis product. During PET pyrolysis, the oil yield is quite low compared to other plastics and ranges from 23 to 40 m/m% [55, 56, 67]. The oil obtained from PET pyrolysis contains a high content of benzoic acid and terephthalic acid (up to 0.5 kg per kg PET) [108]. The high acidity of the oil negatively affects its characteristics, making it highly corrosive, while benzoic acid sublimates and clogs pipelines [55,56].

PUR (PU) pyrolysis

Polyurethane plastic is used as often as PET. Research on the pyrolysis of PUR has been negligible. The studies carried out have been mainly related to the study of the kinetics of the pyrolysis process and the analysis of volatiles released during heating without oxygen access [57, 58]. The thermal decomposition of polyurethane foam proceeds in three stages in the temperature ranges 38 °C – 400 °C, 400 °C – 550 °C, and 550 °C – 1000 °C; 81% of the sample from the initial mass decomposes at a temperature of up to 1000 °C [58], which indicates the presence of fillers in polyurethane. Pyrolysis at temperatures above 1000 °C produces soot, which is considered a valuable nano-scale material based on carbon [59].

Polyolefin pyrolysis

As stated in the 2019 European Commission report “A circular economy for plastics – Insights from research and innovation to inform policy and funding decisions”, since polyolefins (PE and PP) are the most used polymers by volume, accounting for about half of the plastic consumed by EU recyclers, and this type of plastics cannot be depolymerized back to ethylene and propylene; using pyrolysis with a conventional

refining of the products obtained in the process, there can be a large technological gap. At the same time, polymeric waste does not require preliminary removal of contaminants and additives [60].

1.7.1 Mechanism of pyrolysis

Guoxun Yan et al. [61] describe in their research work the mechanism of pyrolysis of PE-LD and PP plastics. They assumed that with a short residence time in the reactor at atmospheric pressure, the thermal decomposition of polymers would occur according to the mechanism shown in Figure 9.

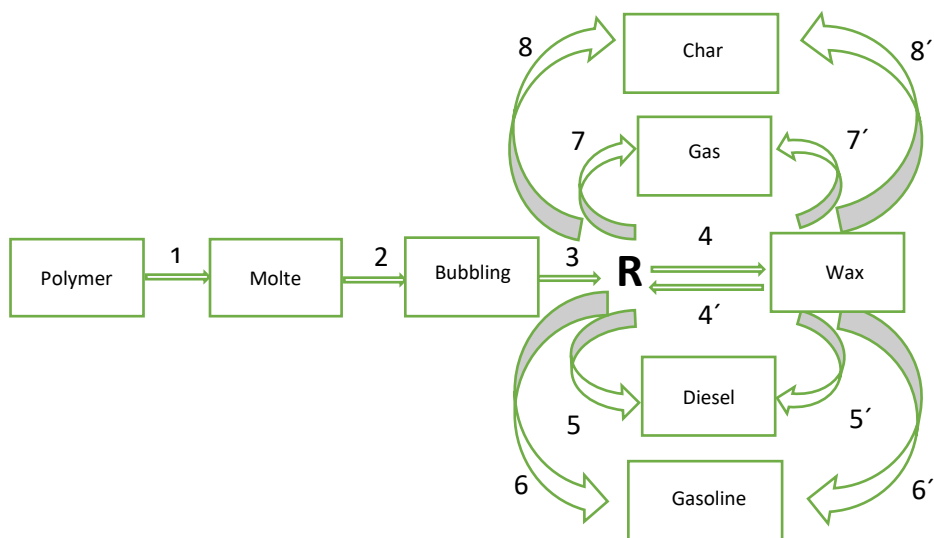


Figure 9. Main pathway in the thermal degradation of polymer.

The polymer first melts, then begins to bubble, which continues at temperatures from 100 to 400 °C (paths 1 and 2). It was also noted that white solid intermediates formed between Paths 1 and 2 at room temperature. An important step in thermal destruction is the formation of radicals R, which occurs at temperatures above 400 °C, which provides a reaction environment conducive to the rupture of C-C bonds. Chain-breaking reactions with the formation of paraffin, diesel fuel and gasoline proceed along Paths 4, 5 and 6 with increasing temperatures, and Paths 5 and 6 occur simultaneously [61].

1.7.2 Pyrolysis process conditions

The pyrolysis process can be thermal or catalytic. Catalysts affect the yield and composition of pyrolysis products [62]. Catalytic pyrolysis takes place at lower temperatures, but cracking reactions are faster and the resulting liquid products have a lower boiling point [63–65]. In a thermal pyrolysis process, reactor residence time, temperature, pressure and reactor type play important roles in the yields and compositions of the pyrolysis products [48]. Thus, during the pyrolysis of polyolefin plastics under various conditions, oil and waxes, aromatic compounds of BTX, and olefin gases (ethene, propene and butadiene) can be formed [66].

The pyrolysis process is classified as slow pyrolysis, fast pyrolysis or flash pyrolysis. This classification is according to the heating rate and the residence time of the pyrolyzable sample in the reactor [67]. Table 5 presents the classification of the pyrolysis process.

Table 5. Main operation parameters for the pyrolysis process.

Parameters	Slow pyrolysis	Fast pyrolysis	Flash pyrolysis
Temperature, °C	550 - 900	850 - 1250	1050 - 1300
Heating rate, °C/s	0,1 - 1	10 - 200	>1000

From a review of the literature by Garten Lopez et al. [68], it was concluded that waxes are the primary product in the thermal pyrolysis of polyolefins. Waxes are formed in the largest quantities at moderate temperatures of about 500 °C and with a short stay in the reactor.

In a review of the pyrolysis of plastic waste by Shafferina Dayana Anuar Sharuddin et al. [69], it was noted that during the pyrolysis of individual plastics at temperatures of 300–500 °C, liquid pyrolysis products are formed, and it was shown that temperature has the greatest impact, as it can affect the composition of pyrolysis products for all plastics. Also, Merve Sogancioglu et al. [55] noted in their study that, with an increase in the temperature of the pyrolysis process from 300 to 700 °C, the yield of liquid products of PE-HD, PE-LD and PP decreased. Table 6 presents the data from this study.

Table 6. Pyrolysis liquid product yield.

Pyrolysis temperature, °C	Pyrolysis liquid product yield, m/m%		
	PE-HD	PE-LD	PP
300	88.5	78.4	79.6
400	87.9	76.6	78.7
500	87.6	69.2	78.6
600	87.6	73.2	77.5
700	83.9	72.9	75.1

The same trend of decreasing the yield of liquid products during PE-LD pyrolysis with increasing temperature has also been noted by other authors [70].

As noted by R. Miandad et al. [71], during the pyrolysis of polyethylene up to 500 °C, they obtained waxes instead of liquid oil, since PE has a structure with a long carbon chain. George Kofi Parku et al. [72] noted that, in addition to temperature, the yield of liquid products of PP pyrolysis is also affected by the heating rate (slow and fast insertion). Propylene pyrolysis was carried out at temperatures of 450, 488, 525 and 600 °C with fast and slow insertion. Table 7 presents the data from this study.

Table 7. Dependence of the yield of liquid products of PP pyrolysis atmospheric pressure on temperature and insertion rate.

Pyrolysis temperature, °C	Slow insertion				Fast insertion			
	Heavy oil	Light oil	Gases	Char	Heavy oil	Light oil	Gases	Char
450	68.6	13.8	5.6	5.7	62.9	14.0	4.0	14.0
488	70.3	15.3	5.8	3.1	69.7	14.8	7.2	3.0
525	63.8	17.1	8.4	2.6	64.6	16.0	10.1	2.6
600	48.0	15.0	27.0	2.5	31.0	29.5	31.8	2.5

Increasing the pyrolysis temperature and heating rate of polypropylene significantly increases the amount of light oil produced, while the amount of total oil decreases as the gas yield increases.

Min-Hwan Cho et al. [73], in their study of the pyrolysis of plastic waste at temperatures of 667, 710, 735 and 773 °C, note that at a temperature of 735 °C the content of BTX aromatic compounds in oil increased significantly, while the maximum BTX yield was obtained at 719 °C (18 m/m% of organic product).

The results of the thermal pyrolysis of PE-HD at temperatures of 600–800 °C showed that 700 °C is optimal for the yields of ethylene (36%), propylene (15%) and butenes (9.4%). With an increase in temperature above 700 °C, the yields of methane and PAHs increase, which is undesirable [68].

In their study, Azubuike Anene et al. [74] noted that during the pyrolysis of PP and PE-LD in a series of experiments at temperatures below 450 °C, waxes were formed in the product lines. During the pyrolysis of these plastics at 460 °C, the yield of the liquid fraction from PE-LD was 86%, and from PP it was 94%. An analysis of the resulting liquid fractions by GC-FID showed that both consist of C7–C40 hydrocarbons. In PE-LD plastic oil, the gasoline fraction was 24%, the diesel fraction 30% and the heavy fraction 46%. In oil from PP plastic, the gasoline fraction was 44%, the diesel fraction 33% and the heavy fraction 23%.

The effect of temperature and residence time in the reactor on the pyrolysis of polyolefins to obtain certain products is characterized by the following scheme [68], shown in Figure 10.

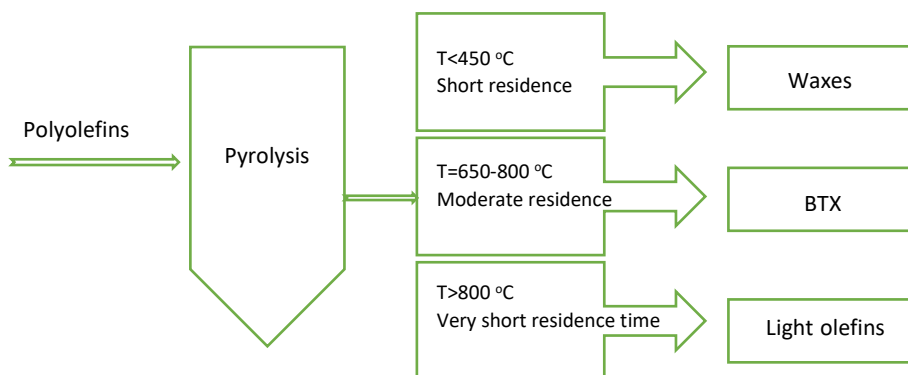


Figure 10. Conditions for the selective production of waxes, BTX and light polyolefins by pyrolysis.

As mentioned above, pyrolysis is affected by the type of reactor in which the process takes place. Table 8 shows data on the effects on the yield of pyrolysis products of polyolefins of such parameters as the type of reactor, residence time in the reactor, temperature and pressure [69].

Table 8. Yield of pyrolysis products of polyolefins.

Type of plastic	Reactor	Process parameters				Yield, wt%		
		t, °C	Pre-ssure	Heating rate, °C/min	Durationmin	Oil	Gas	Solid
PE-HD	Horizontal steel	350	-	20	30	80.9	17.2	1.9
PE-HD	Semi-batch	400	1atm	7	-	82.0	16.0	2.0
PE-HD	Batch	450	-	-	60	74.5	5.8	19.7
PE-HD	Semi-batch	450	1atm	25	-	91.2	4.1	4.7
PE-HD	Fluidized bed	500	-	-	60	85.0	10.0	5.0
PE-HD	Batch	550	-	5	-	84.7	16.3	0
PE-HD	Fluidized bed	650	-	-	20-25	68.5	31.5	0
PE-LD	Pressurized batch	425	0.8-4.3 kPa	10	60	89.5	10.0	0.5
PE-LD	Batch	430	-	3	-	75.6	8.2	7.5
PE-LD	-	500	1 atm	6	-	80.4	19.4	0.16
PE-LD	Fixed bed	500	-	10	20	95.0	5.0	0.0
PE-LD	Batch	550	-	5	-	93.1	14.6	0.0
PE-LD	Fluidized bed	600	1 atm	-	-	51.0	24.2	0.0
PP	Horizontal steel	300	-	20	30	69.8	28.8	1.3
PP	Batch	380	1 atm	3	-	80.1	6.6	13.3
PP	Semi-batch	400	1 atm	7	-	85.0	13.0	2.0
PP	Semi-batch	450	1 atm	25	-	92.3	4.1	3.6
PP	-	500	1 atm	6	-	82.1	17.8	0.1
PP	Batch	740	-	-	-	48.8	49.6	1.6

From the data presented in Table 8, it can be seen that an increase in the pyrolysis temperature of the plastics PE-HD, PE-LD and PP leads to a significant decrease in oil yield for all types of reactors. Most of the gas-vapor mixture does not condense, but passes into a gas. For PE-HD and PP plastics, the optimal temperature for the highest oil yield is 450 °C, and for PE-LD plastic, the temperature is 500 °C.

1.8 Tire pyrolysis

Tire pyrolysis has been widely studied by many authors [75–79]. From an environmental point of view, pyrolysis is the best alternative to direct combustion, which releases the pollutants PAHs, CO, CO₂, NO_x, SO_x etc. [80] Pyrolysis is a versatile process that allows for the co-pyrolysis of tires with waste plastics, biomass and solid fuels [81]. The yield of pyrolysis products is affected by the process temperature and the type of reactor. Table 9 shows data on the influence of these parameters [82].

Table 9. Effect of temperature and reactor type on the yield of tire pyrolysis products.

Reactor	t, °C	Yield, wt%		
		Oil	Char	Gas
Fixed, batch	700	38.5	43.7	17.8
Closed batch reactor	450	~63	~30	~7
Fixed bed, batch, internal fire tubes	475	55	36	9
Fixed bed, batch	720	58.8	26.4	14.8
Fixed bed, batch	600	40.3	47.9	11.9
Fixed bed, batch	500	58.0	37.0	5.0
Fixed bed, batch	425	60.0	~30	~10
Fixed bed, batch	475	58.2	37.3	4.5
Fluidised bed	700	26.8	35.8	19
Fluidised bed	450	55.0	42.5	2.5
Fluidised bed	740	30.2	48.5	20.9
Rotary kiln	550	38.1	49.1	2.4
Rotary kiln	500	45.1	41.3	13.6
Circulating fluidized bed	450	~52	~28	~15

As can be seen in Table 9, an increase in tire pyrolysis temperature leads to a decrease in oil yield and the formation of more gas. The optimum pyrolysis temperature to obtain liquid products is 425–500 °C.

The resulting pyrolysis oil is a mixture of hydrocarbons from C₆ to C₃₇, mostly C₈–C₁₃. About 65% are non-condensed pentenes, isoprene, butadiene and pentadienes. The oil contains large amounts of aromatics, naphthenes and terpenes, especially limonene [81].

1.9 Theory of the study of kinetic parameters

Thermogravimetry (TG) is a research and analysis method based on the registration of changes in the mass of a sample depending on its temperature or time under certain and controlled conditions of changes in the ambient temperature. Thermogravimetric analysis is quite accurate and fast, and it is used to study the characteristics and kinetics of the pyrolysis of materials with complex matrices, such as solid fuels. In pyrolysis

kinetics analysis, the activation energy (E_a) is an important parameter describing the pyrolysis process of a sample [83]. There are a number of methods for calculating E_a , based on the mathematical processing of the TGA curve. The least time-consuming and most accurate for polymers and oil shale is the double logarithm method. The condition for the applicability of the Coats-Redfern method is the first order of the decomposition reaction. When calculating the kinetics of oil shale pyrolysis and polymer decomposition, it is usually assumed that these reactions are of the first order [84–88].

The rate constant of the decomposition reaction of the test substance is found from the Arrhenius' equation:

$$K = A \cdot e^{-\frac{E_a}{RT}} \quad (1)$$

where

A = pre-exponential factor, sec^{-1}

E = activation energy, kJ/mol

T = temperature of the test substance, K

$$\frac{d\alpha}{d\tau} = K \cdot (1-\alpha)^n, \quad (2)$$

where

K = the rate constant of the decomposition reaction of the test substance

α = conversion rate

n = reaction order

τ = thermal decomposition time in sec^{-1}

The degree of decomposition of the material can be calculated following the established procedure for each reaction stage separately, and the conversion rate (α) is calculated by comparing the mass at time τ (m_τ) with the initial (m_0) and final (m_f) masses as per eq.:

$$\alpha = \frac{m_0 - m_\tau}{m_0 - m_f} \quad (3)$$

Substituting equation (2) into equation (1), we obtain the dependence: (4)

$$\frac{d\alpha}{d\tau} = A \cdot e^{-\frac{E}{RT}} \cdot (1-\alpha)^n. \quad (4)$$

$$\beta = \frac{dT}{d\tau},$$

Dividing the left and right sides of equation (4) by the heating rate, the following dependence is obtained:

$$\frac{d\alpha}{dT} = \frac{A}{\beta} e^{-\frac{E}{RT}} \cdot (1-\alpha)^n. \quad (5)$$

By dividing the variables in equation (5) and integrating the right and left sides, the following dependence is obtained:

$$\int_0^\alpha \frac{d\alpha}{(1-\alpha)} = \frac{A}{\beta} \int_{T_{\min}}^{T_{\max}} e^{-\frac{E}{RT}}. \quad (6)$$

The temperature integral can be calculated using the following equation:

$$\int_{T_{\min}}^{T_{\max}} e^{-\frac{E}{RT}} = \frac{R}{E} T_{\text{ext}}^2 \cdot e^{-\frac{E}{RT}}, \quad (7)$$

where

T_{ext} = reference temperature, which corresponds to the extremum of the decomposition rate of the substance. Replacing the integral over temperature and integrating the right and left sides of the equation, we obtain:

$$-\ln(1-\alpha) = \frac{A R}{\beta E} T_{\text{ext}}^2 \cdot e^{-\frac{E}{RT}}. \quad (8)$$

After taking the logarithm of the right and left sides of equation (8) [84-88], we get:

$$\ln(-\ln(1-\alpha)) = \ln\left(\frac{A R}{\beta E} T_{\text{ext}}^2\right) - \frac{E}{RT}. \quad (9)$$

From equation (9) it follows that the value of the activation energy E can be defined as the tangent of the slope of the linear portion of the curve plotted in coordinates

$\ln(-\ln(1-\alpha)); \frac{1000}{T}$.

After analyzing the curves of thermal decomposition, it is possible to select linear sections, approximate them by a linear equation of the type

$y = a \cdot x + b$, where the value of the parameter a corresponds to the value $\frac{R}{E}$, and b

corresponds to the complex $\ln\left(\frac{A R}{\beta E} T_{\text{ext}}^2\right)$, from which the value of the pre-exponential factor can be found.

2. EXPERIMENTAL

2.1 Sample characterization

The oil shale sample used in this study was Estonian oil shale from an underground mine called Ojamaa. The polyethylene (PE-HD and PE-LD), polypropylene (PP) and the tires used in this study were collected from the Uikala municipal waste dump.

One of the most important characteristics of fuels is the calorific value, which determines the fuel's quality. The calorific value was determined in calorimetric bomb Parr 6300, the net calorific value was calculated by EVS-ISO 1928 and corrected for non-decomposed carbonates. The need to correct the values of the calorific values for oil shales that contain more than 23% mass of the carbon dioxide of carbonates is described in Publication I. An analysis of the determination of the calorific values of oil shale from various deposits, including the Estonian oil shale, showed that for shale with a carbon dioxide content in carbonates of more than 23% on mass basis, it is necessary to introduce a correction for the value of the gross calorific value. The gross calorific value correction for some oil shale can be as high as 800 kJ/kg, but the ASTM and ISO international standards for determining the calorific value of solid fuels did not indicate this. Since the net calorific value is a critical characteristic of a fuel for industry and is calculated via gross calorific value, a correction for non-decomposed carbonates must be taken into account, as this will also affect the value of the net calorific value.

The elemental composition was determined using a "Vario Macro Cube" device by ASTM D5373, and the fixed carbon was determined by calculation from the equation: $FC (m/m\%) = 100 - A^d - \text{mass of the residue at } 815 \text{ } ^\circ\text{C}$ after heating the sample in a nitrogen atmosphere (TGA analysis). The ash content was determined by the International Standard ISO 1171. The data are shown in Table 10.

Table 10. Proximate and Ultimate analysis results.

Sample	Proximate analysis*, m/m%			Ultimate analysis*, m/m%			
	Ash content	Fixed carbon (FC)	Net calorific value, MJ/kg	C Total	H	N	S Total
EOS	50.1	2.7	8.807	27.5	2.7	0.07	1.60
PE-HD	0.4	< 1.0	44.575	84.0	15.5	0.02	<0.1
PE-LD	1.30	< 1.0	44.286	83.0	15.5	0.05	<0.1
PP	< 0.1	< 1.0	44.876	84.1	15.8	0.01	<0.1
Tires	8.0	24.6	34.388	78.7	7.7	0.47	1.25

*on dry basis

For a characterization of the mineral part of the oil shale, the content of metal oxides was determined. The content of metal oxides was determined by atomic emission spectrometry with microwave plasma generation (MP-AES). At the first stage of the analysis, the sample was treated with H₂O₂ and HNO₃, and then the decomposition of the sample continued in an ETHOS ONE microwave system. At the next stage, the content of metals in the resulting solutions was determined by atomic emission spectrometry with microwave plasma on a Shimadzu 4200MP-AES instrument. Based on the amount of metals, the content of metal oxides was recalculated through the molar mass. Based on the ash content in the oil shale sample, the content of the metal oxides was recalculated to ash. The data are shown in Table 11.

Table 11. Metals content in the oil shale and oil shale ash.

Sample	SiO ₂	Al ₂ O ₃	Fe ₂ O ₃	CaO	MgO	Na ₂ O	K ₂ O	TiO ₂
	m/m%							
EOS	12.9	2.8	2.3	24.6	2.2	0.2	1.4	0.2
Oil shale ash	25.7	5.6	4.6	49.2	4.4	0.4	2.8	0.4

The studied samples were analyzed on a Thermo Nicolet Summit FTIR spectrophotometer instrument in order to determine the functional groups included in their compositions. The FTIR spectra are shown in Figure 11 and Figure 12.

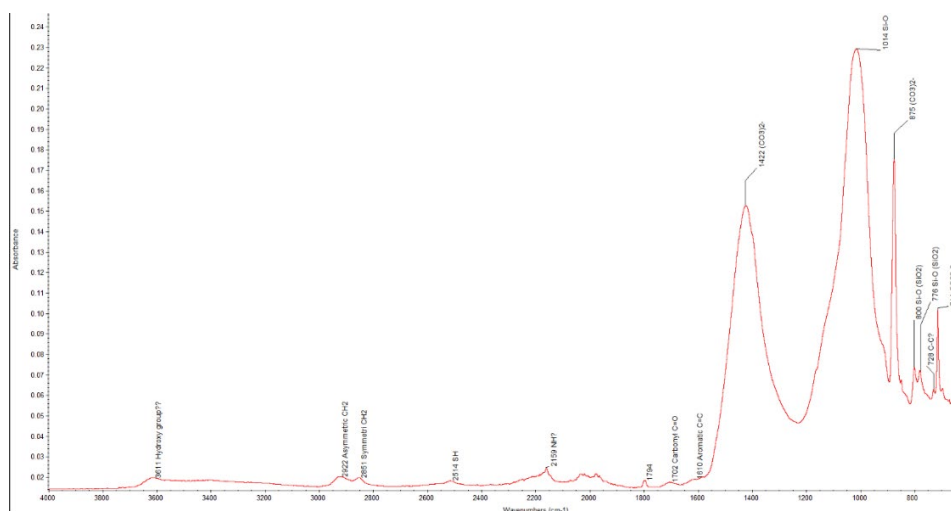


Figure 11. FTIR spectra of Estonian oil shale.

In principle, the FTIR method is the interaction of infrared radiation with the vibrating dipole moments of the molecules of the substance under study. The FTIR spectra show the molecular absorption of various chemical bonds and specific bonds in an oil shale sample. A peak with an intensity of 3615 cm⁻¹ indicates stretching vibrations of the hydroxy group, H-bonded OH stretch. The original oil shale sample had asymmetric and symmetric CH₂ groups stretching vibrations of kerogen at around 2922 and 2857 cm⁻¹, respectively. From near 1706 cm⁻¹ carbonyl C=O stretch bands and from 1622 cm⁻¹ C=C aromatic structures were apparent. The right side of the FTIR spectra shows the mineral

bands of shale samples. The distinct broad peak at around 1422 cm^{-1} represents stretching vibrations of the CO_3^{2-} ion from dolomite and calcite. The other two sharp peaks at 874 and 727 cm^{-1} represent carbonate ions from dolomite and calcite. The other broad peak at around 1012 cm^{-1} with small peaks around 778 and 695 cm^{-1} represent Si-O stretching vibrations of quartz and silica. The intensity of the peaks around 2922 and 2857 cm^{-1} may indicate that the kerogen of the oil shale has aliphatic content.

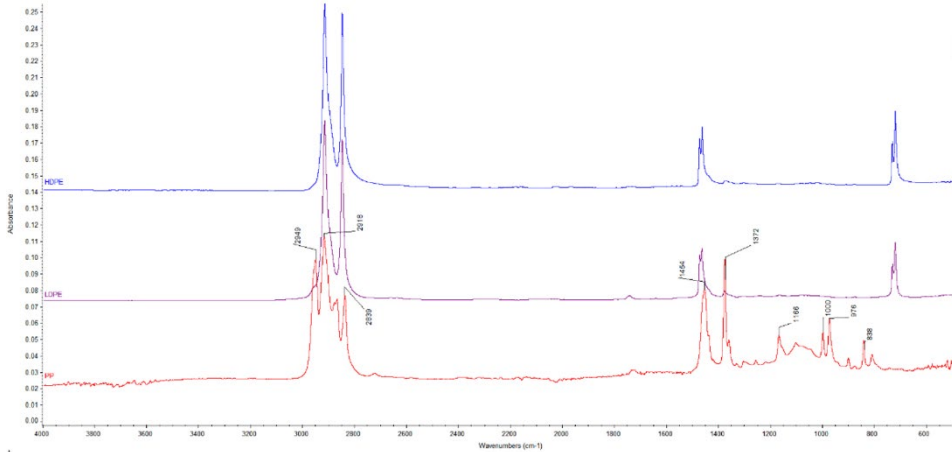


Figure 12. FTIR spectra of PE-HD, PE-LD, PP.

The spectra of high and low density polyethylene were identical to each other. At wavelengths of 2918 and 2839 cm^{-1} there were asymmetric and symmetric stretching vibrations of the CH_2 groups (methylene C–H asymmetric stretch), and at 1454 cm^{-1} and 750 cm^{-1} there were scissoring vibrations and pendulum vibrations of the CH_2 groups, respectively. The FTIR spectrum of polypropylene had the same asymmetric and symmetric stretching vibrations of the CH_2 groups at 2918 and 2839 cm^{-1} as PE, and the asymmetric and symmetric in-plane C–H ($-\text{CH}_3$) at 1454, and a shoulder at 1354 cm^{-1} confirmed that it was a polypropylene. The peak at 1372 cm^{-1} was C–H scissoring and bending assigned to $-\text{CH}_3$ alkanes.

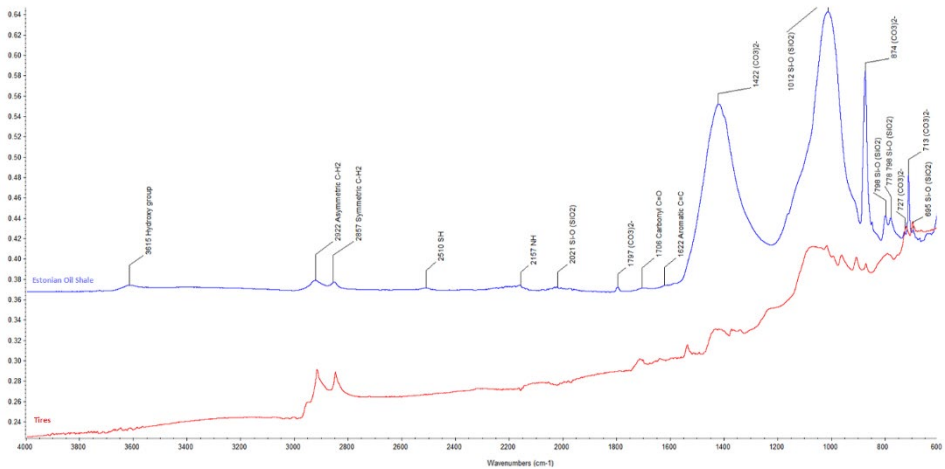


Figure 13. FTIR spectra of Estonian oil shale and tires.

The tire spectrum (Figure 13) contained symmetric and asymmetric stretching vibrations of CH₂ groups (2850–2950 cm⁻¹). The spectrum also showed that the tires had a mineral filler. When compared with the spectrum of the oil shale, it was clear that the tires had stretching vibrations of the CO₃²⁻ ion from the calcium carbonate used as tire filler. The other two peaks at 874 and 727 cm⁻¹ also testified to this.

For all samples, the yield of pyrolysis products was determined in accordance with the standard ISO 647. The method is based on heating the test sample in an aluminum retort to a temperature of 520 °C for 80 minutes. The data are shown in Table 12.

Table 12. Yield of pyrolysis products.

Samples	Yield of pyrolysis products, m/m%			
	oil	semi-coke	pyrogenetic water	gas + loss
EOS	16.5	77.3	1.5	4.7
PE-LD	92.3	1.2	0.3	6.2
PE-HD	92.1	1.9	0.0	6.0
PP	93.4	0.3	0.0	6.3
Tires	54.2	38.8	0.1	6.9

Before analysis, the samples were dried and ground in a mill Retch SK-100 to an analytical sample (up to 0.2 mm).

Test mixtures of samples were prepared from oil shale and individual components of polymer wastes in a ratio of 50/50 (EOS + PE-LD, EOS + PE-HD, EOS + PP, EOS + tires), as well as a mixture of oil shale 50% and 50% (EOS + mix) of the four components of polymer wastes in an equal ratio. The resulting mixtures were subjected to pyrolysis under the same conditions as the individual components of the mixtures. The pyrolysis products were analyzed. Data for this part of the study are presented in Publication III.

2.2 Methods for the analysis of co-pyrolysis products

In the oils and semi-cokes obtained by co-pyrolysis, the elemental composition was determined on a “Vario Macro Cube” device. Carbon, hydrogen, nitrogen and sulfur were determined concurrently in a single instrumental procedure. The quantitative conversion of the carbon, hydrogen, nitrogen and sulfur into their corresponding gases (CO₂, H₂O, N₂/NO_x and SO₂) occurred during the combustion of the sample at 1150 °C in an atmosphere of oxygen. Combustion products which would interfere with the subsequent gas analysis were removed by a helium purge. The oxides of nitrogen (NO_x) produced during the combustion were reduced to N₂ before detection. The carbon dioxide, water vapor, elemental nitrogen and sulfur dioxide in the gas stream were then determined quantitatively by appropriate instrumental gas analysis procedures.

The relative density of the liquid pyrolysis products was determined by the ratio of the oil density to the density of distilled water at room temperature.

The group composition of the obtained oils was determined by adsorption chromatography. Separation into groups of compounds occurred when the mobile phase moved along the column as a result of interaction with silica gel, which has active sites on the surface. The mobile phase was a polar solvent with increasing eluting power. At the next stage, each group of compounds was analyzed on a GAS-CHROMATO-MASS-SPECTROMETER (GC-MS), which had the following characteristics:

Equipment: Gas chromatograph mass spectrometer "Shimadzu GCMS-QP2010 Plus"

Ionization mode: Electron ionization (EI)

Injection: Split @ 280 °C, 3 µl / auto sampler AOC-20i

Column: Zebron ZB-1

Dimensions: L = 100m, ID = 0.25 mm and FT = 0.50 µm

Detector: MSD @ 280 °C

Carrier Gas: Helium @ 30mL/min (constant flow)

The studied samples were analyzed on a Thermo Nicolet Summit FTIR spectrophotometer instrument in order to determine the functional groups included in their compositions. The spectrometer had the following characteristics:

Range: 4000-400 cm⁻¹

Number of scans: 16

Optics: KBr

An analysis of the component composition of the gas was performed on an Agilent Technologies 7890B gas chromatograph. The gas chromatograph had two types of detectors: TCD (thermal conductivity) and FID (flame ionization). High purity helium and nitrogen were used as carrier gases. The obtained data were processed using specialized OpenLab software; for analysis, a method developed on the basis of international standards was used: UOP 539-12 Refinery Gas Analysis by Gas Chromatography and EVS-EN ISO 6976.

2.3 Thermogravimetric analysis

A thermogravimetric analysis (TGA) of the oil shale samples and polymer wastes was undertaken using a TGA 1 STARe System METTLER TOLEDO. The initial TGA temperature for all samples was 25 °C and the final temperature was 950 °C. The heating rate was 20 °C/min and the tests were carried out under nitrogen purging at a rate of 20 ml/min. Nitrogen gas was used as an inert purge gas to displace air in the pyrolysis zone, thus avoiding unwanted oxidation of the sample. In this work, about 20–25 mg of each sample were analyzed in an Al₂O₃ dish and used for TGA analysis.

From the TG curve, according to the international standard EVS-EN ISO 11358-1, points T_A, T_B and T_C were determined (Figure 14), where:

- A is the starting point: the point of intersection of the starting-mass baseline and the tangent to the TG curve at the point of maximum gradient;
- B is the end point: the point of intersection of the final-mass baseline and the tangent to the TG curve at the point of maximum gradient;
- C is the mid-point: the point of intersection of the TG curve with the temperature at which both baselines are equidistant.

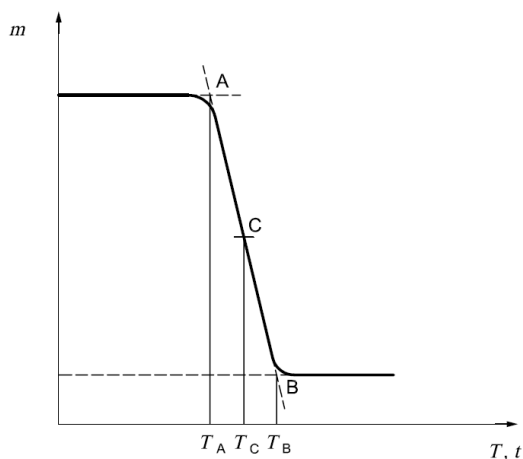


Figure 14. Processing of the obtained TG curve.

The thermogravimetric analysis of the sample in an inert atmosphere, in this study under nitrogen, simulated the process of pyrolysis. Based on the obtained mass loss curves and the differential mass loss curve, the main kinetic parameters of co-pyrolysis were determined. Data on the main kinetic parameters of co-pyrolysis are presented in Publication III.

Also, based on the data of the thermogravimetric analysis, the thermal stability of the polymers was determined, which characterizes the ability of the polymer to maintain its properties.

3. RESULTS AND DISCUSSION

3.1 Decomposition of Estonia oil shale, polymers and mixtures of polymer wastes with oil shale

The curves of mass loss (TG) of oil shale and polymers waste when heated under these conditions and a differential weight loss (DTG) curve are shown in Figures 15 and 16.

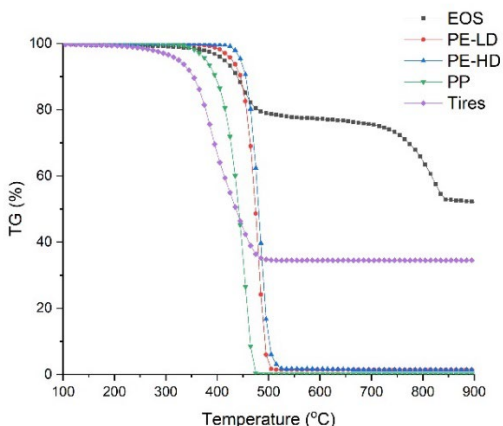


Figure 15. Curves of oil shale and polymer waste weight loss (heating to 950 °C).

The oil shale weight loss curve indicates a two-stage decomposition of the sample. Such a two-stage decomposition is typical for oil shales with an insignificant stage of moisture loss at 100°C, as pointed out by other authors [89, 90]. The decomposition of plastics in a nitrogen environment occurs in one stage, since they basically lack the mineral part (see the results of the analysis of the ash content in Table 10).

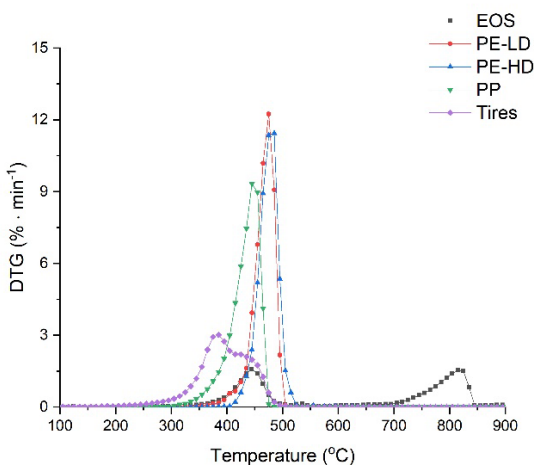


Figure 16. Curves of oil shale and polymer waste differential weight loss (heating to 950 °C).

The graphs indicate that, in the temperature range from 300 to 550 °C, the organic part of oil shale decomposed, with a maximum weight loss at 445 °C, and in the temperature range from 670 to 870 °C, the mineral part of the oil shale decomposed, with a maximum weight loss at the second stage at 799 °C. Although PE-HD and PE-LD plastics are identical in composition, their degradation starts and ends at different temperatures. PE-HD decomposed in the temperature range of 400–550 °C, with a maximum mass loss point at 482 °C, and PE-LD decomposed at 350–580 °C, with a maximum mass loss point at 472 °C. As can be seen from the weight loss curve of PP, its decomposition began at a lower temperature, in the range of 300–520 °C, with a maximum weight loss at 442 °C. The obtained data on TGA analysis correspond to the data obtained by other authors [91, 92]. The tire began to decompose in the temperature range of 250–550 °C (organic part), with a maximum weight loss at 400 °C. A residue of about 34% at the end of decomposition at 950°C indicated the presence of a filler. The mineral part of the filler partially decomposed in the temperature range of 650–740 °C; however, this peak is not clearly visible on the DTG curve, since the content of the organic part was much higher than the mineral part. In the temperature range of 250–550 °C, the active pyrolysis of the studied samples took place. Subsequent heating of the samples to 950 °C led to the thermal destruction of stronger bonds in the solid residue and a weight loss of less than 1%. The values of the beginning (T_{onset}) and end (T_{endset}) of the active destruction of organic matter, the destruction of the mineral part and the maximum weight loss (T_{midpoint}) during these processes are presented in Table 13.

Table 13. The TGA parameters for Estonian oil shale and polymers.

TGA parameter	Raw materials					
	EOS		PE-LD	PE-HD	PP	Tires
	Step 1	Step 2	Step 1	Step 1	Step 1	Step 1
T_{onset} , °C	412.8	766.0	455.6	460.5	419.5	353.6
T_{midpoint} , °C	444.7	798.8	480.7	480.4	442.3	400.3
T_{endset} , °C	476.6	839.4	493.9	500.3	468.9	451.0

The thermal stability of polymers is estimated by the temperature of the beginning of decomposition, at which the mass loss begins and the TG curve deviates from the initial zero value, as well as by the values of T_{10} , T_{20} , T_{50} , at which 10%, 20% and 50%, respectively, of the mass occurs under the same experimental conditions. The data of thermal stability for each polymer are shown in Table 14.

Table 14. Thermal stability (T_{10} , T_{20} , T_{50}) of the studied polymers.

	Raw materials			
	PE-LD	PE-HD	PP	Tire
T_{10}	445.5	455.5	396.4	358.0
T_{20}	456.9	465.1	415.6	385.1
T_{50}	474.3	480.4	441.8	452.8

From the data presented in Table 14, it can be seen that PE-HD plastic was the most thermally stable of the studied polymers, and the tires were the least stable. The data obtained by thermogravimetric analysis for PE-HD and PE-LD are logical, since the bonds of PE-HD molecules are stronger than those of PE-LD.

The kinetics of the co-pyrolysis of oil shale with polymer wastes has not been studied much. To study this process, the following mixtures were prepared:

- Estonian oil shale/ PE-HD – 50/50
- Estonian oil shale/ PE-LD – 50/50
- Estonian oil shale/ PP– 50/50
- Estonian oil shale/ Tires – 50/50
- Estonian oil shale/ PE-HD/ PE-LD/ PP/ Tires – 50/12.5/12.5/12.5/12.5

The thermogravimetric analysis of the samples was carried out under the following conditions: the initial TGA temperature for all samples was 25 °C and the final temperature was 950 °C, the heating rate was 20 °C/min and the tests were carried out under nitrogen purging at a rate of 20 ml/min. Figures 17 and 18 show a simple weight loss (TG) curve of the studied test mixtures and a differential weight loss (DTG) curve.

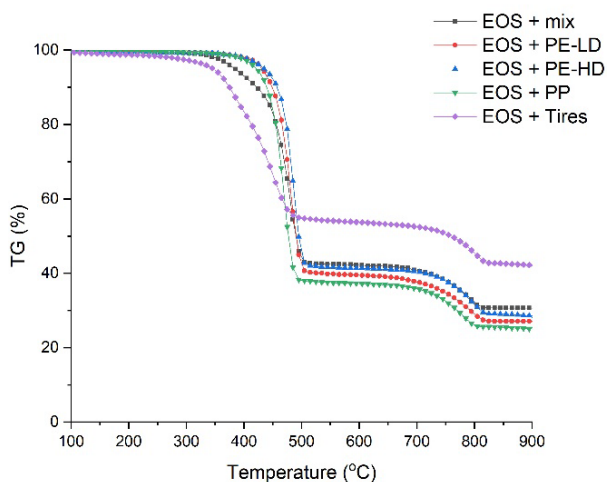


Figure 17. Simple weight loss (TG) curve of the studied mixtures of Estonian oil shale with polymer wastes.

The mass loss curves during the co-pyrolysis of the studied mixtures indicate that the process occurred in two stages. The first stage was the decomposition of the organic part of the mixtures, and the second stage was the mineral part of the oil shale and filler in the mixtures that included tires.

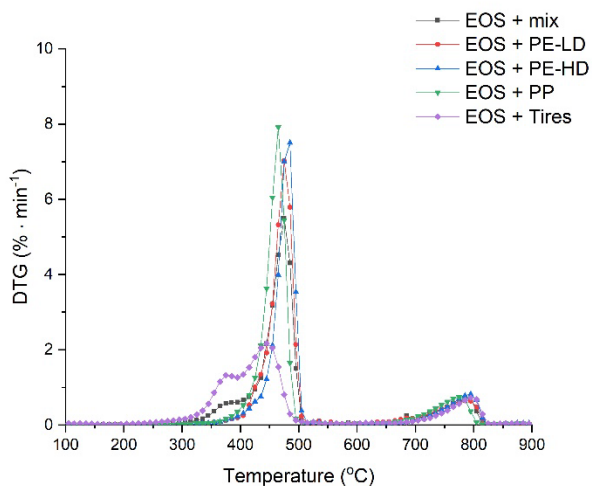


Figure 18. Differential weight loss (DTG) curve of the studied mixtures Estonian oil shale and polymer wastes.

It can be seen from the DTG curve (Figure 18) that the addition of polymers to the oil shale affected the temperature at which the samples began to decompose. While the temperature of the beginning of the decomposition of the oil shale and PP began at 300 °C, and that of the plastics PE-HD and PE-LD at 370 °C, during co-pyrolysis the onset of decomposition for all mixtures shifted and began at 350 °C and ended for all mixtures at 500°C. Between 350 and 500 °C, there was a total weight loss of 58.4 and 57.5 m/m% for oil shale with PE-LD and PE-HD, respectively, and 61.0 for PP and 39 for tires, which corresponds to the overlapping decomposition of the organic matter of the oil shale and polymers. These data are in good agreement with a study of the co-pyrolysis of oil shale from a Moroccan deposit with plastic PE-HD in a ratio of 1:1 [93]. When a tire was added to the oil shale, the decomposition of which began at 250 °C, the decomposition of the mixture began at 300 °C, i. e. at the same temperature as the decomposition of only oil shale. This may be due to the fact that tires contain less organic matter than plastic, so the effect on the co-pyrolysis process was not as significant. The values of the beginning (T_{onset}) and end (T_{endset}) of the active intensity of the destruction of organic matter, the destruction of the mineral part and the maximum weight loss (T_{midpoint}) during these processes are presented in Table 15.

Table 15. TGA parameters for mixtures of oil shales and polymer wastes.

TGA parameter	Mixture									
	EOS + PE-LD		EOS + PE-HD		EOS + PP		EOS + tire		EOS + mix	
	Step 1	Step 2	Step 1	Step 2	Step 1	Step 2	Step 1	Step 2	Step 1	Step 2
Tonset, °C	456.8	732.7	464.0	746.9	446.6	727.8	378.1	761.4	456.6	727.2
Tmidpoint, °C	476.0	759.9	481.4	778.1	464.9	760.7	425.1	780.6	471.7	757.7
Tendset, °C	496.3	798.2	499.2	814.5	483.8	798.6	477.0	817.8	495.5	796.2

From the data presented in Table 15, it is clear that the stage of active decomposition of the organic part (T_{onset}) of all mixtures with polymers occurred in the temperature range of 447–464 °C and ended (T_{endset}) at 500 °C. The maximum weight loss temperature (T_{midpoint}) of this stage was in the temperature range of 465–481 °C. The stage of active decomposition of the organic part of the mixture with the tires occurred at a temperature of 378 °C and ended at 477 °C, with the maximum weight loss temperature at 425 °C. During the co-pyrolysis of mixtures of oil shale and polymers, the mineral part of the samples began and ended decomposition at lower temperatures than during the pyrolysis of oil shale. Such a shift in temperature may have been due to a deeper decomposition of the organic part of the oil shale during co-pyrolysis and the weakening of chemical bonds in the solid residue.

3.2 Study of additivity based on the TG analysis

Based on the data of the thermogravimetric analysis of each initial sample separately (oil shale, plastics and tires), the principle of additivity was studied during the thermal decomposition of mixtures of oil shale with individual plastics, tires and a multicomponent mixture (mixtures of oil shale with these polymeric wastes). Figure 19 shows the experimental and calculated data on the contribution of each component to the thermal decomposition process.

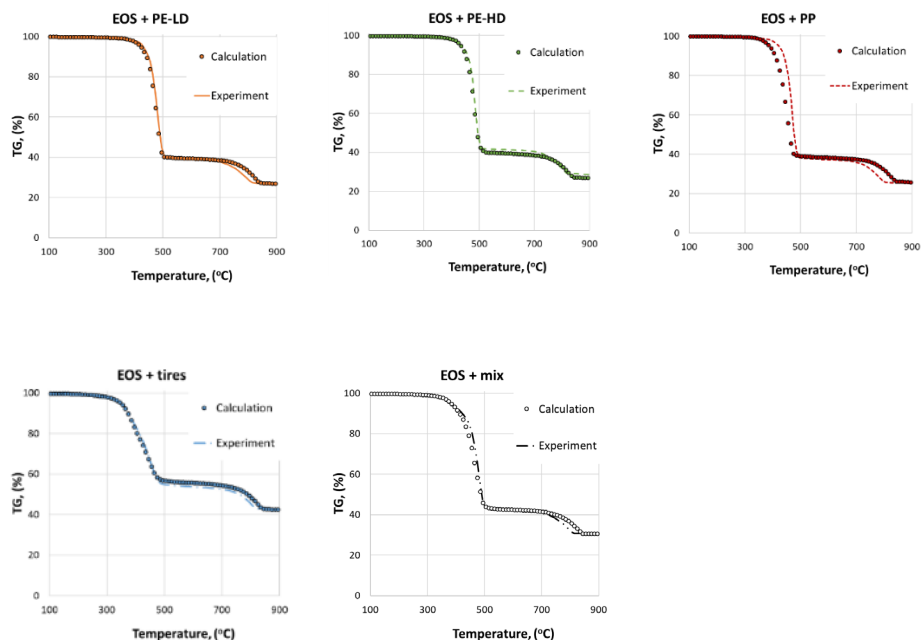


Figure 19. Calculated and experimental curves of weight loss (TG) for mixtures of Estonian oil shale with individual components and a mixture of polymer wastes.

As can be seen in Figure 19, the mass loss curves during the thermal decomposition of the samples, constructed on the basis of the calculated data and experimental data, are in good agreement with each other. This indicates the possibility of calculating the weight loss based on the principle of additivity for mixtures, for example, with other ratios of oil shale/polymer wastes. The possibility of obtaining data based on the principle of additivity allows for mathematical modeling of the process of co-pyrolysis, as well as taking into account the features of this process when regulating the operation of pyrolysis plants in real life.

3.3 Kinetics of co-pyrolysis. Activation energy

The thermal decomposition of the organic part of oil shale, raw materials and their mixtures occurs in a wide temperature range, from 225 to 515 °C. This temperature interval on the DTG curve was chosen to calculate the activation energy. In this interval, weight loss and temperature were determined every 10 °C. To plot the dependence, all temperature values were calculated as $10^3/T$. The results are shown in Figures 20 and 21.

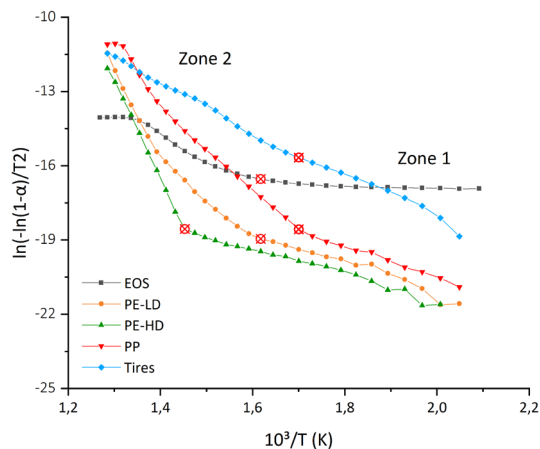


Figure 20. The Coats-Redfern integral method results for raw materials.

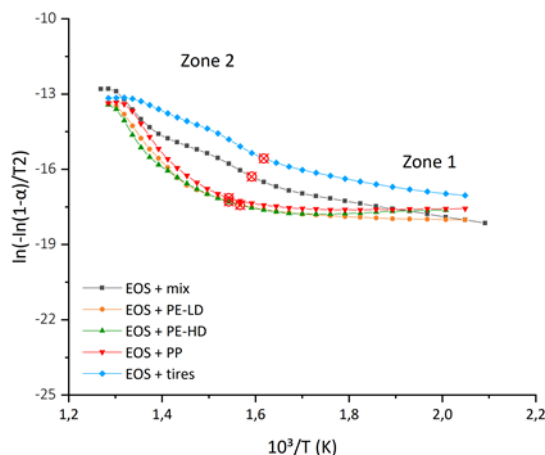


Figure 21. The Coats-Redfern integral method results for mixtures of Estonian oil shale with polymer wastes.

Figures 20 and 21 show that in the studied temperature range there are two zones separated from each other by a “breaking point”. Zone I is the reaction zone at low temperatures, and Zone II is the reaction zone at higher temperatures. The “breaking point” indicates different rates of thermal decomposition in these zones. For the polymers PE-LD and PE-HD, the presence of a “breaking point” is quite clearly expressed, while for PP, tires and oil shale it is not so obvious. The presence of two zones of thermal decomposition in oil shale indicates the occurrence of different reactions, which may overlap slightly [89]. In the case of mixtures of oil shale and plastics, it can be seen that the behavior of the mixtures becomes the same in different temperature zones. During the thermal decomposition of oil shale samples with a mixture of polymeric wastes and with tires, the reactions occurring in the process are almost identical.

Tables 16 and 17 show the kinetic parameters of the pyrolysis of the raw materials and mixtures of polymer wastes and oil shale.

Table 16. The obtained characteristics of the kinetic parameters of the pyrolysis of the raw materials.

Sample	Zone	Raw materials			
		Temperature range, °C	R ²	Activation energy, kJ/mol	log A
EOS	Zone I	225 – 365	0.99	44.38	7.42
	Zone II	375 – 515	0.99	129.33	8.29
PE-LD	Zone I	225 – 365	0.96	50.24	9.06
	Zone II	375 – 515	0.97	210.88	20.44
PE-HD	Zone I	225 – 405	0.98	43.72	10.96
	Zone II	415 – 515	0.99	327.01	38.56
PP	Zone I	225 – 315	0.99	51.60	8.08
	Zone II	325 – 515	0.98	158.08	13.36
Tires	Zone I	225 – 315	0.99	63.48	2.62
	Zone II	325 – 515	0.99	86.72	1.97

Table 17. The obtained characteristics of the kinetic parameters of the pyrolysis of the mixtures of polymer wastes and oil shale.

Sample	Zone	Mixtures			
		Temperature range, °C	R ²	Activation energy, kJ/mol	log A
EOS + mix	Zone I	225 – 445	0.99	59.94	4.51
	Zone II	455 – 515	0.98	234.36	24.48
EOS + PE-LD	Zone I	225 – 415	0.99	46.95	8.31
	Zone II	425 – 515	0.98	233.82	24.14
EOS + PE-HD	Zone I	225 – 425	0.90	54.14	7.23
	Zone II	435 – 515	0.96	249.01	26.29
EOS + PP	Zone I	225 – 395	0.98	46.59	8.50
	Zone II	405 – 515	0.98	224.34	23.18
EOS + Tires	Zone I	225 – 345	0.99	58.43	3.91
	Zone II	355 – 515	0.99	92.10	2.55

Tables 16 and 17 present the calculated activation energy data, pre-exponential factors and R-squared values, ranging from 0.90 to 0.99. The calculated data show that in the addition of the polymers PE-LD, PE-HD and PP and tires to mixtures with oil shale, the activation energy in reaction Zone I (lower thermal decomposition temperatures) was slightly reduced (by a factor of 1.06, 1.2 and 1.06, respectively), while in Zone II (higher thermal decomposition temperatures) its values increased by a factor of 1.1 and 1.4, respectively. An increase in the activation energy indicates that the thermal decomposition of mixtures at high temperatures was slower than the decomposition of raw materials. An exception was the mixture with PE-HD, whose activation energy in the second zone was 1.3 times lower. The faster course of the decomposition reaction may have been due to the branched structure of the PE-HD molecules. Mixtures of oil shale and plastics and a mixture with polymer waste had almost the same values of activation energy in reaction Zones I and II. The thermal decomposition of the mixture of oil shale and tires was much faster than with other mixtures.

3.4 Characteristics of the resulting co-pyrolysis products

For the studied mixtures, the yield of pyrolysis products was determined. The data obtained are presented in Table 18. For comparison of the obtained data, the results were recalculated per apparent organic content.

Table 18. The yield of co-pyrolysis products.

Samples	Yield of co-pyrolysis products, m/m%							
	as received				per apparent organic content			
	Oil	Semi-coke	Pyro-genetic water	Gas + loss	Oil	Semi-coke	Pyro-genetic water	Gas + loss
EOS	16.5	77.3	1.5	4.7	59.8	17.8	5.4	17.0
EOS + PE-LD	55.5	36.5	0.8	7.2	87.3	0.2	1.3	11.3
EOS+PE-HD	53.9	39.7	0.2	6.1	84.7	5.2	0.3	9.6
EOS + PP	55.2	37.8	0.2	6.8	86.7	2.3	0.3	10.8
EOS + tires	34.6	58.2	1.6	5.6	57.9	30.1	2.7	9.3
EOS + mix	49.3	42.1	0.9	7.7	78.7	7.6	1.4	12.3

The pyrolysis of oil shale with polymer wastes significantly increased the yield of liquid pyrolysis products. The yield of semi-coke and pyrogenic water was significantly reduced. The decrease in the content of pyrogenic water occurred because the samples of polymeric wastes with which the experiments were carried out did not contain oxygen.

3.5 Study of a possible synergistic effect in the output of co-pyrolysis products

Previously, the authors of other studies on the co-pyrolysis of various materials containing some organic matter with plastics found a synergistic effect for oil yield. Yunwu Zhenga et al. [94] described the synergistic effect between biomass and PE-HD plastic in co-pyrolysis. This study confirmed the hypothesis that during the pyrolysis of plastic PE-LD, in a vapor-gas mixture a high H/C ratio is formed, which prevents coking and partially reduces the repolymerization of a biomass vapor-gas mixture. Limin Zhou et al. [95], when studying the kinetics of co-pyrolysis, revealed a synergistic effect between coal and a mixture of the plastics PE-HD, PE-LD and PP, especially at high temperatures (550–650 °C). Other authors have also found a synergistic effect in the co-pyrolysis of oil shale from deposits in Turkey and China with plastics. In their study, Yong Li et al. [96] found a significant synergistic effect during the co-pyrolysis of oil shale from Fushun and Longkou with plastics, while the effect was more noticeable during pyrolysis with PE than with PP. The authors explained the synergistic effect by the free radical reaction theory of pyrolysis. Oil shale contains a low amount of hydrogen, so the free radicals formed during pyrolysis polycondensed compounds and, as a result, the yield of liquid products was small and more semi-coke was formed. During the pyrolysis of polymers, the gas-vapor mixture contains a high amount of hydrogen, which is

attached to a free radical of oil shale, making it stable, excluding the polycondensation process. Ultimately, more liquid pyrolysis products are formed. Pinar Acar Bozkurt et al. [97] also supported the theory of a free radical pyrolysis reaction when studying the joint pyrolysis of Turkish oil shale with polypropylene, noting a significant increase in the yield of the liquid product.

To study the occurrence of a possible synergistic effect, the additivity principle was tested for all co-pyrolysis products.

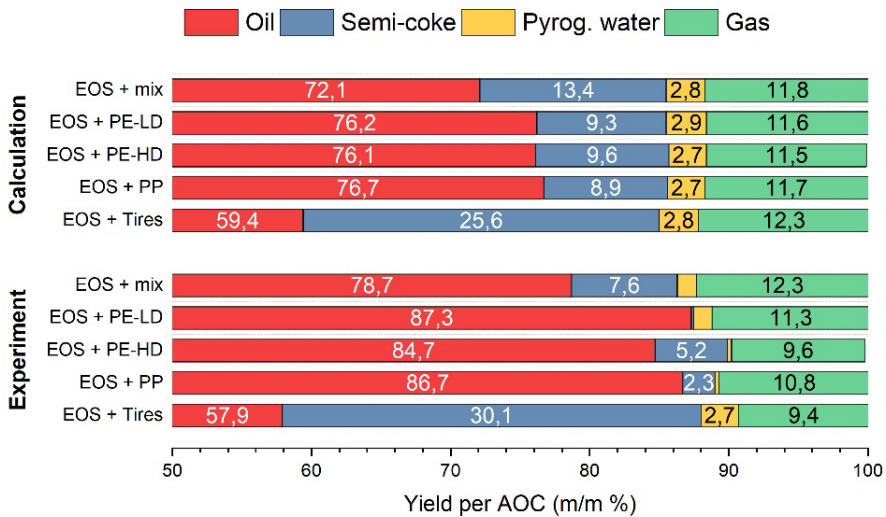


Figure 22. Comparison of experimental and calculated data on the yield of co-pyrolysis products.

As Figure 22 shows, for all mixtures of shale with plastics, a synergistic effect was observed in the release of liquid products. According to the calculated data, based on the result of the pyrolysis of the individual components of the mixture and the additivity method, the yield of liquid products after the experiment increased by 14.6, 11.3 and 15.0 for PE-LD, PE-HD and PP, respectively, and the output of semi-coke and gas was lower than calculated for these plastics. The synergistic effect of the yield of liquid products was not observed in the co-pyrolysis of oil shale with tires. The experimental oil yield was 2.6% lower than the calculated value. However, in a mixture of polymer wastes where tires were also present, a synergistic effect occurred. The yield of liquid products was 9.2% higher than the calculated value. The synergistic effect was observed due to the interaction of volatile oil shale products and polymeric wastes in the gas and condensed phases, where the reaction between the hydrogen of polymers and oil shale kerogen took place.

3.6 Characteristics of liquid products of co-pyrolysis

Liquid products obtained from oil shale with plastics are a mixture of oil and wax, which does not flow at room temperature. When samples were heated to 45 °C, they became liquid. The formation of a mixture of oil and wax during the pyrolysis of PE-HD, PE-LD and PP at a temperature of 520 °C has also been noted by other authors [98, 99]. Oils from a mixture of oil shale and polymers are not as thick at room temperature as oils

from oil shale and plastics. Oil obtained from oil shale with tires is a liquid. The elemental composition and relative density of oils obtained by co-pyrolysis are presented in Table 19.

Table 19. The elemental composition and relative density of oils.

Samples	Elemental composition, m/m%				100 H/C	Relative density, kg/m ³
	C	H	N	S		
EOS	81.6	10.4	0.17	0.82	13	946.0
EOS + PE-LD	84.7	13.6	0.12	0.18	16	845.0
EOS + PE-HD	83.5	13.4	0.09	0.19	16	812.5
EOS + PP	84.8	13.8	0.05	0.17	16	766.4
EOS + tires	85.0	11.0	0.35	0.97	13	926.0
EOS + mix	87.1	14.4	0.18	0.27	17	844.7

Oils from a mixture of oil shale and individual plastics were similar in their elemental compositions and relative densities, but the relative density of the oil obtained by co-pyrolysis with PP was lower than from other mixtures. These oils also had low sulfur contents. Oil obtained by co-pyrolysis with tires was of lower quality than shale oil. The nitrogen content in the oil was almost doubled, the sulfur content increased by 18%, and the relative density of the oil was almost the same as that of shale oil. The oil obtained from oil shale and a mixture of polymer wastes was of a fairly high quality, although the mixture contained one part tires. This oil had a low sulfur content, lower density and the highest 100 H/C ratio of all of the co-pyrolysis blends. The higher the 100 H/C ratio, the higher the energy efficiency of the fuel and the lower the CO₂ air emission levels during its combustion [100]. The results of the analysis of the obtained oils showed that the oils of the co-pyrolysis of oil shale with polymers were of significantly higher quality than shale oil.

From the data presented in Table 19, the sulfur content of the oil was well below the expected value based on the additivity principle. Figure 23 shows that in all oils, except for oil obtained from oil shale with tires in a ratio of 1:1, the calculated sulfur content was much higher than that obtained in the experiment.

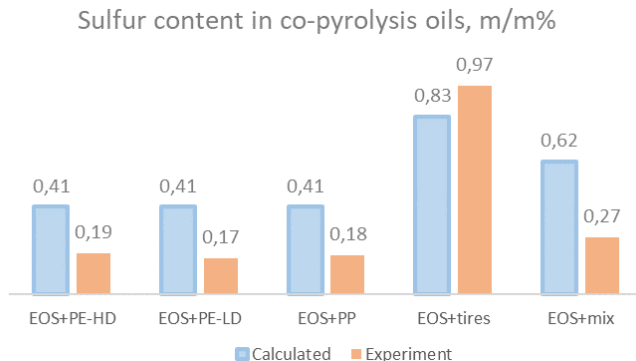


Figure 23. Calculated by the additivity principle and the experimental results of the sulfur content in co-pyrolysis oils.

The sulfur contents in oils of co-pyrolysis with polymers after the experiment were 53, 56 and 59% lower than the calculated values based on the additivity principle, for PE-HD, PE-LD and PP, respectively. For oil obtained from oil shale with tires, the sulfur content was 17% higher than the calculated value. However, in the oil of the co-pyrolysis of oil shale mixed with polymer wastes, the sulfur content was lower than the calculated value by 57%, which indicates that the presence of tires in small amounts in polymer wastes did not significantly affect this indicator.

The studied samples of oils were analyzed to determine the functional groups included in their compositions. The FTIR spectra are shown in Figure 24.

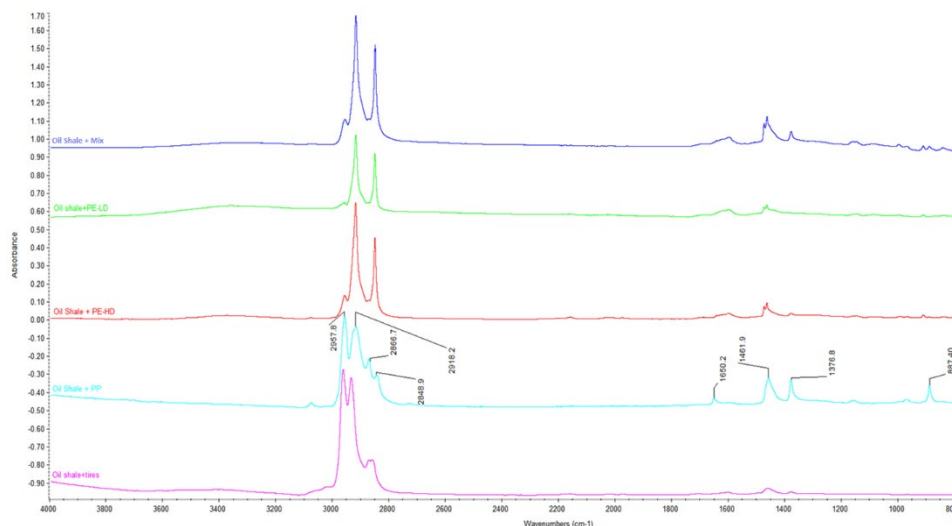


Figure 24. Co-pyrolysis oils FTIR spectra.

A stretched peak between 3600 and 3100 cm^{-1} indicates the presence of OH groups, which in this case belong to phenols, which were formed during the pyrolysis of oil shale. The IR spectra show intense absorption bands of 2867, 2918, 2958, 1462, and 1377 cm^{-1} , which indicate the presence of CH_2 and CH_3 groups. The peak at 1650 cm^{-1} indicates the C=O bonds of aldehydes or ketones. The wave range of 1600–1500 cm^{-1} indicates the formation of the C-C stretching of aromatic compounds. The peaks between 1350–1140 cm^{-1} indicate oxygenated functional groups with sulfur and nitrogen and indicate the presence of sulfonamide at a wave rate of 1160 cm^{-1} . The peak at 960 cm^{-1} indicates the C=C stretching of alkene compounds. The peaks at wave numbers 887 cm^{-1} in the wave range of 900–880 cm^{-1} indicate alkenes [101, 102].

3.7 Semi-coke and gas

In pyrolysis with a solid heat carrier, the resulting semi-coke plays an important role, part of which is its use for additional combustion and its return to the process, so its composition has been studied. Table 20 shows the elemental composition of co-pyrolysis semi-coke and, for comparison, oil shale pyrolysis semi-coke.

Table 20. The elemental composition of semi-coke.

Samples	Elemental composition, m/m%			
	C	H	N	S
EOS	13.5	<0.1	0.07	0.90
EOS + PE-LD	15.2	0.3	0.07	1.48
EOS + PE-HD	16.7	0.3	0.06	1.40
EOS + PP	15.7	0.4	0.07	1.33
EOS + tires	30.7	0.3	0.18	1.60
EOS + mix	20.1	0.3	0.11	1.44

The data presented in Table 20 show that co-pyrolysis semi-coke in its elemental composition differs from oil shale pyrolysis semi-coke. Oil shale and tire pyrolysis semi-coke contains a lot of total carbon, which is due to the carbon black fillers contained in tires. The high carbon content in the semi-coke of the co-pyrolysis of a mixture of oil shale and polymeric wastes is also associated with this. Also, in semi-cokes of co-pyrolysis, the sulfur content increases by a factor of 1.6 – 1.8. which can cause problems during the after-burning of semi-coke in an industrial process.

The composition of the co-pyrolysis gas has also been studied. Table 21 shows the main components of the gas; other components contained in the gas in amounts of less than one volume percent is not shown.

Table 21. Main components and characteristics of gas.

Component, V/V%	EOS	EOS+PE-LD	EOS+PE-HD	EOS+PP	EOS+tires	EOS+mix
C6+	2.7	1.7	1.3	2.0	3.3	1.7
Hydrogen	4.7	5.9	4.4	1.8	10.9	5.3
Methane	10.5	13.7	15.2	8.1	15.4	13.6
Ethane	7.4	12.1	12.1	6.7	7.7	9.2
Ethylene	2.0	6.3	7.4	1.4	4.2	4.4
Propane	3.5	8.1	7.5	3.9	4.5	5.7
Carbon Dioxide	30.4	18.6	19.7	23.6	20.8	21.3
Propylene	3.6	9.8	10.2	18.8	3.9	11.2
n-Butane	1.8	3.7	2.9	0.8	1.9	1.8
Carbon Monoxide	9.9	8.0	7.5	7.6	6.8	7.3
Hydrogen Sulfide	17.6	5.8	6.1	7.6	12.1	7.4
Carbonyl Sulfide	1.9	0.2	0.2	0.4	1.9	0.3
Superior Heat Value, MJ/m ³	37.86	55.90	53.99	64.56	46.46	54.18
Inferior Heat Value, MJ/m ³	34.97	51.60	49.84	59.82	42.82	50.11
Density, kg/m ³	1.663	1.610	1.592	1.924	1.546	1.652

The data presented in Table 21 show that the content of sulfur compounds, such as hydrogen sulfide and carbonyl sulfide, in the semi-coke gas composition was significantly reduced. Moreover, the decrease in sulfur compounds was not consistent with the principles of additivity. The reduction of sulfur compounds in gas mixtures was as follows:

EOS + PE-LD: 69% less

EOS + PE-HD: 68% less

EOS + PP: 59% less

EOS + tires: 28% less

EOS + mix: 60% less

There was also a decrease in CO₂ content in semi-coke gas:

EOS + PE-LD: 39% less

EOS + PE-HD: 35% less

EOS + PP: 23% less

EOS + tires: 32% less

EOS + mix: 30% less

The caloric content of semi-coke gases increased significantly, especially in the gas of the EOS+PP mixture, due to the high content of polypropylene in the gas. In mixtures of EOS + PE-LD and EOS + PE-HD, the content increased due to an increase in the content of ethane, and it increased in a mixture of EOS + tires hydrogen.

3.8 Sulfur compounds balance

The sulfur content is one of the fuel quality indicators. When planning the parameters of the pyrolysis process, it is important to know the distribution of sulfur by products. To create a balance for the distribution of sulfur compounds, its contents in oil (Table 17), semi-coke and pyrolysis gas were determined.

Based on the data obtained, graphs of the distribution of sulfur by pyrolysis products were plotted. Since the yield of pyrogenetic water formed in the process was less than 1% for all mixtures except EOS + tires (1.6%), when calculating the balance, it was assumed that sulfur compounds in this product were equal to zero. When compiling the balance, the sulfur content in the gas was calculated from the difference $100 - \text{the mass of sulfur in oil} - \text{the mass of sulfur in semi-coke}$, since when calculating the mass content of sulfur in gas, the data obtained introduced a large error in the balance. This may have been due to the fact that when determining the yield of pyrolysis products, the gas yield was calculated as gas plus losses. Data on the distribution of sulfur by pyrolysis products are shown in Figure 25.

Sulfur compounds balance, m/m%

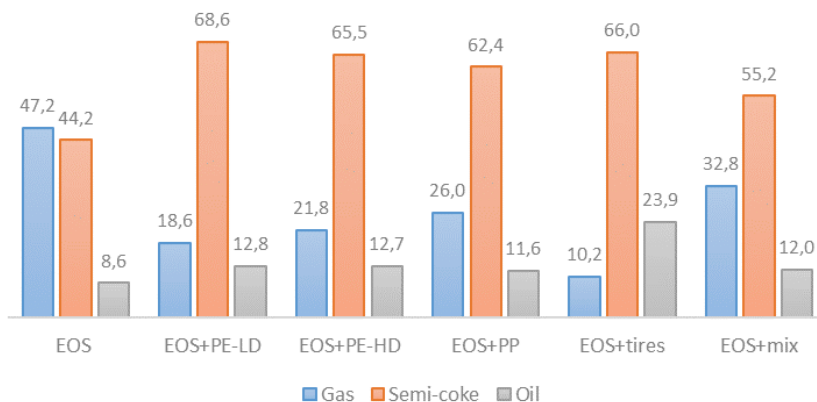


Figure 25. Distribution of sulfur by pyrolysis products.

From the data presented in the graph, it can be seen that during pyrolysis most of the sulfur was concentrated in semi-coke and gas. Thus, during co-pyrolysis with polymers, an increase in the sulfur content in semi-coke and a decrease in its content in gas were noticeable in comparison with the pyrolysis of oil shale. With co-pyrolysis, the amount of sulfur that passed into the oil also increased. Probably, during co-pyrolysis the sulfur molecules of oil shale in a vapor-gas mixture, with hydrocarbons of plastic, additionally formed sulfur compounds. The sulfur concentration in the oils of co-pyrolysis with polymers increased on average by 20% of the amount of sulfur concentrated in the oil of pyrolysis (per apparent organic content). During co-pyrolysis with tires, sulfur was also concentrated to a greater extent in semi-coke, although less of it passed into gas, and more into oil. A rather high percentage of the sulfur in the oil was due to the fact that part of the sulfur in the oil shale, as well as the sulfur contained in the tires, passed into the oil. During co-pyrolysis with a mixture of polymeric wastes, the distribution of sulfur over pyrolysis products was not the average value from all of the results of the co-pyrolysis of oil shale and each component of the mixture.

3.8.1 Sulfur compounds of the fraction up to 150 °C of oil obtained from tires and oil shale

Since car tires and oil shale have high sulfur contents, this also affects the quality of the oil obtained by pyrolysis [103]. In order to quantitatively and qualitatively study the sulfur compounds of the fraction up to 150 °C, oil was obtained from oil shale and tires by pyrolysis. The fraction was chosen for research because sulfur compounds are usually more concentrated in it. Details of how the oil was obtained and under what conditions the sulfur compounds were evaluated are shown in Publication II. The investigated fractions (boiling range fractions up to 150 °C) had the following characteristics, presented in Table 22.

Table 22. Characteristics of the fraction up to 150 °C of oil shale and tire pyrolysis oil.

Item	Method	Fraction up to 150 °C	
		Shale oil	Tire oil
Density at 15 °C, kg/m ³	EVS-EN ISO 12185	776.6	828.2
Total sulfur, S _t , m/m%	EVS-EN ISO 20846	1.04	0.62
Iodine number, gI ₂ /100 g	GOST 2070	107.7	98.5
Acid number, mg KOH/g	ISO 668	3.2	0.05

The fractions were very different from each other. The shale oil fraction contained twice as much sulfur. A high iodine level indicates the presence of a large number of double bonds in chemical compounds that are less stable and, as a result, a high content of oxidation products in the future.

Data on sulfur quantitative content in the fractions of shale oil and oil obtained from tires are presented in Table 23. The fractions were analyzed by gas chromatography.

Table 23. Sulfur quantitative content.

Sulfur compound, mg S/kg	Retention time, min.	Shale oil	Tires oil
Methyl mercaptan	3.74	24.19	14.95
Ethyl mercaptan	4.16	29.97	14.12
2-Propanethiol	4.63	13.11	-
Ethyl methyl sulfide	5,39	35.72	-
1-Methyl1-propanrthiol	6.26	157.53	-
Thiophene	6.35	236.22	145.48
1-Butanethiol	7.23	68.58	-
Dimethyl disulfide	7.98	-	534.29
2-Methylthiophene	8.62	1716.66	1566.00
3-Methylthiophene	8.80	147.60	262.82
1-Pentathiol	9.66	146.59	-
3-Ethylthiophene	11.17	694.53	215.47
Benzothiophene	18.05	-	13.02
∑ unidentified	8.35-19.87	7617	2766
∑ identified		3271	2607
Total gas chromatography method, m/m%		1.09	0.54

The chromatograms of sulfur compounds of the studied samples are presented in Figures 26 and 27.

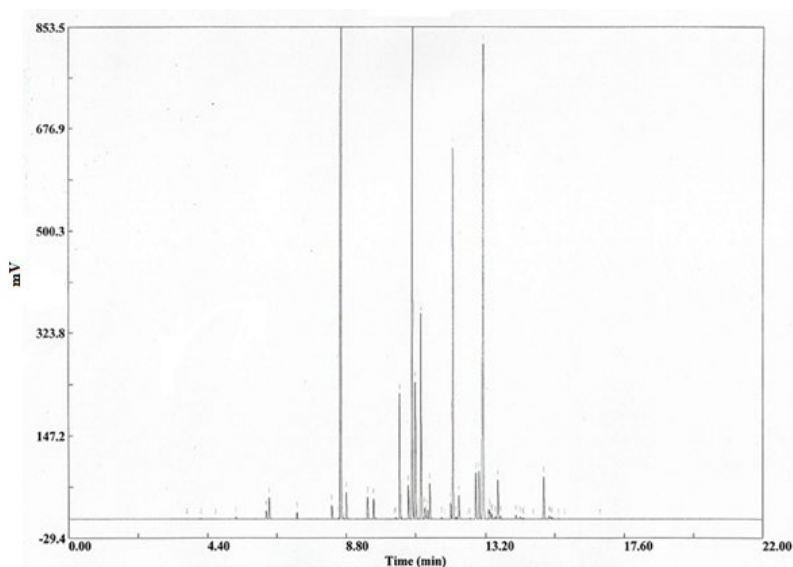


Figure 26. Chromatogram of the fraction of shale oil.

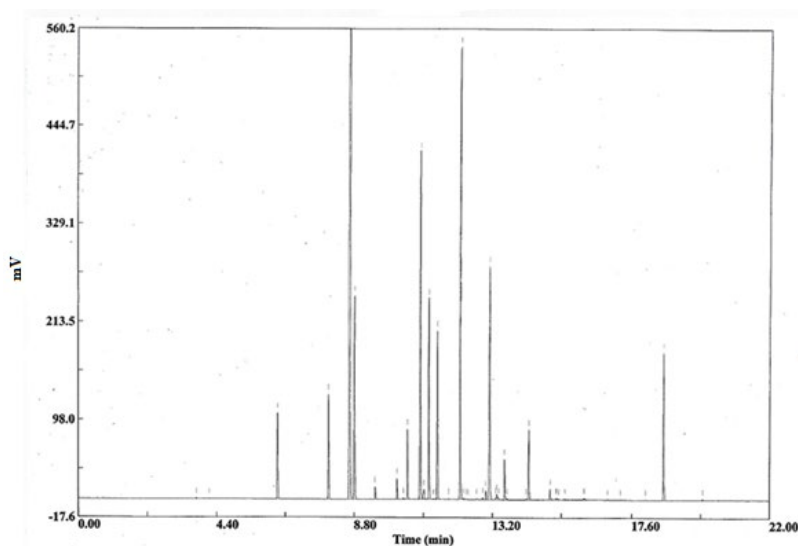


Figure 27. Chromatogram of the fraction obtained from used tires.

As can be seen in Figures 26 and 27, the sulfur compounds in the shale oil and tire fractions up to 150 °C were identical, since the retention time of unidentified compounds for both fractions was the same. Therefore, in the case of co-pyrolysis with oil shale, the addition of tires to the process does not adversely affect the quality of the resulting oil. Since the sulfur components present in gasoline fractions are very diverse, it is not possible to identify everything qualitatively, only quantitatively. The data on the content of total sulfur obtained by gas chromatography are in good agreement with the data presented in Table 22.

3.9 Composition of co-pyrolysis oils

Co-pyrolysis oils have been studied for component composition. Since shale oil is a multicomponent mixture, it can be assumed that when polymer wastes are added, the composition of the co-pyrolysis oil will be quite complex. To achieve more reliable results on the component composition, the obtained oil samples were previously divided into two fractions (a fraction up to 150 °C and a fraction above) by distillation at atmospheric pressure in accordance with the EVS-EN ISO 3405 standard [104]. The results for the yields of the fractions are presented in Table 24.

Table 24. Yields of the fractions co-pyrolysis oil.

Samples	Yields of fractions, v/v%	
	<150 °C	>150 °C
EOS	10.9	89.1
EOS + PE-LD	15.2	84.8
EOS + PE-HD	11.7	88.3
EOS + PP	24.3	75.7
EOS + tires	15.6	84.4
EOS + mix	16.7	83.1

From the data presented in Table 24, it can be seen that the addition of PP to oil shale significantly increased the yield of the gasoline fraction. The content of the <150 °C fraction in the co-pyrolysis oil in the sample increased by a factor of 2.2 (123%). In other mixtures, the amount of the <150 °C fraction increased by 39–53%. The exception was the oil shale with a PE-HD plastic mixture, where the gasoline fraction yield increased by only 7.3%, which may be due to the plastic molecular structure, which has a smaller number of branched side chains than PE-LD plastic. Probably side chains during pyrolysis can break away from the molecule and form a larger amount of low-boiling compounds.

Then each fraction was divided into groups of compounds using a classic separation technique, a column filled with silica gel in aliphatic, aromatics and oxygen-containing compounds. The division of the studied samples into groups of compounds in this way is not ideal. When dividing the gasoline fraction when eluting, aromatic olefinic hydrocarbons, cycloolefins, trienes, some dienes, sulfur- or nitrogen-containing compounds, or high-boiling oxygen-containing compounds can fall into the group of aromatic compounds. Therefore, each group of compounds was analyzed by MS-GC and, according to the results obtained, adjusted for the quantitative content of groups [105]. When dividing the fraction with a boiling point above 150 °C when eluting, condensed naphthenic aromatics, aromatic olefins, asphaltenes, sulfur, nitrogen, oxygenated aromatics and polar aromatic compounds can fall into the group of aromatic compounds. Therefore, the resulting groups were also additionally analyzed by MS-GC [106]. Data on the group composition of both fractions are presented in Table 25.

Table 25. Group composition.

Samples	Fraction <150 °C			Fraction > 150 °C				
	Group						Σ 100	
	aliphatic	aromatics	oxygen-containing	aliphatic	aromatics	oxygen-containing		
	per oil, m/m%							
EOS + PE-LD	11.6	3.4	0.2	53.6	15.2	16.0	Σ 100	
EOS + PE-HD	9.2	2.5	0.4	62.1	13.5	12.7	Σ 100	
EOS + PP	18.9	4.8	0.7	35.5	19.9	20.2	Σ 100	
EOS + tires	9.1	5.7	0.8	20.2	50.1	14.1	Σ 100	
EOS + mix	11.4	5.1	0.4	58.8	15.6	8.7	Σ 100	
	per fraction, m/m%							
EOS	70.7	20.3	9.0	Σ 100	20.0	32.0	48.0	Σ 100
EOS + PE-LD	76.3	22.4	1.3	Σ 100	63.2	17.9	18.9	Σ 100
EOS + PE-HD	76.0	20.7	3.3	Σ 100	70.3	15.3	14.4	Σ 100
EOS + PP	77.5	19.7	2.9	Σ 100	57.0	16.3	26.7	Σ 100
EOS + tires	58.3	36.5	5.1	Σ 100	23.9	59.4	16.7	Σ 100
EOS + mix	67.5	30.2	2.4	Σ 100	70.8	18.8	10.5	Σ 100

The data obtained by GC-MS were regrouped according to the groups of compounds (Table 25). Thus, in fractions up to 150 °C for samples of EOS + PE-HD, EOS + PE-LD and EOS + PP, in comparison with the oil shale fraction, the content of aliphatics increased, while the content of aromatics remained approximately at the same level. As plastics were added to the process, more aliphatic compounds were formed, since PE and PP mostly degrade into aliphatic compounds. Such a composition of the oil obtained by the co-pyrolysis of oil shale and plastics is also noted by other authors [107]. In sample of EOS + tires in the light fraction, the content of aliphatic compounds was lower and that of aromatics was higher than the oil shale fraction. The content of oxygen-containing compounds in all studied samples is significantly lower compared to the oil shale fraction. This decrease in oxygen-containing compounds is due to the fact that plastics do not contain oxygen in their composition. The sample EOS + mix was approximately the average of all the above samples in terms of its group composition.

Fractions with a boiling point above 150 °C were also distinguished by high levels of aliphatics, and lower levels of aromatics and oxygen-containing compounds. An exception was the EOS + tires sample, in which the content of aliphatics was practically at the same level as in the shale sample, and aromatics almost two times higher. Moreover, the high content of aromatic compounds formed during the co-pyrolysis of oil shale and tires did not affect the oil obtained by the pyrolysis of oil shale and a mixture of polymer wastes. A significant reduction in oxygen-containing compounds in the obtained liquid products of co-pyrolysis had a positive effect on the quality of the gasoline fraction and oil, increasing their stability.

As described above, the co-pyrolysis oils were divided into two fractions: up to 150 °C and above 150 °C. However, when analyzing the data obtained by MS-GC, the fraction with a boiling point below 150 °C contained aliphatic compounds with a boiling point

above 150 °C (C10–C13). This is explained by the fact that the fractionation of oils by simple atmospheric distillation is not ideal. In this case, there were no theoretical plates or adjustable reflux ratios, which would have allowed for a more accurate fractionation of the oils. For the same reason, the fraction with a boiling point above 150 °C contained aliphatics with boiling points below 150 °C (C7–C10).

The content of alkanes and alkenes C10–C13 (m/m %) in the fraction up to 150 °C was: sample OS + PE-LD – 9.7 %; OS + PE-HD – 10.7 %; OS + PP – 11.3 %; OS + Tires – 4.7 %; OS + mix – 10.6%. Table 26 shows the alkane/alkene composition of the aliphatic group of the light fraction.

Table 26. The aliphatic group of the fraction up to 150 °C.

Fraction,m/m%	Samples				
	EOS+PE-LD	EOS+PE-HD	EOS+PP	EOS+tires	EOS+mix
C4	-	-	0.36	0.74	0.81
C5	3.8	1.7	8.4	6.3	2.7
C6	19.0	16.4	15.8	20.5	13.3
C7	28.7	28.5	6.1	37.0	15.9
C8	16.9	20.5	7.3	17.5	20.3
C9	12.7	12.6	49.7	7.4	31.7
C10	9.2	9.6	1.0	6.0	4.7
C11	4.7	5.6	4.1	4.3	2.1
C12	2.9	3.0	4.1	0.4	7.0
C13	2.1	2.1	3.0	-	1.5

As seen from the table in the mixtures of OS + PE-LD and OS + PE-HD, the total content of alkanes/alkenes in the fraction less than 150 °C was almost identical. However, the OS + PE-LD mixture in total had a large amount of C4–C6. The highest amount of light alkanes/alkenes was found in the sample of OS + Tires. This sample had the highest content of fractions C6 and C7. The OS + PP sample was characterized by a high level of the C9 fraction. The total content of alkanes/alkenes up to C9 was maximal in the samples OS + Tires and OS + PP, and, as a result, in the sample OS + mix.

The content of alkanes and alkenes C7–C10 (m/m %) in the fraction above 150 °C was: sample OS + PE-LD – 1.8 %; OS + PE-HD – 3.1 %; OS + PP – 4.0 %; OS + Tires – 6.1 %; OS + mix – 4.8 %. Table 27 shows the alkane/alkene composition of the aliphatic group of the fraction with a boiling point above 150 °C.

Table 27. The aliphatic group of the fraction above 150 °C.

Fraction,m/m%	Samples				
	EOS+PE-LD	EOS+PE-HD	EOS+PP	EOS+tires	EOS+mix
C7	-	1.5	1.4	3.5	-
C8	-	-	-	4.2	-
C9	0.8	0.7	8.3	5.2	5.6
C10	2.5	2.8	1.8	18.0	2.5
C11	4.0	5.3	4.7	7.4	5.3
C12	4.8	4.9	41.8	6.3	9.4
C13	5.9	6.5	0.7	6.3	7.2
C14	6.3	5.7	6.5	3.1	8.3
C15	5.9	5.7	2.4	3.7	4.5
C16	6.1	6.0	2.5	12.0	4.6
C17	2.9	6.0	2.0	9.0	3.5
C18	3.2	6.5	2.9	2.3	2.7
C19	7.0	5.7	5.4	5.9	5.8
C20	8.9	6.4	8.6	3.7	8.4
>C20	41.8	36.2	11.0	9.5	32.5

As seen in Figure 27, in mixtures of OS + PE-LD and OS + PE-HD, the total content of alkanes/alkenes in this fraction was almost identical. In these samples, the content of the > C20 fraction was higher than in other samples. Sample OS + Tires contained C7 – > C20 in almost equal amounts (with the exception of C10). Sample OS + PP contained a high level of fraction C12 compared to other samples. The sample EOS + mix was approximately the average of all of the above samples in terms of its C7 – > C20 composition.

4. CONCLUSION

The goal of this thesis was to prepare a theoretical and practical basis for the co-pyrolysis of Estonian oil shale and polymer wastes. The product of co-processing of oil shale and polymer wastes is pyrolysis oil, which can be used in the chemical industry to produce new products. The advantage of the co-pyrolysis process is that some of the fossil fuel can be replaced with mixed and untreated polymer waste.

The novelty of the study is that the impact on the co-pyrolysis process of adding the various most common polymer wastes to Estonian oil shale, both for individual components and in mixtures, including car tires, was studied. Both the kinetics of co-pyrolysis and the properties of the resulting products, such as oil, oil fractions (fractions with a boiling point up to 150 °C and above 150 °C), co-pyrolysis gas and semi-coke, were studied. The effects of adding polymeric wastes on reducing emissions of CO₂ and sulfur compounds was also studied.

The conclusions of this study are as follows:

- The analysis of mixtures by TGA showed that during the co-pyrolysis of oil shale with plastics, the decomposition of the organic part of all mixtures shifted to a narrower temperature range, from 350 to 500 °C, and the decomposition of the mineral part occurred at lower temperatures. The exception was a mixture of oil shale with tires. In this case, when adding 50% polymer wastes to the industrial pyrolysis process, temperature changes had to be taken into account.
- The calculation of mass loss during heating according to the additivity principle for mixtures makes it possible to obtain data based on mathematical modeling of the co-pyrolysis process, and also makes it possible to take into account the features of this process when regulating the operation of industrial plants in real life conditions.
- The obtained data on the value of the activation energy indicates that when the pyrolysis temperature reaches 350 °C in mixtures of Estonian oil shale and polymer waste, reactions begin to take place, requiring almost twice as much energy in order for them to proceed. The exception is a mixture of oil shale with tires. In the case of the pyrolysis of such a mixture, the value of the activation energy decreases, which indicates a faster reaction of decomposition of the organic part of the mixture.
- According to the calculated data based on the results of the pyrolysis of individual components of the mixture by the additivity method, a synergistic effect occurred, in which the yield of liquid products increased by 14.6, 11.3 and 15.0% for PE-LD, PE-HD, PP, respectively, and the outputs of semi-coke and gas were lower than calculated for these plastics. The synergistic effect of the yield of liquid products was not observed in the co-pyrolysis of Estonian oil shale with tires.
- The liquid products obtained by co-pyrolysis were of significantly higher quality than shale oil. Co-pyrolysis oils have a lower density, and the sulfur content is reduced. The exception is the oil of co-pyrolysis with tires. Co-pyrolysis oils have a higher ratio of 100 H/C, except for the oil shale-tire mixture. However, it must be taken into account that during co-pyrolysis with PE-LD, PE-HD and PP, carried out at 520 °C, the resulting liquid products were very thick at room temperature, since part of the plastic oil is paraffin, which becomes liquid when heated to 45 °C.
- When polymer waste was added to oil shale, the reduction of sulfur content in liquid products did not follow the principles of additivity. The sulfur content was reduced by more than half. The sulfur balance showed that, during co-pyrolysis, more sulfur passed into semi-coke, and less into oil and gas than with oil shale pyrolysis. During co-pyrolysis

with tires, sulfur was also concentrated to a greater extent in semi-coke, although less of it passed into gas, and more into oil.

- An analysis of the gasoline fractions of the original high sulfur samples of oil shale and tires showed that the sulfur compounds in them were identical. Therefore, in the co-pyrolysis with oil shale, the addition of tires to the process did not adversely affect the quality of the resulting oil.
- In co-pyrolysis semi-cokes, the sulfur content increased by a factor of 1.6 – 1.8 compared with oil shale semi-coke, which can cause problems during the after-burning of semi-coke in an industrial process.
- The semi-coke gas of the co-pyrolysis of oil shale with polymeric wastes was characterized by high heating values. The addition of polymer wastes to the pyrolysis process can significantly reduce the content of sulfur compounds in semi-coke gas and CO₂ emissions, which is also important for the industrial process.
- The addition of plastic wastes (PE-LD, PP and tires) to oil shale significantly increased the yield of the fraction up to 150 °C. The exception was the oil shale with a PE-HD plastic mixture.
- The study of the group composition showed that when polymer waste was added to oil shale, it changed the amount of aromatics and oxygen-containing compounds in liquid pyrolysis products. The amount of aromatic compounds increased in fractions up to 150 °C, and decreased in fractions with a boiling point above 150 °C. In both fractions, there was a significant decrease in oxygen-containing compounds.
- The study of the composition of the aliphatic group of fractions with a boiling point below 150 °C and above showed that both fractions of the mixtures of EOS + PE-LD and EOS + PE-HD were almost identical in terms of the content of alkanes and alkenes. The EOS + PP mixture was distinguished by a high content of C₉ in the fraction up to 150 °C, and C₁₂ in the fraction above 150 °C. The EOS + Tires mixture differed from the other mixtures in its total high content of high-boiling compounds.

List of figures

Figure 1. Plastics demand by country in the European Union in 2020.	13
Figure 2. Distribution of plastics converters demand by segment in 2020.....	14
Figure 3. The demand for plastics by type.	14
Figure 4. A stronghold of European manufacturing.....	15
Figure 5. Life cycle of plastics.	16
Figure 6. Classification of plastics.	17
Figure 7. EU-28 plastic waste exports, 2002-2019.....	22
Figure 8. Global Revenues from Polymer Recycling by Process.....	24
Figure 9. Main pathway in the thermal degradation of polymer.....	27
Figure 10. Conditions for the selective production of waxes, BTX and light polyolefins by pyrolysis.....	29
Figure 11. FTIR spectra of Estonian oil shale.....	35
Figure 12. FTIR spectra of PE-HD, PE-LD, PP.	36
Figure 13. FTIR spectra of Estonian oil shale and tires.....	36
Figure 14. Processing of the obtained TG curve.	39
Figure 15. Curves of oil shale and polymer waste weight loss (heating to 950 °C).....	40
Figure 16. Curves of oil shale and polymer waste differential weight loss (heating to 950 °C).	40
Figure 17. Simple weight loss (TG) curve of the studied mixtures of Estonian oil shale with polymer wastes.....	42
Figure 18. Differential weight loss (DTG) curve of the studied mixtures Estonian oil shale and polymer wastes.	43
Figure 19. Calculated and experimental curves of weight loss (TG) for mixtures of Estonian oil shale with individual components and a mixture of polymer wastes.....	45
Figure 20. The Coats-Redfern integral method results for raw materials.	46
Figure 21. The Coats-Redfern integral method results for mixtures of Estonian oil shale with polymer wastes.....	46
Figure 22. Comparison of experimental and calculated data on the yield of co-pyrolysis products.....	50
Figure 23. Calculated by the additivity principle and the experimental results of the sulfur content in co-pyrolysis oils.	51
Figure 24. Co-pyrolysis oils FTIR spectra.....	52
Figure 25. Distribution of sulfur by pyrolysis products.....	55
Figure 26. Chromatogram of the fraction of shale oil.....	57
Figure 27. Chromatogram of the fraction obtained from used tires.	57

List of tables

Table 1. Chemical formulas of thermosetting and thermoplastic polymers.	19
Table 2. Typical materials used in tire manufacturing in Europe according to the percentage of the total weight.	21
Table 3. The main types of synthetic rubbers.	22
Table 4. Common definitions of polymer recycling.	23
Table 5. Main operation parameters for the pyrolysis process.	28
Table 6. Pyrolysis liquid product yield.....	28
Table 7. Dependence of the yield of liquid products of PP pyrolysis atmospheric pressure on temperature and insertion rate.	29
Table 8. Yield of pyrolysis products of polyolefins.	30
Table 9. Effect of temperature and reactor type on the yield of tire pyrolysis products. .	31
Table 10. Proximate and Ultimate analysis results.	34
Table 11. Metals content in the oil shale and oil shale ash.	35
Table 12. Yield of pyrolysis products.....	37
Table 13. The TGA parameters for Estonian oil shale and polymers.	41
Table 14. Thermal stability (T_{10} , T_{20} , T_{50}) of the studied polymers.....	42
Table 15. TGA parameters for mixtures of oil shales and polymer wastes.....	44
Table 16. The obtained characteristics of the kinetic parameters of the pyrolysis of the raw materials.	47
Table 17. The obtained characteristics of the kinetic parameters of the pyrolysis of the mixtures of polymer wastes and oil shale.	48
Table 18. The yield of co-pyrolysis products.....	49
Table 19. The elemental composition and relative density of oils.	51
Table 20. The elemental composition of semi-coke.	53
Table 21. Main components and characteristics of gas.	53
Table 22. Characteristics of the fraction up to 150 °C of oil shale and tire pyrolysis oil. .	56
Table 23. Sulfur quantitative content.	56
Table 24. Yields of the fractions co-pyrolysis oil.	58
Table 25. Group composition.....	59
Table 26. The aliphatic group of the fraction up to 150 °C.	60
Table 27. The aliphatic group of the fraction above 150 °C.....	61

References

- [1] Andres Siirde, Laenen Ben, Barbra Harvie, Mihkel Veiderma; A study on the EU oil shale industry – viewed in the light of the Estonian experience; A report by EASAC to the Committee on Industry, Research and Energy of the European Parliament, 2007
- [2] Survey of Energy Resources World Energy Council, 2010 [Online]. Available: <https://www.worldenergy.org> [Accessed: 25-Jun-2021]
- [3] World Energy Council, “World Energy Resources: 2016. [Online]. Available: <https://www.worldenergy.org/publications/entry/world-energy-resources-2016>. [Accessed: 12-Aug-2021]
- [4] Eesti põlevkivitööstuse aastaraamat 2022. [Online]. Available: <https://taltech.ee/polevkivi-kompetentsikeskus-aastaraamat>. [Accessed: 15-Aug-2021]
- [5] Strategy "Estonia 2035" , 12 mai 2021. [Online]. Available: <https://valitsus.ee/strateegia-eesti-2035-arengukavad-ja-planeering/strateegia/materjalid>. [Accessed: 24-Sept-2021]
- [6] DIRECTIVE (EU) 2018/851 OF THE EUROPEAN PARLIAMENT AND OF THE COUNCIL of 30 May 2018 amending Directive 2008/98/EC on waste. [Online]. Available: https://eur-lex.europa.eu/legal-content/EN/TXT/?uri=uriserv:OJ.L_.2018.150.01.0109.01.ENG [Accessed: 12-Aug-2021]
- [7] Harish Jeswani, Christian Krüger, Manfred Russ, Maike Horlacher, Florian Antony, Simon Hann, Adisa Azapagic; Life cycle environmental impacts of chemical recycling via pyrolysis of mixed plastic waste in comparison with mechanical recycling and energy recovery. *Science of The Total Environment*, Vol. 769, 144483, 2021
- [8] L. Tiikma, H. Luik, N. Pryadka, ‘Co-Pyrolysis Of Estonian Shales With Low-Density Polyethylene’, *Oil Shale*, Vol. 21 Issue 1, pp. 75–85, 2004
- [9] Tiikma, L.; Johannes, I.; Luik, H. Fixation of chlorine evolved in pyrolysis of PVC waste by Estonian oil shales. *Journal of Analytical and Applied Pyrolysis*, 75 (2), 205–210, 2006
- [10] N. E. Altun, C. Hiçyılmaz, J.-Y. Hwang, A. Suat bağcı, M. V. Kökoil „Oil shales in the world and turkey; reserves, current situation and future prospects: a review”; *Oil shale*, Vol. 23, No. 3, pp. 211–227, 2006
- [11] “Production of plastics worldwide from 1950 to 2019 (in million metric tons)”. [Online]. Available: <https://www.statista.com/statistics/282732/global-production-of-plastics-since-1950/>. [Accessed: 12-Aug-2020]
- [12] ‘Plastic - the Facts 2021’. [Online]. Available: <https://plasticseurope.org/knowledge-hub/plastics-the-facts-2021/>. [Accessed: 27-Nov-2021]
- [13] The European Tyre Industry Facts and Figures - 2020 Edition, [Online]. [Accessed: 12-Aug-2020]
- [14] ‘Europe – 91% of all End of Life Tyres collected and treated in 2018’. [Online]. Available: <https://www.etrma.org/library/europe-91-of-all-end-of-life-tyres-collected-and-treated-in-2018/>. [Accessed: 28-Det-2020]

- [15] Communication from the Commission to the European Parliament, the Council, the European Economic and Social Committee and the Committee of the Regions Closing the Loop—An EU Action Plan for the Circular Economy COM/2015/0614 Final. [Online]. Available: <https://eur-lex.europa.eu/legal-content/EN/TXT/?uri=CELEX%3A52015DC0614> (accessed 24-Jan-2022).
- [16] Directive 2000/53/EC of the European Parliament and of the Council of 18 September 2000 on End-of Life Vehicles—Commission Statements. [Online]. Available:<https://eur-lex.europa.eu/legal-content/EN/ALL/?uri=CELEX%3A32000L0053> [accessed 29-Det-2021]
- [17] The environmental impacts of plastics and micro-plastics use, waste and pollution: EU and national measures, Policy Department for Citizens' Rights and Constitutional Affairs, Directorate-General for Internal Policies PE 658.279 - October 2020. [Online]. Available:[https://www.europarl.europa.eu/thinktank/en/document/IPOL_STU\(2020\)658279](https://www.europarl.europa.eu/thinktank/en/document/IPOL_STU(2020)658279). [accessed 15-Det-2021]
- [18] An overview of chemical additives present in plastics: Migration, release, fate and environmental impact during their use, disposal and recycling, John N.Hahladakis, Roland Weber, Eleni Iacovidou, PhilPurnella, Journal of Hazardous Materials Volume 344, pp. 179–199, 2018
- [19] Giulia Cerminara, Raffaello Cossu; Waste Input to Landfills, Solid Waste Landfilling Concepts, Processes, Technologies, pp. 15–39, 2018
- [20] ISO 472:2013. Plastics — Vocabulary
- [21] Priit Kulu, Jakob Kübarsepp, Andres Laansoo, Renno Veinthal; MATERJALITEHNIKA I, Tehnomaterjalid, TTÜ, 2015
- [22] A.Demaid, V.Spedding, J.Zucker Classification of plastics materials, Artificial intelligence in engineering, Vol. 10, No. 1, pp. 9–20,1996
- [23] Vannessa Goodship; Plastic recycling, Science Progress, 90(4), pp. 245–268, 2007
- [24] Delilah Lithner; Environmental and Health Hazards of Chemicals in Plastic Polymers and Products, , Ph.D. thesis, 2011
- [25] Donald R. Askeland; Polymers, The Science and Engineering of Materials, pp. 488–548, 1996
- [26] Maciej Sienkiewicz, Justyna Kucinska-Lipka, Helena Janik, Adolf Balas; Progress in used tyres management in the European Union: A review, Waste Management, 32(10):1742–51, 2012
- [27] Б.А.Догодкин. Химия эластомеров. Издательство «Химия», Москва, Стр. 19-279, 1972
- [28] О.Б.Литвин. Основы технологии синтеза каучуков. Государственное научно-техническое издательство химической литературы. Москва. Стр. 11–21, 1959
- [29] Plastics, the circular economy and Europe’s environment — A priority for action, Luxembourg: Publications Office of the European Union, 2021. [Online]. Available: <https://www.eea.europa.eu/publications/plastics-the-circular-economy-and>. [accessed 08-Nov-2021]
- [30] Zongguo Wen, Yiling Xie, Muhan Chen & Christian Doh Dinga; China’s plastic import ban increases prospects of environmental impact mitigation of plastic waste trade flow worldwide, Nature Communications volume 12, Article number: 425, 2021

- [31] A European Strategy for Plastics in a Circular Economy. [Online]. Available COM/2018/028, <https://eur-lex.europa.eu/legal-content/EN/TXT/?uri=COM%3A2018%3A28%3AFIN>. [accessed 18-Nov-2021]
- [32] Zoé O. G. Schyns, Michael P Shaver; Mechanical Recycling of Packaging Plastics: A Review, *Macromolecular Rapid Communication*, 2000415, 2020
- [33] ASTM D7209-06 Standard Guide for Waste Reduction, Resource Recovery, and Use of Recycled Polymeric Materials and Products (Withdrawn 2015)
- [34] ISO 15270:2008 Plastics — Guidelines for the recovery and recycling of plastics waste
- [35] Polymer Recycling Technologies 2020-2030. End of life options for plastic waste: tools, trends and markets. [Online]. Available: <https://www.idtechex.com/en/research-report/polymer-recycling-technologies-2020-2030/760>. [accessed on 28-Feb-2021]
- [36] Javier Pose-Rodrigue, Dirk Marsitzky, Yann Ménière, Wibke Meiser; Patents for tomorrow's plastics Global innovation trends in recycling, circular design and alternative sources, European Patent Office, 2021, [Online]. Available <https://www.researchgate.net/publication/355466896>. [accessed on 30-Mai-2021]
- [37] Raju Francis *Recycling of Polymers: Methods, Characterization and Applications*, Publisher John Wiley & Sons, 2016
- [38] Kim Ragaert, Laurens Delva, Kevin Van Geem; Mechanical and chemical recycling of solid plastic waste, *Waste Management*, Vol. 69, pp. 24–58, 2017
- [39] Rinku Verma, K. S. Vinoda, M. Papireddy, A.N.S Gowda; Toxic Pollutants from Plastic Waste- A Review, *Procedia Environmental Sciences; International Conference on Solid Waste Management, 5IconSWM 2015*, Vol. 35, pp. 701–708, 2016
- [40] Wilson Uzochukwu Eze, Reginald Umunakwe, Henry Chinedu Obasi, Michael Ifeanyichukwu Ugbaja, Cosmas Chinedu Uche and Innocent Chimezie Madufor, *Plastics waste management: A review of pyrolysis technology*, *Claen Technology and Recycling*, 1(1): 50–69, 2021
- [41] Madalina Elena Grigore; *Methods of Recycling, Properties and Applications of Recycled Thermoplastic Polymers*, *Recycling*, 2017
- [42] Dr. Julia Vogel, Dr. Franziska Krüger, Matthias Fabian; *Chemical recycling, background*, German Environment Agency, 2020
- [43] Yi-Bo Zhao, Xu-Dong Lv, Hong-Gang Ni; Solvent-based separation and recycling of waste plastics: A review, *Chemosphere*, Vol. 209, pp. 707–720, 2018
- [44] Sanjana D. Gunasee, Bart Danon, Johann F. Görgens, Romeela Mohee; Copyrolysis of LDPE and cellulose: Synergies during devolatilization and condensation, *Journal of Analytical and Applied Pyrolysis*, Vol. 126, pp. 307–314, 2017
- [45] Natalia Yu. Kovaleva, Elena G. Raevskaya, and Alexander V. Roshchin; Plastic waste pyrolysis – a review; *CHEMICAL SAFETY SCIENCE*, 4, (1), pp. 48–79, 2020
- [46] Juan Baena-González, Arantzazu Santamaria-Echart, Juan Luis Aguirre, Sergio González, *Chemical recycling of plastic waste: Bitumen, solvents, and polystyrene from pyrolysis oil*, *Waste Management*, Vol. 118, pp. 139–149, 2020

- [47] Miriam Arabiourrutia, Gartzzen Lopez, Maite Artetxe, Jon Alvarez, Javier Bilbao, Martin Olazar; Waste tyre valorization by catalytic pyrolysis – A review; *Renewable and Sustainable Energy Reviews*, Vol. 129, 2020
- [48] Itsaso Barbarias, Aitor Arregi, Maite Artetxe, Laura Santamaria, Gartzzen Lopez, María Cortazar, Maider Amutio, Javier Bilbao and Martin Olazar; Recent Advances in Pyrolysis, 2020, [Online]. Available: <https://www.intechopen.com/chapters/66047>. [accessed on 05-Feb-2022]
- [49] Anandhu Vijayakumar, Jilse Sebastian; Pyrolysis process to produce fuel from different types of plastic – a review, *IOP Conf. Series: Materials Science and Engineering* 396, 2018
- [50] Jan Nisar, Muhammad Sufaid Khan, Munawar Iqbal, Afzal Shah, Ghulam Ali, Murtaza Sayed, Rafaqat Ali Khan, Faheem Shah, Tariq Mahmood; Thermal decomposition study of polyvinyl chloride in the presence of commercially available oxides catalysts, *Advances in Polymer Technology*, Vol. 37, Issue 6, pp. 2336–2343, 2018
- [51] Miranda R, Jin Y, Roy C, Vasile C; Vacuum pyrolysis of PVC kinetic study, *Polymer Degradation and Stability*, Vol. 64, pp. 127–44, 1998
- [52] Yihan Wang, Kai Wu, Qingyu Liu, Huiyan Zhang; Low chlorine oil production through fast pyrolysis of mixed plastics combined with hydrothermal dechlorination pretreatment, *Process Safety and Environmental Protection*, Vol. 149, pp. 105–114, 2021
- [53] Bidhya Kunwar, H.N.Cheng, Sriram R Chandrashekar, Brajendra K Sharma; Plastics to fuel: a review, *Renewable and Sustainable Energy Reviews*, Vol. 54, pp. 421–428, 2016
- [54] AliReza Rahimi, Jeannette M. García; Chemical recycling of waste plastics for new materials production, *Nature reviews. Chemistry*, Vol. 1 (6), 2017
- [55] Merve Sogancioglu, E. Yel; A Comparative Study on Waste Plastics Pyrolysis Liquid Products Quantity and Energy Recovery Potential, *Energy Procedia*, Vol. 118, pp. 221–226, 2017
- [56] Raoul Meys, Felicitas Frick, Stefan Westhues, Andre Sternberg, Jurgen Klankermayer, Andre Bardow; Towards a circular economy for plastic packaging wastes – the environmental potential of chemical recycling, *Resources Conservation & Recycling*, Vol. 162, 105010, 2020
- [57] R. Font, A. Fullana, J.A. Caballero, J. Candela, A. García; Pyrolysis study of polyurethane, *Journal of Analytical and Applied Pyrolysis*, 58–59, pp. 63–77, 2001
- [58] Zhitong Yao, Shaoqi Yu, Weiping Su, Weihong Wu, Junhong Tang and Wei Qi; Comparative study on the pyrolysis kinetics of polyurethane foam from waste refrigerators, *Waste Management & Research*, Vol. 38(3), pp. 271– 278, 2020
- [59] Xuebin Wang, Qiming Jin, Jiaye Zhang, Yan Li, Shuaishuai Li, Hrvoje Mikulčić, Milan Vujanović, Houzhang Tana, Neven Duić; Soot formation during polyurethane (PU) plastic pyrolysis: The effects of temperature and volatile residence time, *Energy Conversion and Management*, Vol. 164, pp. 353–362, 2018
- [60] Edited by Michiel De Smet and Mats Linder, *A circular economy for plastics – Insights from research and innovation to inform policy and funding decisions*, Belgium, pp. 147, 2019

- [61] Guoxun Yan, Xiaodong Jing, Hao Wen, and Shuguang Xiang, Thermal Cracking of Virgin and Waste Plastics of PP and LDPE in a Semibatch Reactor under Atmospheric Pressure, *Energy and Fuels*, Vol. 29, pp. 2289–2298, 2015
- [62] Rashid Miandad, Mohammad Rehan, Mohhamad A. Barakat, Asad S. Aburiazaiza, Hizbullah Khan, Iqbal M. I. Ismail, Jeya Dhavamani, Jabbar Gardy, Ali Hassanpour, Abdul-Sattar Nizami; Catalytic Pyrolysis of Plastic Waste: Moving Toward Pyrolysis Based Biorefineries, *Frontiers in Energy Research*, 2019, [Online]. Available: <https://doi.org/10.3389/fenrg.2019.00027>. [accessed 15-Nov-2021]
- [63] Almeida, D.; de Fatima Marques, M. Thermal and catalytic pyrolysis of plastic waste. *Polímeros*, Vol. 26, pp. 44–51, 2016
- [64] López, A.; de Marco, I.; Caballero, B.M.; Laresgoiti, M.F.; Adrados, A.; Aranzabal, A. Catalytic pyrolysis of plastic wastes with two different types of catalysts: ZSM-5 zeolite and Red Mud; *Applied Catalysis B: Environmental*, Vol. 104, pp. 211–219, 2011
- [65] Azubuike Francis Anene, Siw Bodil Fredriksen, Kai Arne Sætre, Lars-Andre Tokheim; Experimental Study of Thermal and Catalytic Pyrolysis of PlasticWaste Components, *Sustainability*, 3979, 2018
- [66] E. Butler, G. Devlin, K. McDonnell; Waste Polyolefins to Liquid Fuels via Pyrolysis: Review of Commercial State-of-the-Art and Recent Laboratory Research, *Waste and Biomass Valorization*, Vol. 2, pp. 227–255, 2011
- [67] Tariq Maqsood, Jinze Dai, Yaning Zhang, Mengmeng Guang, Bingxi Li; Pyrolysis of plastic species: A review of resources and products, *Journal of Analytical and Applied Pyrolysis*, Vol. 159, 105295, 2021
- [68] Gartzten Lopez, Maite Artetxe, Maider Amutio, Javier Bilbao, Martin Olazar; Thermochemical routes for the valorization of waste polyolefinic plastics to produce fuels and chemicals. A review, *Renewable and Sustainable Energy Reviews*, Vol. 73, pp. 346–386, 2017
- [69] Shafferina Dayana Anuar Sharuddin, Faisal Abnisa, Wan Mohd Ashri Wan Daud, Mohamed Kheireddine Aroua; A review on pyrolysis of plastic wastes, *Energy Conversion and Management*, Vol. 115, pp. 308–326, 2016
- [70] Jude A. Onwudili, Nagi Insura, Paul T. Williams; Composition of products from the pyrolysis of polyethylene and polystyrene in a closed batch reactor: Effects of temperature and residence time, *Journal of Analytical and Applied Pyrolysis*, Vol. 86, pp. 293–303, 2009
- [71] R.Miandad, M.A.Barakat, Asad S.Aburiazaiza, M.Rehan, I.M.I.Ismail, A.S.Nizami; Effect of plastic waste types on pyrolysis liquid oil, *International Biodeterioration & Biodegradation*, 2017
- [72] George Kofi Parku, François-Xavier Collard, Johann F. Görgens; Pyrolysis of waste polypropylene plastics for energy recovery: Influence of heating rate and vacuum conditions on composition of fuel product, *Fuel Processing Technology*, Vol. 209, 106522119, pp. 239–252, 2020
- [73] Min-Hwan Cho, Su-Hwa Jung, Joo-Sik Kim; Pyrolysis of Mixed Plastic Wastes for the Recovery of Benzene, Toluene, and Xylene (BTX) Aromatics in a Fluidized Bed and Chlorine Removal by Applying Various Additives, *Energy Fuels*, 24, 2, pp. 1389–1395, 2010

- [74] Azubuike Francis Anene, Siw Bodil Fredriksen, Kai Arne Sætre, Lars-Andre Tokheim; Experimental Study of Thermal and Catalytic Pyrolysis of Plastic Waste Components, *Sustainability*, 10(11):3979, 2018
- [75] Mohan Akhil, Dutta Saikat, Madav Vasudeva; Characterization and upgradation of crude tire pyrolysis oil (CTPO) obtained from a rotating autoclave reactor, *Fuel (Guildford)*, Vol. 250, pp. 339–351, 2019
- [76] Palos, Roberto, Rodríguez, Elena, Gutiérrez, Alazne, Bilbao, Javier, Arandes, José M; Kinetic modeling for the catalytic cracking of tires pyrolysis oil, *Fuel (Guildford)*, Vol. 309, p. 122055, 2022
- [77] Okoye Chiemeka Onyeka, Zhu Mingming, Jones Isabelle, Zhang Juan, Zhang Zhezi, Zhang Dongke; Preparation and characterization of carbon black (CB) using heavy residue fraction of spent tyre pyrolysis oil, *Journal of environmental chemical engineering*, Vol. 9 (6), p. 106561, 2021
- [78] Muelas Álvaro, Callén María Soledad, Murillo Ramón, Ballester Javier; Production and droplet combustion characteristics of waste tire pyrolysis oil, *Fuel processing technology*, Vol. 196, p. 106149, 2019
- [79] Karagöz Mustafa, Ağbulut Ümit, Sarıdemir Suat; Waste to energy: Production of waste tire pyrolysis oil and comprehensive analysis of its usability in diesel engines, *Fuel (Guildford)*, Vol. 275, p. 117844, 2020
- [80] L.Lombardi, E.Carnevale, A.Corti; A review of technologies and performances of thermal treatment systems for energy recovery from waste, *Waste Manag*, Vol. 37, pp. 26–44, 2015
- [81] Idoia Hita, Miriam Arabiourrutia, Martin Olazar, Javier Bilbao, José María Arandes, Pedro Castaño; Opportunities and barriers for producing high quality fuels from the pyrolysis of scrap tires, *Renewable and Sustainable Energy Reviews*, Vol. 56, pp. 745–759, 2016
- [82] S.T.Kumaravel, A.Murugesan, A.Kumaravel; Tyre pyrolysis oil as an alternative fuel for diesel engines – A review, *Renewable and Sustainable Energy Reviews*, Vol. 60, pp. 1678–1685, 2016
- [83] Mingshu Chi, Xiangcheng Xu, Da Cui, Hongxi Zhang, Qing Wang, A Tg-Ftir Investigation and Kinetic Analysis of Oil Shale Kerogen Pyrolysis Using the Distributed Activation Energy Model, *Oil Shale*, Vol. 33, No. 3, pp. 228–247, 2016
- [84] S.M. Al-Salema, P. Lettieri, J. Baeyens, Kinetics and product distribution of end of life tyres (ELTs) pyrolysis: A novel approach in polyisoprene and SBR thermal cracking, *Journal of Hazardous Materials*, Vol. 172, no. 2, pp. 1690–1694, 2009
- [85] Juliana P. Foltin, Guilherme N. Prado, Antonio C. L. Lisboa, Kinetic analysis of the oil shale pyrolysis using thermogravimetry and differential scanning calorimetry, *Chemical Engineering Transactions*, Vol. 61, pp. 559-564, 2017
- [86] Shabbar Syed, Rana Qudaihllham, Talabsam Janajreh, Kinetics of pyrolysis and combustion of oil shale sample from thermogravimetric data, *Fuel*, Vol. 90, no. 4, pp. 1631–1637, 2011
- [87] A. A. Koptelov, I. A. Koptelov, A. A. Rogozina, E. S. Yushkov, Potential of thermal analysis as applied to studying the kinetics of thermal degradation of polymers, *Russian Journal of Applied Chemistry*, Vol. 89, no. 9, pp. 1454–1460, 2016

- [88] Pankaj Tiwari, Milind Deo, Detailed kinetic analysis of oil shale pyrolysis TGA data, *AIChE Journal*, Vol. 58, no. 2, pp. 505–515, 2012
- [89] Birgit Maaten, Lauri Loo, Alar Konist, Dmitri Nešumajev, Tõnu Pihu, Indrek Külaots; Decomposition kinetics of American, Chinese and Estonian Oil Shales Kerogen, *Oil Shale*, Vol. 33, pp. 167–183, 2016
- [90] Gamzenur Özsin, Murat Kılıç, Esin Apaydin-Varol, Ayşe Eren Pütün, Ersan Pütün; A thermo- kinetic study on co-pyrolysis of oil shale and polyethylene terephthalate using TGA/FT-IR, *Korean Journal of Chemical Engineers*, Vol. 37, pp. 1888–1898, 2020
- [91] Rashid Miandad, Mohammad Rehan, Mohammad A. Barakat, Asad S. Aburizaiza, Hizbullah Khan, Iqbal M. I. Ismail, Jeya Dhavamani, Jabbar Gardy, Ali Hassanpour, Abdul-Sattar Nizami; Catalytic Pyrolysis of Plastic Waste: Moving Toward Pyrolysis Based Biorefineries, *Frontiers in Energy Research*, Vol. 7, Article 27, 2019
- [92] Markus Gall, Paul J. Freudenthaler, Joerg Fischer, Reinhold W. Lang; Characterization of Composition and Structure-Property Relationships of Commercial Post-Consumer Polyethylene and Polypropylene Recyclates, *Polymers*, 13, 1574, 2021
- [93] A. Aboulkas, K. El harfi, A. El bouadili, M. Benchanaa, A. Mokhlisse, A. Outzourit; Kinetics of co-pyrolysis of Tarfaya (Morocco) oil shale with high-density polyethylene, *Oil Shale*, Vol. 24, No. 1, pp. 15–33, 2007
- [94] Yunwu Zheng, Lei Tao, Xiaoqing Yang, Yuanbo Huang, Can Liu, Zhifeng Zheng; Study of the thermal behavior, kinetics, and product characterization of biomass and low-density polyethylene co-pyrolysis by thermogravimetric analysis and pyrolysis-GC/MS, *Journal of Analytical and Applied Pyrolysis*, Vol. 133, pp. 185–197, 2018
- [95] Limin Zhou, Taian Luo, Qunwu Huang; Co-pyrolysis characteristics and kinetics of coal and plastic blends, *Energy Conversion and Management*, Vol. 50, pp. 705–710, 2009
- [96] Yong Li, Jingui He, Yanhui LIU; Preparation of shale oil from copyrolysis of oil shale/plastics mixtures, *Advanced Materials Research*, Vol. 512–515, pp. 2162–2165, 2012
- [97] Pınar Acar Bozkurt; Nagehan Merve Kutlu, Muammer Canel; Co-Pyrolysis of Göynük Oil Shale with Polypropylene and Structural Characterization of Pyrolysis Liquid, *Journal of the Turkish Chemical Society*, Vol. 3, no. 3, pp. 247–264, 2016
- [98] M.Predel, W.Kaminsky; Fluidised bed pyrolysis of low density polyethylene to produce petrochemical feedstock, *Journal of Analytical and Applied Pyrolysis*, Vol. 51, Issues 1–2, pp. 107–126, 1999
- [99] M.Predel, W.Kaminsky; Pyrolysis of mixed polyolefins in a fluidised-bed reactor and on a pyro-GC/MS to yield aliphatic waxes, *Polymer Degradation and Stability*, Vol. 70, Issue 3, pp. 373–385, 2000
- [100] Balachandar Gopalakrishnan, Namita Khanna, Debabrata Das; Chapter 4 - Dark-Fermentative Biohydrogen Production, *Biohydrogen*, pp. 79–122, 2019
- [101] R.K. Singh, S. Mondal, Biswajit Rujb, A.K. Sadhukhan, P. Gupta; Interaction of three categories of tyre waste during co-pyrolysis: Effect on product yield and quality, *Journal of Analytical and Applied Pyrolysis*, Vol. 141, 2016

- [102] Pinar Acar Bozkurt, Onur Tosun, Muammer Canel; The synergistic effect of co-pyrolysis of oil shale and low density polyethylene mixtures and characterization of pyrolysis liquid, *Journal of the Energy Institute*, Vol. 90, pp. 355–362, 2017
- [103] Hao Wang, Hongyun Hu, Yuhan Yang, Huan Liuay, HuaTang, Sihua Xu, Aijun Li, Hong Yao; Effect of high heating rates on products distribution and sulfur transformation during the pyrolysis of waste tires, *Waste Management*, Vol. 118, pp. 9–17, 2020
- [104] EVS-EN ISO 3405:2019 - Petroleum and related products from natural or synthetic sources - Determination of distillation characteristics at atmospheric pressure
- [105] EVS-EN 15553:2007 - Petroleum products and related materials - Determination of hydrocarbon types - Fluorescent indicator adsorption method
- [106] Method of determining the content of aromatic constituents in products with a distillation end point exceeding 315 °C. European Commission. Explanatory notes to the Combined Nomenclature of the European Union. Official Journal of the European Union, C 119, 29 (OJ 2019/C 119/146), 2019
- [107] A. Aboulkas, T. Makayssi, L. Bilali, K. El harfi, M. Nadifiyine, M. Benchanaa; Co-pyrolysis of oil shale and High density polyethylene: Structural characterization of the oil, *Fuel Processing Technology*, Vol. 96, pp. 203–208, 2012
- [108] Hang Jia, Haoxi Ben, Ying Luo, Rui Wang; Catalytic Fast Pyrolysis of Poly (Ethylene Terephthalate) (PET) with Zeolite and Nickel Chloride, *Polymers (Basel)*, 12(3): 705, 2020

List of other publications

1. M. Y. Nazarenko, S. N. Saltykova, V. A. Rudko, **O. Pihl**; Production of Isotropic Coke from Shale Tar at Various Parameters of the Delayed Coking Process. *ACS Omega*, Vol. 6 (34), pp. 22173–22179, 2021
2. B. Maaten, O. Järvik, **O. Pihl**, A. Konist, A. Siirde; Oil shale pyrolysis products and the fate of sulfur. *Oil Shale*, Vol. 37 (1), pp. 51–69, 2020
3. **O. A Pihl**, Yu. Kh. Soone, L. V Kekisheva, M. A. Kaev; Tire processing using pyrolysis and hydrogenation methods. *Solid Fuel Chemistry*, Vol. 47 (3), pp. 183–192, 2013

Acknowledgments

I am grateful to my supervisor and co-supervisor for their help and support in defending this doctoral thesis. I would like to express my deep gratitude to all of the staff of the Laboratory of Fuels Technology for their help in the analysis of samples, data processing and the valuable advice that I received. I am also grateful to the staff of the Oil Shale Competence Center.

Special thanks to my family for their support, especially to my beloved daughter, sister and husband.

I gratefully acknowledge the partial financial support from the European Regional Development Fund and the project “Increasing the value of oil shale (products) and expanding the scope of activities of the Oil Shale Competence Center” (2014-2020.5.04.19-0376).

Abstract

Co-pyrolysis of Estonian oil shale with polymer wastes

Every year, millions of tons of polymer waste around the world remains unrecycled. One of the possible ways to dispose of this waste is chemical processing, for example by pyrolysis. Pyrolysis oil can be used to create new products. In accordance with the EU Green Deal, Estonia is aiming for zero carbon emissions by 2050. The main source of CO₂ in Estonia is oil shale processing, mostly from the direct burning of oil shale, but a significant part comes from the pyrolysis process. Therefore, there are currently plans to shut down oil shale processing by 2040. Before 2040, it is necessary to gradually reduce CO₂ emissions, and one way to move to zero emissions may be the co-pyrolysis of oil shale and polymer waste.

The goal of this thesis was to study the theoretical and practical basis of the co-pyrolysis of Estonian oil shale and polymer waste using modern research methods of analysis. For this study, the most used plastics (PP, PE-HD and PE-LD) and used car tires were selected.

The novelty of the study lies in examining the impact of adding various common polymer waste materials to Estonian oil shale, both as individual components and as mixtures, including car tires, on the co-pyrolysis process. Both the kinetics of co-pyrolysis and the properties of the resulting products, such as oil, oil fractions (fractions with a boiling point up to 150 °C and above 150 °C), co-pyrolysis gas and semi-coke, were studied. The effects of adding polymeric wastes on reducing emissions of CO₂ and sulfur compounds in co-pyrolysis gas were studied.

For the studies, mixtures of oil shale and plastic PE-LD (50/50), oil shale and a mixture of the polymers PE-LD, PE-HD, PP and tires (50/50) and oil shale and tires (50/50) were prepared. Using the thermogravimetric method of analysis, the process of mass loss of each sample separately and mixtures of samples upon heating in an inert environment were studied. The contribution of each component to the co-pyrolysis process was considered. It has been shown that when determining the mass loss during the heating of mixtures, additive properties appeared. Based on the thermogravimetric data on the mass loss of individual components, it is possible to calculate the mass loss of a mixture of oil shale and polymer waste in various ratios. On the basis of the experimental data, a synergistic effect was observed during co-pyrolysis, which was expressed by an increase in the yield of liquid products compared to the calculated data. The kinetic parameters were calculated by the Coates-Redfern method; it was determined that during the pyrolysis of mixtures of oil shale with polymeric waste, more energy had to be expended to decompose the mixtures than in the pyrolysis of oil shale.

According to the data obtained by co-pyrolysis, it was shown that the addition of polymer wastes improves the quality of liquid products, and sulfur is distributed among the pyrolysis products differently than in oil shale pyrolysis. Fractions with a boiling point of up to 150 °C and above were studied. The yield of the up to 150 °C fraction significantly increased, and the addition of polymer wastes changed the group composition of both fractions. To study the group composition, column chromatography on silica gel to separate the fractions and a GC-MS analyzer were used.

Lühikokkuvõte

Eesti põlevkivi ja polümeerjätmete koospürolüüs

Igal aastal jääb miljoneid tonne polümeerjätmeid üle maailma ringlusse võtmata. Üks võimalik viis nende jäätmete kõrvaldamiseks on keemiline töötlemine, näiteks pürolüüs. Sel viisil saadud pürolüüsiõli saab kasutada uute toodete saamiseks. EL-i rohelise kokkuleppe valguses on Eesti eesmärgiks saavutada 2050. aastaks null süsinikuheide. Põhiline CO₂ voog Eestis tuleb põlevkivi ümbertöötlemisest. Suurem osa põlevkivi otsepõletamisest, kuid osa pürolüüsi protsessist, mistõttu on täna plaanis põlevkivi ümbertöötlemine 2040. aastaks lõpetada. Aastani 2040 on vaja järk-järgult vähendada CO₂ emissiooni ning üheks võimaluseks nullheitele liikumiseks võiks olla põlevkivi ja polümeerjätmete koospürolüüs.

Käesoleva töö eesmärgiks oli uurida Eesti põlevkivi ja polümeerjätmete koospürolüüsi teoreetilisi ja praktilisi aluseid kasutades kaasaegseid uurimismeetodeid analüüsimiseks. Uuringuks valiti polümeerjätmed – enim kasutatud plastid (PP, PE-HD ja PE-LD) ja kasutatud autorehvid.

Uuringu uudsus seisneb selles, et mõju koospürolüüsi protsessile uuriti erinevate enamlevinud polümeerjätmete lisamisega Eesti põlevkivile nii üksikute komponentidena kui ka seguna (sh autorehvid). Põhjalikult uuriti nii koospürolüüsi protsessi kui ka sellest tekkivaidprodukte nagu õli, õlifraktsioonid (fraktsioonid keemistemperatuuriga kuni 150 °C ja üle 150 °C) ja poolkoks. Uuriti polümeerjätmete lisamise mõju CO₂ ja väävlühendite emissiooni vähenemisele.

Katsete jaoks valmistati viis segu: põlevkivi ja plast PE-LD (50/50), põlevkivi ja plast PE-HD (50/50), põlevkivi ja plast PP (50/50), põlevkivi ja polümeerid PE-LD, PE-HD, PP, rehvid (50/50) ning põlevkivi ja rehvid (50/50). Termogravimeetrilise analüüsimeetodi abil uuriti iga proovi eraldi ja proovide segu massikadu kuumutamisel inertses keskkonnas. Uuriti iga komponendi panust koospürolüüsi protsessi. Näidati, et massikao määramisel segude kuumutamisel ilmnevad aditiivsed omadused. Üksikute komponentide massikao termogravimeetriliste andmete põhjal on võimalik arvutada põlevkivi ja polümeerjätmete erinevates vahekordades segu massikadu. Katseandmete põhjal leiti, et koospürolüüsi käigus täheldatakse sünergilist efekti, mis väljendub vedelate toodete saagise suurenemises võrreldes arvutuslike andmetega.

Kineetilised parameetrid arvutati Coates-Redferni meetodil. Tehti kindlaks, et põlevkivi ja polümeerjätmete segude pürolüüsil tuleb segude lagundamisele kulutada rohkem energiat võrreldes põlevkivi pürolüüsiga.

Koospürolüüsi meetodil saadud andmete põhjal näidati, et polümeerjätmete lisamine parandab oluliselt vedelate toodete kvaliteeti, väävel jaotub pürolüüsi saaduste vahel teisiti kui põlevkivi pürolüüsil. Uuriti õlifraktsioone, mille keemistemperatuur on kuni 150 °C ja üle selle. Näidati, et tõuseb fraktsiooni kuni 150 °C saagis. Samuti näidati, et polümeerjätmete lisamine muudab mõlema fraktsiooni rühmakoostist. Rühmakoostise uurimiseks kasutati kolonnkromatograafiat, kus adsorbendiks oli silikageel ja saadud fraktsioonide komponendid määrati GC-MS analüsaatoriga.

Appendix 1

PUBLICATION I

O. Pihl, M. Tsepelevitsh, M. Burko, A. Siirde; Applying the correction for undecomposed carbonates to gross calorific values of oil shales from different deposits, *Oil Shale*, 36 (2), pp. 250–256, 2019

APPLYING THE CORRECTION FOR UNDECOMPOSED CARBONATES TO GROSS CALORIFIC VALUES OF OIL SHALES FROM DIFFERENT DEPOSITS

OLGA PIHL^{(a)*}, MARIA TSHEPELEVITSH^(a),
MARIA BURKO^(b), ANDRES SIIRDE^(c)

- ^(a) Oil Shale Competence Centre, TalTech Virumaa College, School of Engineering, Tallinn University of Technology, Ehitajate tee 5, 19086 Tallinn, Estonia
^(b) Virumaa College, School of Engineering, Tallinn University of Technology, Ehitajate tee 5, 19086 Tallinn, Estonia
^(c) School of Engineering, Department of Energy Technology, Tallinn University of Technology, Ehitajate tee 5, 19086 Tallinn, Estonia

Abstract. *The relationship between the carbon dioxide content of carbonates in the bomb calorimeter combustion residues and that in the corresponding oil shale samples originated from different deposits was investigated. As a result, a criterion for applying a correction for undecomposed carbonates to gross calorific value was established. A suitable standard method for determination of gross calorific value of oil shale samples was also suggested.*

Keywords: *gross calorific value, carbonates in oil shale, carbon dioxide, calorimetric bomb.*

1. Introduction

Calorific value is the most important quality characteristic of fuel. The influence of the composition of mineral matter on the calorific value of low-calorific fuels, e.g. oil shales and lignites, has been widely investigated [1–9]. For instance, Jaber et al. [7] reported that in case of Jordan oil shale, the calcium carbonate content has some influence on its gross calorific value. Such influence was quantitatively evaluated for Israel lignite in which the relatively high CaCO₃ content decreases the calorific value of the fuel due to endothermic decarbonisation. When the sum of ash and carbon dioxide contents was plotted against the sum of high calorific value

* Corresponding author: e-mail olga.pihl@taltech.ee

and decarbonisation heat consumption, a good linear relationship was observed [8].

Warne and Dubrawski [9] addressed the possibilities of calculating corrections to the gross calorific values using the differential thermal analysis (DTA) method.

There are some national and international standards covering the determination of calorific value of coals and cokes [10–13]. Oil shale has not been included in the scope of these standards.

GOST 147-95 covers the analysis of coals, peat and oil shale and takes the specificities of oil shale analysis into account [14]. The presence of undecomposed carbonates in the bomb combustion residue requires applying the corresponding correction to the gross calorific value. According to the standard, such correction is required for calorific values below 5.440 MJ/kg. However, the standard only concerns oil shales from the Baltic deposit and the Volga deposit.

The aim of this work was to determine a criterion for applying the correction to gross calorific value for undecomposed carbonates that would be applicable to oil shales from different deposits.

2. Experimental

2.1. Selection of samples

More than 1000 oil shale samples from different deposits were analysed by our research group in the course of previous investigations. About 50 samples were chosen for the present research based on their carbon dioxide content of carbonates, $(\text{CO}_2)_M$, and calorific values by bomb, Q_b^\dagger . The data on oil shale samples from the Baltic deposit obtained in our previous studies along with the data from literature [15] were plotted in Figure 1 to estimate the value of carbon dioxide content which corresponded to the calorific value of 5.440 MJ/kg.

As seen from Figure 1, there is a clear linear dependence between the carbon dioxide content of carbonates and the calorific value in case of oil shale samples from the Baltic deposit (the squared value of the correlation coefficient is 0.9256). It can be explained by the fact that the mineral matter composition of Baltic oil shale samples is rather constant. The plot indicates that for the Baltic oil shale with a calorific value of 5.440 MJ/kg the carbon dioxide content of carbonates is about 25% by mass.

Based on these values, the samples were selected so that each of the following groups would be represented: $Q_b \geq 5.4$ MJ/kg and $(\text{CO}_2)_M \geq 25\%$; $Q_b \geq 5.4$ MJ/kg and $(\text{CO}_2)_M \leq 25\%$; $Q_b \leq 5.4$ MJ/kg and $(\text{CO}_2)_M \geq 25\%$; $Q_b \leq 5.4$ MJ/kg and $(\text{CO}_2)_M \leq 25\%$. Figure 2 illustrates this selection further.

[†] Calorific value by bomb, Q_b , is the heat of combustion in the calorimetric bomb not corrected to acid formation and carbonates decomposition.

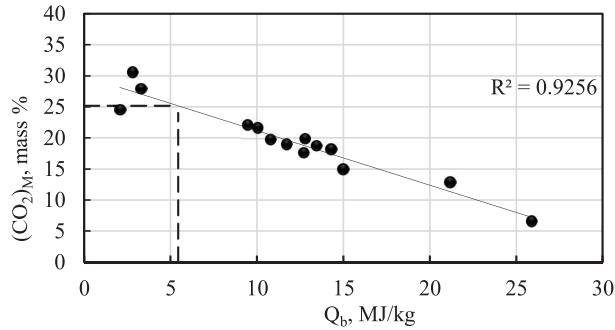


Fig. 1. Data on oil shale samples from the Baltic deposit.

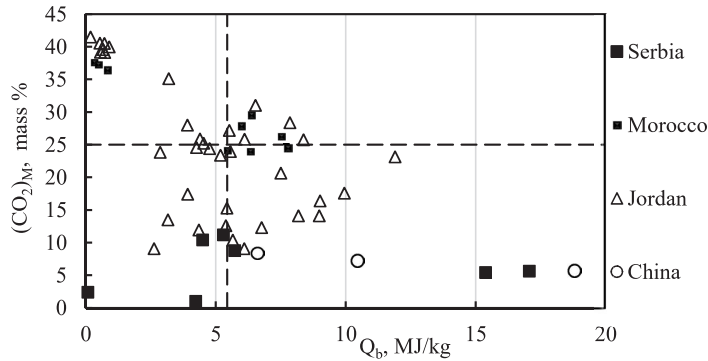


Fig. 2. Characteristics of oil shale samples from different deposits taken for the study.

Thus, the samples from Jordan, Moroccan, Serbian and Chinese oil shales with $(CO_2)_M$ in the range of 1.0–41.5% by mass and Q_b between 0.079 and 25.900 MJ/kg were selected for this study.

2.2. Determination of the carbon dioxide content of undecomposed carbonates

The studied samples were combusted in the Parr 6300 calorimetric bomb. The mass of the weighted portion was 1.0–1.2 g. To fulfil the requirements of the standard methods a benzoic acid of qualification "for calorimetry" was added to the weighted portions of low-calorific oil shale samples to provide the temperature rise equal to that during calorimeter calibration. After combustion, the residues were transferred into weighing vessels and dried completely in a drying oven at 160 °C.

The determination of the carbon dioxide content of carbonates in the residues was carried out using a Vario Macro Cube SoliTIC module device. The test portions were acidified and heated to 50 °C. The amount of released carbon dioxide was quantified by a thermal conductivity detector. The obtained values ranged from 0.06 to 27% by mass.

3. Results and discussion

The relationship between the carbon dioxide content of carbonates present in the residue and the calorific value by the bomb was investigated. It can be seen from Figure 3 that there is a general reverse dependence between the calorific value and the amount of undecomposed carbonates in the residue. However, this correlation is not significant.

It is not possible to determine the degree of influence of the calorific value on the content of undecomposed carbonates in the residue since benzoic acid is added to the samples during analysis.

The dependence between the carbon dioxide content of carbonates in the residue and the carbon dioxide content of carbonates in oil shale is illustrated in Figure 4.

Figure 4 shows that the data points form two distinct groups based on their $(\text{CO}_2)_M$ value in oil shale. As the figure reveals, for oil shale samples with the carbon dioxide content of carbonates less than 23% mass, the latter has almost no influence on the content of undecomposed carbonates in the residue. On the other hand, for samples with the $(\text{CO}_2)_M$ mass percentage exceeding 23, this influence is significant and a linear correlation between the two parameters is observed. The R-squared value is 0.9654.

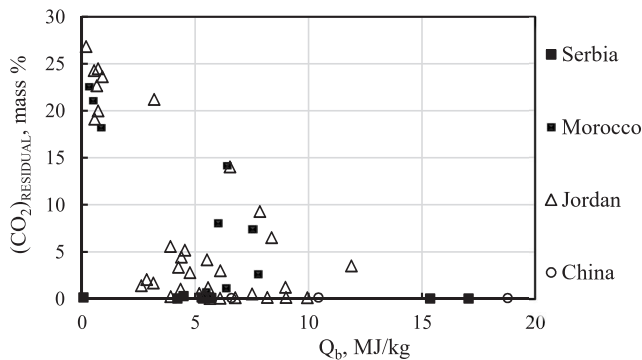


Fig. 3. The relationship between the carbon dioxide content of carbonates in the residue and the calorific value by the bomb.

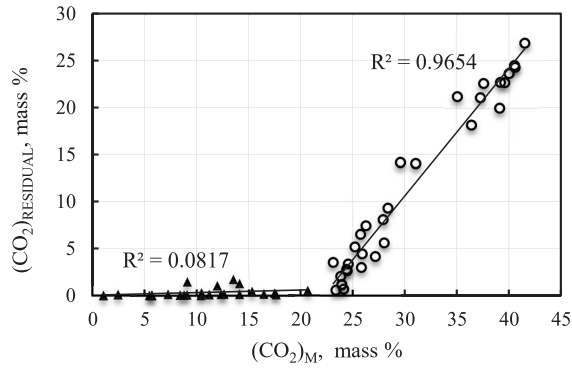


Fig. 4. The dependence of the carbon dioxide content of carbonates in the residue on the carbon dioxide content of carbonates in oil shale.

The obtained values of the carbon dioxide content of carbonates in the residue were recalculated as a mass percentage of the original oil shale sample, taking the yield of residue into account, for further calculations of correction to the gross calorific value.

To calculate the corrections to gross calorific value, the carbon dioxide content of carbonates in the residue, expressed as a mass percentage of the original oil shale sample, was multiplied by the constant ε . This constant takes into account the heat of the decomposition of carbonates and is equal to 40 kJ/kg per 1% of the CO_2 of carbonates. The obtained values are shown in Figure 5.

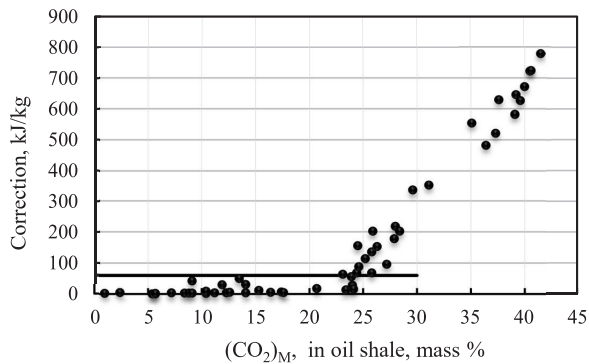


Fig. 5. The dependence of corrections to gross calorific value on the carbon dioxide content of carbonates in oil shale.

As can be seen from Figure 5, in case of oil shale samples with the carbon dioxide content of carbonates greater than 23% on mass basis, the value of the correction to the gross calorific value is higher than 60 kJ/kg, which is half the limit of the repeatability of the standard methods and therefore cannot be disregarded. As is clear from the figure, the correction to gross calorific value can reach 800 kJ/kg for some oil shales.

It should be noted that for Estonian oil shale, the correction needs to be applied only to samples with a calorific value lower than 5.440 MJ/kg since they contain more than 23% mass of the carbon dioxide of carbonates. This calorific value cannot be used as a criterion for oil shales from other deposits.

The results of this research were used when adapting ISO 1928-2009 as an Estonian national standard (EVS-ISO 1928-2016) [16].

4. Conclusions

A correction to gross calorific value for undecomposed carbonates is required for oil shales that contain more than 23% mass of the carbon dioxide of carbonates.

Currently both standard methods, ISO 1928-2009 and EVS-ISO 1928-2016, are valid. However, when dealing with solid fuels such as oil shale, it is more appropriate to use EVS-ISO 1928-2016 rather than ISO 1928-2009 because the requirements taking the specificities of oil shale analysis into consideration were included in this standard.

Since the net calorific value is calculated via gross calorific value, the correction to undecomposed carbonates will also have an influence on the net calorific value.

REFERENCES

1. Aints, M., Paris, P., Tufail, I., Jõgi, I., Aosaar, H., Riisalu, H., Laan, M. Determination of the calorific value and moisture content of crushed oil shale by LIBS. *Oil Shale*, 2018, **35**(4), 339–355.
2. Campbell, J. H. *The Kinetics of Decomposition of Colorado Oil Shale II. Carbonate Minerals*. Lawrence Livermore National Laboratory, Report UCRL-52089 Part 2, 1978.
3. *Impact of Mineral Impurities in Solid Fuel Combustion* (Gupta, R., Wall, T., Baxter, L., eds.). Papers presented at the Engineering Foundation Conference on Mineral Matter in Fuels, held November 2–7, 1997, in Kona, Hawaii. Kluwer Academic/Plenum, New York [etc.], 1999.
4. Plamus, K. *The Impact of Oil Shale Calorific Value on CFB Boiler Thermal Efficiency and Environment*. PhD Thesis, Tallinn University of Technology, 2012.
5. Zhang, H., Zhou, M., Wang, C., Sun, M., Li, M., Wei, X. Influence of mineral matters on the calorific value of an anthracite under oxygen bomb conditions. *Energ. Fuel.*, 2004, **18**(6), 1883–1887.

6. Sato, S., Enomoto, M. Development of new estimation method for CO₂ evolved from oil shale. *Fuel Process. Technol.*, 1997, **53**(1–2), 41–47.
7. Jaber, J. O., Amri, A., Ibrahim, K. Experimental investigation of effects of oil shale composition on its calorific value and oil yield. *Int. J. Oil Gas Coal T.*, 2011, **4**(4), 307–321.
8. Kafri, U., Gersh, S., Dosoretz, C. Corrections to calorific values of lignites of the Hula Basin, Israel, for contained CaCO₃. *Fuel*, 1980, **59**(11), 787–789.
9. Warne, S. S. J., Dubrawski, J. V. Potential for coal calorific value corrections, dependent on the carbonate mineral type present. *J. Therm. Analysis*, 1988, **33**(2), 435–440.
10. ASTM D5865-13. *Standard Test Method for Gross Calorific Value of Coal and Coke*. ASTM International, West Conshohocken, PA, 2013.
11. JIS M 8814 (2003). *Coal and coke - Determination of gross calorific value by the bomb calorimetric method, and calculation of net calorific value*, 2003.
12. DIN 51900-2:2003. *Testing of solid and liquid fuels - Determination of the gross calorific value by the bomb calorimeter and calculation of the net calorific value - Part 2: Method using isoperibol or static, jacket calorimeter*, 2003.
13. ISO 1928:2009. *Solid mineral fuels – Determination of gross calorific value by the bomb calorimetric method and calculation of net calorific value*.
14. GOST 147-95. *Solid mineral fuel. Determination of the highest combustion heat and calculation of the lowest combustion heat* (in Russian).
15. Yefimov, V. M., Purre, T. A., Rappu, L. I. The characteristics of oil shale as a technological raw material. *Chemistry and Technology of Oil Shales*, 1973, **19**, 7–15 (in Russian).
16. EVS-ISO 1928-2016. *Solid mineral fuels. Determination of gross calorific value by the bomb calorimetric method and calculation of net calorific value* (ISO 1928:2009, modified) (in Estonian).

Received January 18, 2019

Appendix 2

PUBLICATION II

O. Pihl, A. Niidu, N. Merkulova, M. Fomitsov, A. Siirde, M. Tshepelevitsh; Gas-chromatographic determination of sulfur compounds in the gasoline fractions of shale oil and oil obtained from used tires, *Oil Shale*, 36 (2), pp. 188–196, 2019

GAS-CHROMATOGRAPHIC DETERMINATION OF SULFUR COMPOUNDS IN THE GASOLINE FRACTIONS OF SHALE OIL AND OIL OBTAINED FROM USED TIRES

OLGA PIHL^{(a)*}, ALLAN NIIDU^(b), NADEZDA MERKULOVA^(a), MIHHAIL FOMITSOV^(a), ANDRES SIIRDE^(c), MARIA TSHEPELEVITSH^(a)

- ^(a) Oil Shale Competence Centre, TalTech Virumaa College, School of Engineering, Tallinn University of Technology, Ehitajate tee 5, 19086 Tallinn, Estonia
^(b) School of Science, Department of Chemistry and Biotechnology, Division of Chemistry, Tallinn University of Technology, Ehitajate tee 5, 19086 Tallinn, Estonia
^(c) School of Engineering, Department of Energy Technology, Tallinn University of Technology, Ehitajate tee 5, 19086 Tallinn, Estonia

Abstract. *The sulfur compounds content of the gasoline fractions of shale oil and oil obtained from used tires was investigated by the method of gas chromatography (GC). There was a marked difference in quantitative chromatograms estimation between the normalization method and the internal standardization method. The application of the internal standardization method proved to be preferable. In addition, the results obtained on the content of sulfur compounds in the studied gasoline fractions allow us to conclude that the co-processing of used tires with oil shale will not affect the quality of the light fraction of oil produced and thus, it enables not to change the method of purification from sulfur compounds.*

Keywords: *shale oil, used tires, gasoline fraction, sulfur, gas chromatography.*

1. Introduction

The oil shale processing industry has suffered many changes due to fluctuations in the petroleum market over the last several years. Record-breaking low prices of petroleum have hindered large investments in shale oil quality improvement [1, 2]. During this period, possibilities of oil production from different solid wastes and co-processing of oil shale with waste materials

* Corresponding author: e-mail olga.pihl@taltech.ee

have been considered, thereby reducing the cost of production of the obtained liquid fuels.

One possible option to pursue could be co-processing of oil shale and pyrolysis of used tires, which has been researched previously to some extent [3–6]. The main task of co-processing is to obtain oil of quality that would meet the requirements of the market. One of the basic requirements for fuel quality is low sulfur content. The determination of sulfur quantity as well as sulfur compounds in fuels is an important task in the face of tightening requirements for sulfur content levels in fuels. Gas chromatography (GC) is one possible technique for identifying sulfur compounds. GC permits quantitative estimation of chromatograms. Three methods are used to determine sulfur concentrations in both gasoline fractions. The internal standardization method consists in analyzing a sample of unknown quantitative composition, to which a known quantity of a substance not contained in it (internal standard) is added. The response areas of each sulfur compound of interest are compared to that of the internal standard. The external standardization method draws a relationship between peak parameter (area or height) and content of the substance in a sample via the results of a series of analyses. A calibration coefficient is then determined. The response areas of each sulfur compound of interest are compared to that of the external standard. The third method is the normalization method. This method is based on a principle that the sum of areas (heights) of all peaks on the chromatogram is taken as 100%.

The aim of the present work is to study possible gas chromatographic methods for the exact determination of sulfur compounds in the 90–150 °C gasoline fractions of shale oil and oil obtained from pyrolysis of used tires.

2. Experiments

2.1. Pyrolysis

Oil shale of the Estonian deposit and rubber crumb of particle sizes of 4 mm and smaller obtained from used tires were applied as raw materials for oil production. Experiments were carried out on the laboratory retorting unit. The unit consisted of a reactor with external heating, an air condenser and a water condenser with condensation temperatures of 10–12 °C, and a gas-liquid separator. Gas was directed from the system and the liquid product bleeding from the tank was carried out manually.

A diagram of the experimental retorting unit is shown in Figure 1.

In the process of retorting, a sample was placed in the middle of the reactor and heated for 8 hours up to the final temperature of 520 °C. A precise graph of sample heating is depicted in Figure 2.

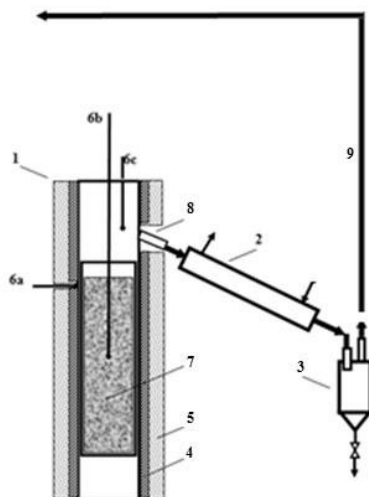


Fig. 1. Retorting unit: 1 – reactor; 2 – air condenser and water condenser; 3 – gas-liquid separator; 4 – heating element; 5 – insulation; 6 – thermocouples (6a – on the wall, 6b – in the mixture, 6c – in the vapours); 7 – initial raw material; 8 – output of steam-gas mixture; 9 – non-condensable gases.

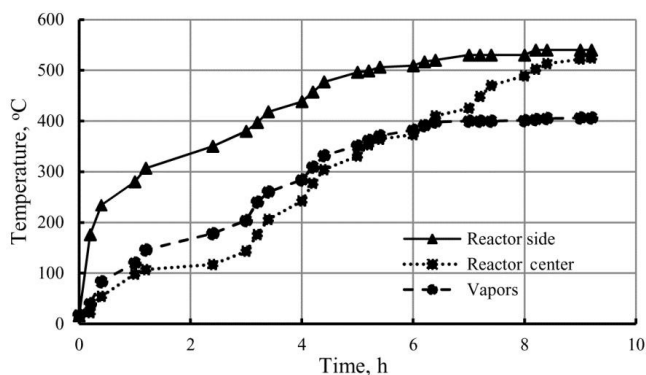


Fig. 2. The graph of temperature change in the process of retorting.

2.2. Distillation

For further research, the 90–150 °C fractions on the B/R Instrument distillation column were separated from shale oil and oil from rubber crumb at atmospheric pressure and a reflux ratio of 1. The column height was 40 cm

with 200 theoretical plates. Oils characteristics are given in Table 1. As seen from the table, the density of oil obtained from used tires is higher than that of shale oil. On the other hand, the sulfur mass percent content of shale oil is twice that present in used tire oil. The iodine number is in the same range whereas the acid number is much higher for shale oil.

Table 1. Characteristics of shale oil and used tire oil (boiling range fraction 90–150 °C)

Item	Method	Shale oil	Used tire oil
Density at 15 °C, kg/m ³	EVS-EN ISO 12185	776.6	828.2
Sulfur total, S _t , %, mass	EVS-EN ISO 20846	1.04	0.50
Iodine number, gI ₂ /100 g	GOST 2070	107.7	98.5
Acid number, mg KOH/g	ISO 668	3.2	0.05

2.3. Analysis of sulfur compounds

Since there are no standard methods for total sulfur determination of the gasoline fractions from both shale oil and oil from the rubber crumb of used tires, in this work, the standards for light petrochemicals were applied.

Determination of the quantitative content of total sulfur in the studied samples was carried out according to the Standard EVS EN ISO 20846 (Petroleum products – Determination of sulfur content of automotive fuels – Ultraviolet fluorescence method) [7]. EVS-EN ISO 20846 specifies an ultraviolet (UV) fluorescence test method for the determination of the sulfur content of motor gasolines containing up to 3.7 % (m/m) oxygen (including those blended with ethanol up to approximately 10 % (V/V)) and of diesel fuels, including those containing up to approximately 10% (V/V) fatty acid methylester (FAME) with sulfur contents in the range of 3–500 mg/kg. Other products can be analysed and other sulfur contents can be determined according to this test method. However, no precise data for products other than automotive fuels or for results outside the specified range have been established in EVS-EN ISO 20846 [7].

Sulfur compounds in the fractions were determined by gas chromatography according to ASTM D 5623 test, which is applied to distillates, gasoline motor fuels (including those containing oxygenates species) and other petroleum liquids with a final boiling point of approximately 230 °C or lower at atmospheric pressure. This test method covers the determination of volatile sulfur-containing compounds in light petroleum liquids [8].

Chromatographic analysis of the studied samples was implemented using the normalization and internal standardization methods. The above methods of quantitative estimation of chromatograms are also described in ASTM D 5623 test [8].

Sulfur compounds in the fractions were determined by gas chromatography employing a TRACE GC chromatograph with a flame photometric detector (FDP). The Zebron ZB-5HT Inferno column with a nonpolar phase and a length of 60 m was used for separation with a helium carrier gas.

Analysis was carried out in the programmable temperature rise mode: 40 °C (3 min), rising rate of 8 °C/min up to 250 °C (1 min hold time), then up to 280 °C (5 min hold time), and injector temperature of 280 °C.

When determining sulfur compounds by the normalization method, the sulfur content of each compound was calculated as a sulfur share of all components. Further, knowing the total sulfur content in a sample as determined by the ultraviolet fluorescence method, the contents of individual sulfur compounds were calculated.

To determine sulfur compounds by the internal standardization method, the chromatograph was calibrated. Since the response of the device detector is not linear, a calibrating linear equation in a narrow range of concentrations was determined for each compound. Shale oil and oil from the rubber crumb of used tires are mixtures containing dozens of different sulfur compounds. In the internal standardization method, it is necessary to apply reference substances. It is practically impossible to identify each individual component in the samples with such complex compositions. When determining calibration linear equations for unidentified sulfur compounds, the equations of nearby identified individual components were applied.

The chromatograms of sulfur compounds of the studied samples are shown in Figures 3 and 4.

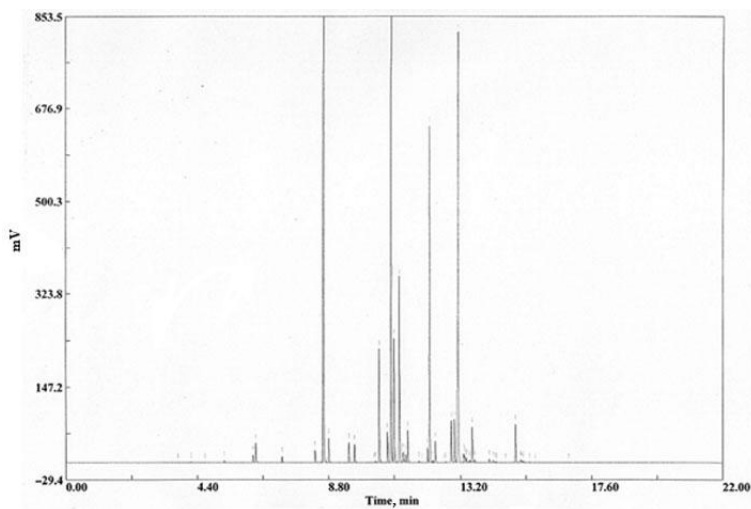


Fig. 3. Chromatogram of the fraction of shale oil (boiling point range 90–150 °C).

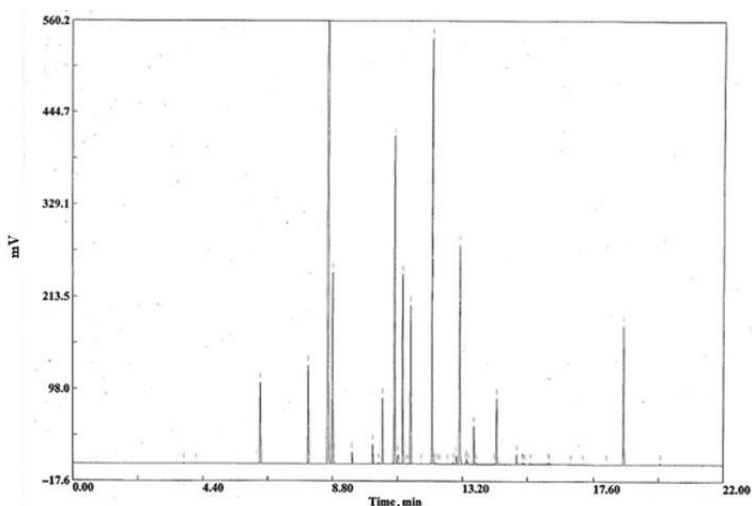


Fig. 4. Chromatogram of oil obtained from used tires (boiling point range 90–150 °C).

3. Results and discussion

Data on quantitative sulfur content in the gasoline fractions of shale oil and oil obtained from the rubber crumb of used tires by different methods are presented in Table 2.

The results presented in Table 2 show that sulfur compounds contents determined by the normalization method differ considerably from those obtained by the internal standardization method. In most cases, the contents of sulfur compounds determined by the former method are lower for the components with minor content. Sulfur compounds of higher content in the samples are, on the contrary, overestimated. The total quantity of identified mercaptans in the gasoline fraction of shale oil determined by the internal standardization method is 440 ppm, and by the normalization method, 101 ppm. For the gasoline fraction of oil from the rubber crumb of used car tires, the respective values are 29 ppm and 2 ppm. There is an opposite tendency in the identification of thiophenes. The sulfur quantity in the gasoline fraction of shale oil determined by the internal standardization method is 2795 ppm, being 4135 ppm by the normalization method. In the gasoline fraction of oil from the rubber crumb, the quantities are 2203 ppm and 4260 ppm, respectively. In the total amount of identified and unidentified compounds, the difference between the results obtained by the methods of internal standardization and normalization is 972 ppm and 1460 ppm, respectively, for the shale gasoline fraction, and respectively 817 ppm and 1638 ppm for the gasoline fraction from the rubber crumb.

Table 2. Quantitative sulfur content in the gasoline fractions of shale oil and oil from the rubber crumb of used tires

Sulfur compound	Retention time, min	Sulfur in shale oil, mg S/kg		Sulfur in used tire oil, mg S/kg	
		Internal standardization method	Normalization method	Internal standardization method	Normalization method
Methyl mercaptan	3.74	24.19	0.62	14.95	1.27
Ethyl mercaptan	4.16	29.97	1.87	14.12	0.58
2-Propanethiol	4.63	13.11	1.34	–	–
Ethyl methyl sulfide	5.39	35.72	6.13	–	–
1-Methyl-1-propanthiol	6.26	157.53	24.18	–	–
Thiophene	6.35	236.22	59.73	145.48	106.76
1-Butanethiol	7.23	68.58	18.29	–	–
DMDS	7.98	–	–	534.29	141.25
Unidentified	8.35	110.03	39.72	–	–
Unidentified	8.55	72.71	4.44	–	–
2-Methylthiophene	8.62	1716.66	3398.03	1566.00	3601.67
3-Methylthiophene	8.80	147.60	76.11	262.82	278.21
Unidentified	9.48	132.74	61.86	48.28	16.67
1-Pentathiol	9.66	146.59	55.11	–	–
Unidentified	10.15	–	–	57.00	27.19
Unidentified	10.30	69.24	1.56	–	–
Unidentified	10.36	72.71	4.92	36.07	2.07
Unidentified	10.49	447.67	364.20	119.20	100.86
Unidentified	10.77	162.09	89.87	–	–
Unidentified	10.89	1567.67	2663.79	431.40	479.51
Unidentified	10.99	56230	474.28	–	–
Unidentified	11.03	–	–	52.18	25.09
3-Ethylthiophene	11.17	694.53	601.05	215.47	273.16
Unidentified	11.30	101.03	31.23	41.01	0.57
Unidentified	11.33	76.20	7.86	41.50	1.05
Unidentified	11.39	95.24	25.73	41.04	0.43
Unidentified	11.44	174.20	101.73	198.38	260.83
Unidentified	11.83–13.00	1024.93	391.25	299.05	23.00
Unidentified	13.12	1174.28	1498.95	277.12	417.88
Unidentified	13.28–16.84	1773.78	395.93	746.57	216.19
Benzothiophene	18.05	–	–	13.02	0.45
Unidentified	18.63–19.87	–	–	176.30	217.00
Unidentified	18.63	–	–	42.04	1.74
Σunidentified, mg S/kg		7617	6157	2766	4404
Σidentified, mg S/kg		3271	4243	2607	1790
Total, mg S/kg		10888		5373	
Σgas chromatography method, mass %		1.09		0.54	
Σultraviolet fluorescence method, mass %		1.04		0.62	

Since the total sulfur content calculated by the internal standardization method is close to the result determined by method of ultraviolet fluorescence, it can be deduced that the obtained results for the quantitative sulfur compounds are reliable.

4. Conclusions

In this research paper, the sulfur compounds determined quantitatively by the normalization method are considerably different from those obtained by the internal standardization method.

It is shown that for precise determination of sulfur compounds content in gasoline fractions by gas chromatography, the use of the internal standardization method is more appropriate than the normalization method.

The sulfur content in the gasoline fraction determined in the used tire oil is lower than the sulfur content of the shale gasoline. The sulfur compounds in both fractions are similar. As a result, the use of the rubber crumb in co-processing with oil shale does not negatively influence the quality of the final product.

REFERENCES

1. *Gas Prices Explained*. Available at <http://gaspricesexplained.com/?from=222.62.178.84%3A6300#/> (accessed 12 November 2018).
2. *Estonian Oil Shale Industry Yearbook 2017* (Beger, M., ed.). https://www.ttu.ee/public/p/polevkivi-kompetentsikeskus/aastaraamat/Polevkivi_aastaraamat_EST_2018-06-27c.pdf (in Estonian).
3. Pikhil', O. A., Soone, Yu. Kh., Kekisheva, L. V., Kaev, M. A. Tire processing using pyrolysis and hydrogenation methods. *Solid Fuel Chem.*, 2013, **47**(3), 183–192.
4. Senchugov, K., Kaidalov, A., Shaparenko, L., Popov, A., Kindorkin, B., Lushnyak, V., Chikul, V., Elenurm, A., Marguste, M. Utilization of rubber waste in mixture with oil shale in destructive thermal processing using the method of solid heat carrier. *Research Gate*. Available at https://www.researchgate.net/publication/298527687_Utilization_of_rubber_waste_in_mixture_with_oil_shale_in_destructive_thermal_processing_using_the_method_of_solid_heat_carrier (accessed 12 November 2018).
5. Orav, A., Kailas, T., Müürisepp, M., Kann, J. Composition of the oil from waste tires. 1. Fraction boilong at up to 160 °C. *Proc. Est. Acad. Sci.*, 1999, **48**(1), 30–39.
6. Eesti Energia tries to obtain oil from used tires. *Põhjarannik*, 14 September 2016 (in Estonian). Available at <https://dea.digar.ee/cgi-bin/dea?a=d&d=pohjarannik20160914.2.6.3>
7. EVS-EN ISO 20846:2011. *Petroleum products – Determination of sulfur content of automotive fuels – Ultraviolet fluorescence method (ISO*

-
- 20846:2011). <https://www.evs.ee/tooted/evs-en-iso-20846-2011> (accessed 12 November 2018).
8. ASTM D5623-94(2014). *Standard Test Method for Sulfur Compounds in Light Petroleum Liquids by Gas Chromatography and Sulfur Selective Detection*.

Received January 23, 2019

Appendix 3

PUBLICATION III

O. Pihl, V. Khaskhachikh, J. Kravetskaja, A. Niidu, A. Siirde; Co-Pyrolysis of Estonian Oil Shale with Polymer Wastes, ACS Omega, 6, 47, pp. 31658–31666, 2021

Co-Pyrolysis of Estonian Oil Shale with Polymer Wastes

Olga Pihl,* Vladimir Khaskhachikh, Julia Kravetskaja, Allan Niidu, and Andres Siirde

Cite This: *ACS Omega* 2021, 6, 31658–31666

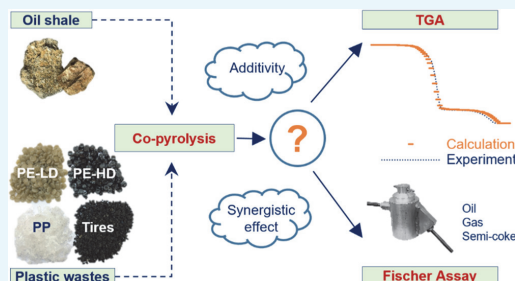
Read Online

ACCESS |

Metrics & More

Article Recommendations

ABSTRACT: Recycling of polymeric wastes is important for both energy recovery and raw material processing. In light of the EU Green Deal, the oil shale industry is looking for new opportunities to use its production potential. As an intermediate stage, the co-pyrolysis of oil shale with waste plastic and tires will be considered acceptable. The article presents the kinetics of pyrolysis of Estonian oil shale, the main polymer components of municipal waste, and their mixtures with oil shale by the thermogravimetric analysis method. The influence of each component separately on the process of sample weight loss during co-pyrolysis was also studied. It is shown that when plastics are added to oil shale, the experimental and calculated data coincide according to the principle of the additive contribution of each component. Kinetic parameters were calculated according to the Coats–Redfern integral method and show that during the co-pyrolysis of mixtures of oil shale with polymer wastes, the value of the activation energy increases in comparison with the pyrolysis of oil shale. Based on the experimental data, it was determined that there is a manifestation of a synergistic effect in the form of an increase in the yield of liquid products during the co-pyrolysis of oil shale and polymer wastes.



1. INTRODUCTION

In recent years, the topic of reuse of polymer wastes, including plastics and used car tires, has become increasingly important. Annual increase in production of polymer/plastic materials inevitably leads to an increase in the waste produced that requires recycling. According to Statista, more plastic has been produced in the past 15 years than in the 50 years prior.¹ In the European Union, only the demand for plastics in 2019 amounted to 50.7 million tons. The most common plastics that are used on a daily basis and are universally applicable are polyethylene (PE-HD and PE-LD) and polypropylene (PP).² According to PlasticsEurope association in 2019 in Europe, of the collected 29 million tons of plastic wastes, 42.6% went to energy recovery, 32.5% to recycling, and 24.9% was buried in a landfill amounting to roughly 7 million tons.² In September 2020, ETRMA, the European Tire and Rubber Manufacturers' Association, reported³ that in 2018, 32 countries (EU28, Norway, Serbia, Switzerland, and Turkey) collected 3.58 million tons of end of life tires from which 193 thousand tons have not been reused. Thus, a fair amount of polymer wastes still needs to be incorporated into sustainable waste management and, by the virtue of it, into circular economy.

On the other hand, according to the “Estonian national energy and climate plan (NECP 2030)”, by 2050, Estonia must strive to reduce carbon emissions to zero.⁴ To achieve this goal, the Estonian government announced two dates—the exiting of the production of oil shale electricity no later than 2035 and the

production of shale oil no later than 2040. During this period, it is planned to reduce the negative impact of oil shale production on the natural environment. For this purpose, oil shale processing enterprises are looking for an opportunity to modernize production and switch to a new type of raw material.

From an environmental and economic point of view, the most rational approach is the use of polymer wastes as an alternative fuel, which contain PE-HD, PE-LD, PP, tire, and other components. However, the use of only polymer wastes as raw material is currently not possible due to the peculiarities of the existing oil shale processing plants. Today, the main technology for processing oil shale in Estonia is the Galoter process, which is pyrolysis of raw materials by the solid heat carrier method. Pyrolysis is the thermal decomposition of organic material in an oxygen-free atmosphere to form gaseous, liquid, and solid products.⁵ The solid heat carrier in the Galoter process is its own ash, which is returned to the pyrolysis process. Because the ash content of polymer wastes is quite low, therefore, the first step is to replace part of the oil shale with polymer wastes, which, according to estimates, can reach 50%.

Received: August 5, 2021

Accepted: October 27, 2021

Published: November 15, 2021



Table 1. Proximate and Ultimate Analysis Results

samples	proximate analysis ^a , m/m %			ultimate analysis ^a , m/m %			
	ash (A)	fixed carbon (FC)	net calorific value, MJ/kg	carbon (C)	hydrogen (H)	nitrogen (N)	sulfur (S)
EOS	50.10	2.70	8.807	27.50	2.70	0.07	1.60
PE-HD	0.40	<1.00	44.575	84.02	15.50	0.02	0.06
PE-LD	1.30	<1.00	44.286	83.04	15.54	0.05	0.08
PP	<0.10	<1.00	44.876	84.09	15.77	0.01	0.03
Tires	8.02	24.60	34.388	78.70	7.70	0.47	1.25

^aIn dry basis.

Pyrolysis of plastic wastes components is one of the ways of recycling.^{6–14} The co-pyrolysis of polymer wastes with various materials containing organic matter, including oil shale, has been widely investigated.^{15–26} For example, Tiikma et al.¹⁵ have studied the impact of co-pyrolysis of low-density polyethylene with Estonian kukersite oil shale, its semi coke, and Dictyonema shale on the yield and composition of the pyrolysis oil. They noted that yield and chemical group composition of co-pyrolysis oil depend to a certain degree on the oil shale type used.

Information about the kinetics of the pyrolysis process is important when designing industrial pyrolysis plants. The kinetics of co-pyrolysis of polymer waste with various materials containing organic matter is well studied.^{10,27–29} Thus, Aboulkas et al.³⁰ have studied pyrolysis kinetics of Moroccan oil shale kerogen mixed with high-density polyethylene (PE-HD) using a thermogravimetric analysis (TGA) system at various heating rates of 2, 10, 20, and 50 K/min in the temperature range of 300–1273 K in a nitrogen atmosphere. The thermogravimetric method was extended by the same group³¹ to the studies on the pyrolytic behaviors of Moroccan oil shale kerogen, polyethylene terephthalate, and their mixtures. The experiments were carried out dynamically by increasing the temperature from 298 to 1273 K at a heating rate of 2–100 K/min in a nitrogen atmosphere.

Despite a significant amount of scientific work in the field of co-pyrolysis of oil shale with various polymer wastes, most of the works investigated the process of pyrolysis of oil shale in a mixture with one or two components, while the real polymer wastes contains a significantly larger number of components. The aim of this work is to study the process of pyrolysis of oil shale in a mixture with all the main polymer components of waste and to determine the kinetic parameters of co-pyrolysis.

2. THEORY OF THE STUDY OF KINETIC PARAMETERS

TGA is a research and analysis method based on the registration of changes in the mass of a sample depending on its temperature or time under certain and controlled conditions of changes in the ambient temperature. TGA is quite accurate and fast, and it is used to study characteristics and kinetics of pyrolysis of materials with complex matrices, such as solid fuels. In pyrolysis kinetics analysis, the activation energy is an important parameter describing the pyrolysis process of a sample.³² There are a number of methods for calculating the activation energy, based on mathematical processing of the TGA curve. The least time-consuming and most accurate for polymers and oil shale is the double-logarithm method. The condition for the applicability of the Coats–Redfern method is the first order of the decomposition reaction. When calculating the kinetics of oil shale pyrolysis and polymer decomposition, it is usually assumed that these reactions are of the first order.^{10,33–36}

Arrhenius equation

$$K = A \cdot e^{-E_a/RT} \quad (1)$$

where A is the pre-exponential factor, sek^{-1} ; E_a is the activation energy, kJ/mol ; R is the universal gas constant; and T is the temperature of the test substance, K .

The Coats–Redfern procedure is widely reported in the literature.³⁷ Following the established procedure for each reaction stage separately, the extent of reaction (α) is calculated by comparing the mass at time τ (m_τ) with the initial (m_0) and final (m_f) masses as per eq 2.

$$\alpha = \frac{m_0 - m_\tau}{m_0 - m_f} \quad (2)$$

Then, according to the procedure for first-order reactions, the value of the activation energy E_a can be defined as the tangent of the slope of the linear portion of the curve plotted in coordinates $\ln(-\ln(1 - \alpha)/T^2)$ against $10^3/T$. After analyzing the curves of thermal decomposition, it is possible to select linear sections and approximate them using a linear equation of the type $y = a \cdot x + b$, where the value of the parameter a corresponds to the value $-E_a/R$.

3. EXPERIMENTAL SECTION

3.1. Sample Characterization. The oil shale sample used in this study—Estonian oil shale (EOS) from an under-ground mine called Ojamaa. The polyethylene (PE-HD and PE-LD), PP, and the tires used in this study were collected from the Uikala municipal waste dump.

The calorific value was determined in a calorimetric bomb Parr 6300; the net calorific value was calculated using EVS-ISO 1928 and corrected for undecomposed carbonates.³⁸ Elemental composition was determined using a “vario macro cube” device, fixed carbon determined by calculation. The ash content was determined by the international standard.^{39,40} The data are shown in Table 1.

For all samples, the yield of semi-coking products was determined in accordance with the standard ISO 647.⁴¹ The results were recalculated per apparent organic content. The data are shown in Table 2.

Table 2. Yield of Semi-Coking Products

samples	yield of semi-coking products per apparent organic content, m/m %			
	oil	semi-coke	pyrogenetic water	gas + loss
EOS	59.8	17.8	5.4	17.0
PE-LD	92.7	0.8	0.3	6.2
PE-HD	92.5	1.5	0.0	6.0
PP	93.6	0.1	0.0	6.3
tires	58.9	33.5	0.1	7.5

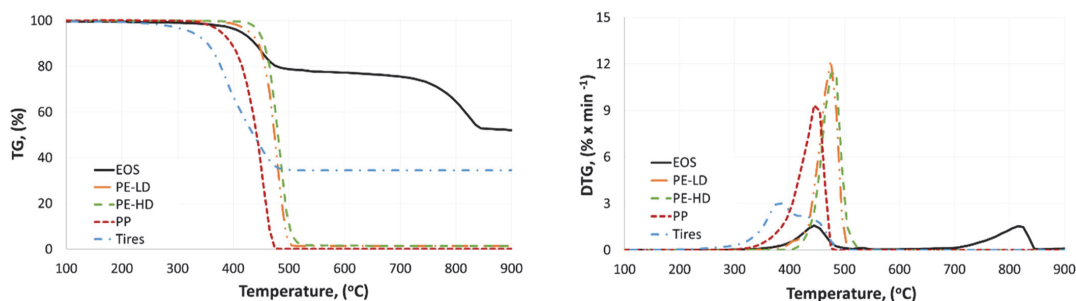


Figure 1. Simple weight loss (TG) curve of the studied raw materials and a DTG curve.

Before analysis, the samples were dried and ground in a mill Retch SK-100 to an analytical sample (up to 0.2 mm). Test mixtures of the samples were prepared from oil shale and individual components of polymer wastes in a ratio of 50/50 (EOS + PE-LD, EOS + PE-HD, EOS + PP, and EOS + tires) and a mixture of oil shale 50% and 50% (EOS + mix) of the four components of polymer wastes in an equal ratio. A mixture of polymer wastes, consisting of various types of plastics and used car tires, is most likely to occur when sorting municipal solid wastes.

3.2. Thermogravimetric Analysis. TGA of a sample of EOS and polymers, as well as oil shale with polymer mixtures, was performed using the TGA 1 STARe METTLER TOLEDO system. The initial TGA temperature for all samples was 25 °C and the final temperature was 950 °C. The heating rate was 20 °C/min, and the tests were carried out under nitrogen purging at a rate of 20 mL/min. Nitrogen gas was used as an inert purge gas to displace air in the pyrolysis zone, thus avoiding unwanted oxidation of the sample. In this work, about 20–25 mg of each sample was analyzed in an Al₂O₃ dish and used for TGA analysis.

The TG curve was used to determine the TGA parameters, the T_{onset} , T_{midpoint} , and T_{endset} points, in accordance with the international standard.⁴²

4. RESULTS AND DISCUSSION

4.1. Decomposition of EOS, Polymers, and Mixtures of Polymer Wastes with Oil Shale. Figure 1 shows a simple weight loss (TG) curve of the studied oil shale and polymers and a differential weight loss (DTG) curve.

The curves show that the loss of mass during heating of the oil shale occurs in two stages (there is also a stage of moisture loss, but it is insignificant). The first major stage is the stage of decomposition of the organic part of the oil shale. It occurs in the temperature ranges from 300 to 550 °C. The second stage is decomposition of the mineral part of the oil shale, which occurs in the temperature ranges of 670–870 °C.

It can be seen from the graphs that the weight loss during pyrolysis for all polymers occurs in one stage. Thermal decomposition of PE-LD and PE-HD occurs in the temperature range of 400–550 °C with maximum weight loss at 480 °C. In PP, the decomposition of the organic part begins at a lower temperature. This process takes place in the range of 300–520 °C, with a maximum loss of mass at 442 °C. This range (300–550 °C) corresponds to the stage of active pyrolysis, in which thermal decomposition of the initial polymer molecule occurs, accompanied by a weight loss of ~98%. Upon subsequent heating in the temperature range from 500 to 945 °C, the

process of passive pyrolysis occurs, accompanied by thermal destruction of stronger bonds in the solid residue and a weight loss of less than 1%. The organic part of tires begins to decompose at a temperature of 250 °C and the decomposition process ends at 550 °C, while the maximum weight loss occurs at 400 °C. A high residual weight at the end of the sample analysis of about 34% indicates a significant amount of filler in the tire composition. Table 3 shows the TGA parameters for EOS and polymers.

Table 3. TGA Parameters for E and Polymers

TGA parameter	raw materials					
	EOS		PE-LD	PE-HD	PP	tires
	step 1	step 2	step 1	step 1	step 1	step 1
T_{onset} °C	412.8	766.0	455.6	460.5	419.5	353.6
T_{midpoint} °C	444.7	798.8	480.7	480.4	442.3	400.3
T_{endset} °C	476.6	839.4	493.9	500.3	468.9	451.0

Table 3 shows that the temperature of the maximum weight loss (T_{midpoint}) of the organic part of the oil shale is 445 °C. These results show that the values of the highest intensity of destruction of organic matter obtained in this work are very similar to those mentioned in the literature.⁴³ The temperature of the maximum weight loss (T_{midpoint}) of the inorganic part of the oil shale is 799 °C. The temperature of the maximum weight loss (T_{midpoint}) for PE-LD and PE-HD is approximately 480 °C, for PP is 442 °C, and for tires is 400 °C.

To study the kinetics of oil shale decomposition with a mixture of polymer wastes in a 50/50 ratio (50% oil shale, 12.5% PE-HD, 12.5% PE-LD, 12.5% PP, and 12.5% tires), TGA of oil shale was also carried out with each polymer separately in a 50/50 ratio. Figure 2 shows a simple weight loss (TG) curve of the studied test mixtures and a DTG curve.

The curves show that when a mixture of oil shale with polymer wastes is heated, weight loss occurs in two stages; while at the first stage, the weight loss increased significantly because polymer wastes consist mainly of organic matter, the second stage involves the decomposition of the mineral part of the oil shale.

From the data in Table 4, it can be seen that the addition of PE-LD and PE-HD plastics to oil shale leads to the fact that the stage of active decomposition of the organic part and the maximum weight loss of the samples occurs at the same temperatures as in the analysis of each polymer separately. Therefore, the stage of active decomposition of the organic part of the polymer PE-LD occurs in the temperature range T_{onset} –

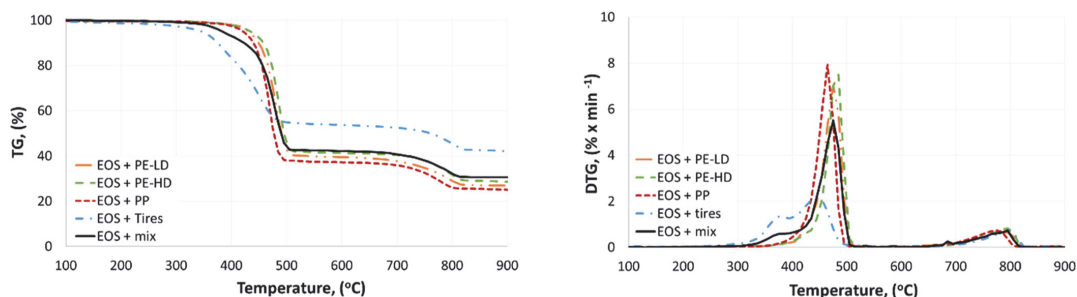


Figure 2. Simple weight loss (TG) curve of the studied mixtures of EOS with polymer wastes and a DTG curve.

Table 4. TGA Parameters for Mixtures Oil Shales with Polymer Wastes

TGA parameter	Materials									
	EOS + PE-LD		EOS + PE-HD		EOS + PP		EOS + tires		EOS + mix	
	step 1	step 2	step 1	step 2	step 1	step 2	step 1	step 2	step 1	step 2
T_{onset} °C	456.8	732.7	464.0	746.9	446.6	727.8	378.1	761.4	456.6	727.2
T_{midpoint} °C	476.0	759.9	481.4	778.1	464.9	760.7	425.1	780.6	471.7	757.7
T_{endset} °C	496.3	798.2	499.2	814.5	483.8	798.6	477.0	817.8	495.5	796.2

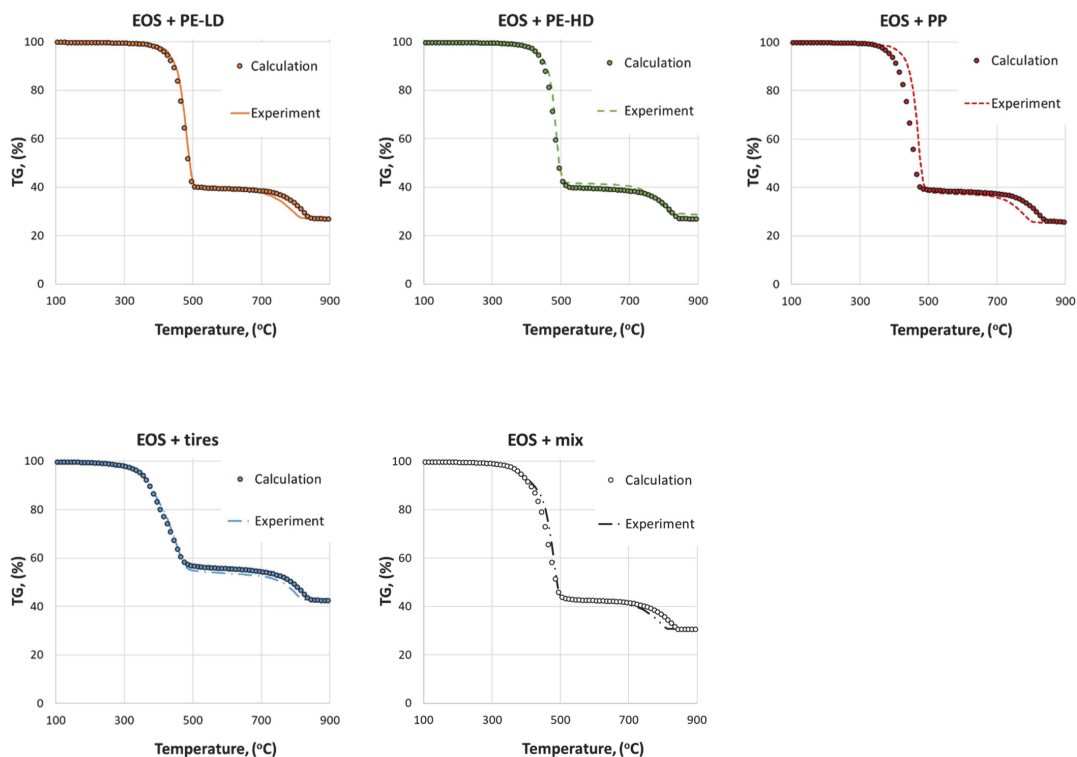


Figure 3. Calculated and experimental curves of weight loss (TG) for mixtures of EOS with polymer wastes.

T_{endset} of 455.6–493.9 °C, and for a mixture of PE-LD with oil shale, this range is 456.8–496.3 °C. For PE-HD plastic and a mixture of oil shale with it, these ranges are $T_{\text{onset}}-T_{\text{endset}}$ 460.5–500.3 and 464.0–499.2 °C, respectively.

For PP and tires, the beginning and end of active decomposition of the organic part is shifted by 20 °C toward higher temperature. In this case, the nature of decomposition of the organic part of the oil shale sample with the mixture (50% oil

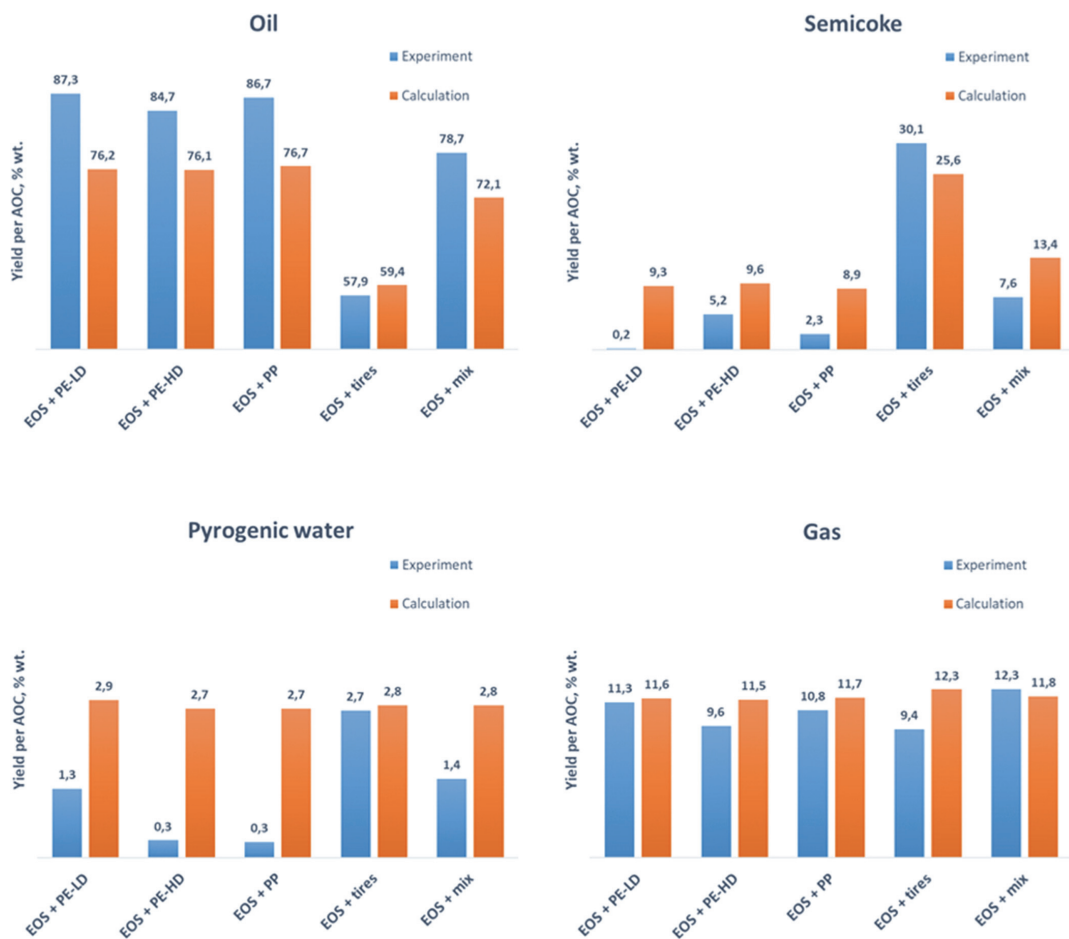


Figure 4. Comparison of experimental and calculated data on the yield of pyrolysis products of a mixture of oil shale with polymer wastes.

shale, 12.5% PE-HD, 12.5% PE-LD, 12.5% PP, and 12.5% tires) becomes the same as for PE-HD and PE-LD because their thermal degradation behavior is similar and their total organic matter in the test mixture predominates. The decomposition of the mineral part for all mixtures of oil shale with polymers is shifted toward lower temperature. Perhaps, this is due to the more complete decomposition of oil shale at the first stage of thermal destruction and the weakening of chemical bonds in the solid residue.

4.2. Study of Additivity Based on TG Analysis. To test the principle of additivity in the process of thermal decomposition of multicomponent mixtures, we studied the data on the co-pyrolysis of mixtures of EOS with polymer wastes by the TGA method. On the basis of TG data, graphs were constructed (Figure 3), comparing experimental and calculated data on the principle of the additive contribution of each component.

As seen in Figure 3, the calculated points are in good agreement with the experimental curves both for a mixture of oil shale with individual components of polymer wastes and for a

multicomponent mixture. This confirms the legitimacy of using the additivity principle for calculating the mass loss of a mixture of oil shale and polymer wastes. Thus, the data obtained can be used in the future for mathematical modeling of the pyrolysis process of multicomponent mixtures, as well as in the design of pyrolysis plants and to determine the yield of pyrolysis products.

4.3. Study of Additivity Based on the Yield of Co-Pyrolysis Products. To verify the principle of additivity, the calculated data on the yields of pyrolysis products for individual components (Table 2) were compared with experimental data on the yield of pyrolysis products for the mixtures under the study. As an evaluation criterion, the yields of product were chosen based per apparent organic content (Figure 4).

As can be seen from Figure 4, for most mixtures, except for the mixture with tires, a manifestation of a synergistic effect is observed in the form of an increase in the yield of liquid pyrolysis products. The difference in oil yield from the calculated one was 11.1, 8.6, and 10.0% for PE-LD, PE-HD, and PP, respectively. Other authors have also previously reported synergistic effects in co-pyrolysis. Bozkurt et al.⁴⁴ reported that in the case of co-

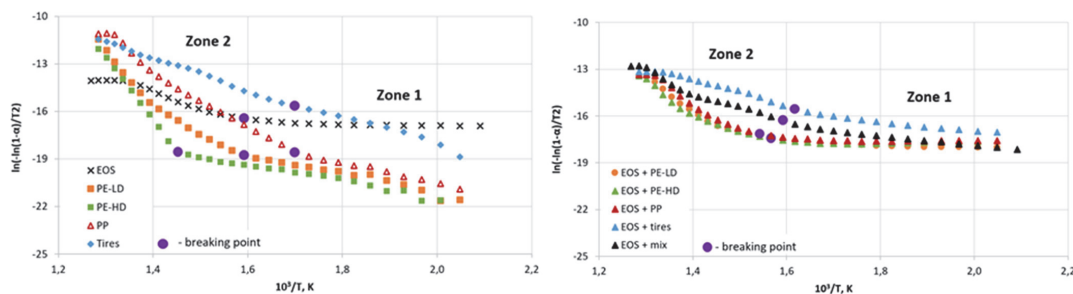


Figure 5. Coats–Redfern integral method results for raw materials and for mixtures of EOS with polymer wastes.

pyrolysis of Turkish oil shale with PP, the yield of pyrolysis products increased. Also, during the co-pyrolysis process, PP acted as a hydrogen source and saturated the free radicals formed as a result of breaking the cross-links and made positive contributions to the liquid product yield by creating a positive synergistic effect. Li et al.⁴⁵ have studied co-pyrolysis of Fushun and Longkou deposit oil shale with varying ratios of PP and polyethylene in mixtures. They noted that plastics have an obvious synergistic effect that increases the yield of shale oil due to the combined pyrolysis of mixtures of oil shale and plastic, and this effect is more significant with polyethylene. The synergistic effect was interpreted based on the free radical reaction in the theory of pyrolysis. Because the hydrogen content in oil shale was low and the hydrogen content in plastic was high, the hydrogen atoms of the plastic were transferred to free radicals, which increased the yield of liquid products. Sinağ et al.⁴⁶ reported that co-pyrolysis of Turkish lignite with PE-LD significantly increased yield of oil, indicating a synergy between lignite and PE-LD. In the case of co-pyrolysis of oil shale and tires, a decrease in the yield of oil is observed, which in turn can be explained by the fact that the rubber contains a significant amount of sulfur, which is bound with alkaline earth metals of the mineral part of oil shale during pyrolysis and leads to an increase in the yield of the solid phase. Despite the negative contribution to the yield of liquid products from tires, the total oil yield for the mixture of all polymer components with oil shale remains 6.5% higher than the calculated values. Thus, it can be stated that the synergistic effect is primarily manifested in the interaction of volatile products of oil shale and polymer wastes in the gas and condensed phases. As a result, the oil yield is higher than expected from the calculated one, and the amount of char and gas for all mixtures, except EOS + tires, decreases.

4.4. Kinetics of Co-Pyrolysis. Activation Energy. To calculate the activation energy from the DTG curve for oil shale, polymer wastes, and their mixtures, a temperature range of 225–515 °C was chosen, which corresponds to the stage of thermal decomposition of the organic part of the materials under the study. Within this interval, a step every 10 °C was chosen. The temperature dependence was transformed, and all temperature values were calculated as $10^3/T$, where T is the temperature in K. According to the data obtained, a graph of dependence $\ln(-\ln(1-\alpha)/T^2)$ on $10^3/T$ was plotted (Figure 5).

The “breaking point” was determined from the graphs plotted over a wide temperature range for the raw materials. Based on the “breaking point”, the graphs were divided into two zones. Zone 1 is a reaction zone at low temperature, and zone 2 is a reaction zone at higher temperature. For polymers PE-LD, PE-HD, and PP, the presence of a “breaking point” is quite clear,

which indicates different rates of decomposition in these zones. For tires and oil shale, the “breaking point” is not so clear. As previously noted by other authors, for oil shale, this is due to various reactions occurring during decomposition, which overlap to some extent and can affect the calculated values.⁴⁷ Tables 5 and 6 shows the kinetic parameters of pyrolysis of the raw materials and mixtures of polymer wastes with oil shale.

Table 5. Obtained Characteristics of Kinetic Parameters of Pyrolysis of the Raw Materials

sample	Zone	temperature range, °C	R ²	activation energy, kJ/mol	log A
EOS	zone II	225–365	0.99	44.38	7.42
	zone I	375–515	0.99	129.33	8.29
PE-LD	zone II	225–365	0.96	50.24	9.06
	zone I	375–515	0.97	210.88	20.44
PE-HD	zone II	225–405	0.98	43.72	10.96
	zone I	415–515	0.99	327.01	38.56
PP	zone II	225–315	0.99	51.60	8.08
	zone I	325–515	0.98	158.08	13.36
Tires	zone II	225–315	0.99	63.48	2.62
	zone I	325–515	0.99	86.72	1.97

Table 6. Obtained Characteristics of Kinetic Parameters of Pyrolysis of the Mixtures of Polymer Wastes with Oil Shale

sample	zone	temperature range, °C	R ²	activation energy, kJ/mol	log A
EOS + mix	zone II	225–445	0.99	59.94	4.51
	zone I	455–515	0.98	234.36	24.48
EOS + PE-LD	zone II	225–415	0.99	46.95	8.31
	zone I	425–515	0.98	233.82	24.14
EOS + PE-HD	zone II	225–425	0.90	54.14	7.23
	zone I	435–515	0.96	249.01	26.29
EOS + PP	zone II	225–395	0.98	46.59	8.50
	zone I	405–515	0.98	224.34	23.18
EOS + tires	zone II	225–345	0.99	58.43	3.91
	zone I	355–515	0.99	92.10	2.55

The results demonstrate a close linear fitting with R² coefficients of determination ranging from 0.90 to 0.99 over the used temperature ranges (Tables 5 and 6). The table also shows the values of the activation energy and the pre-exponential factor. If we compare the kinetic parameters of pyrolysis of individual components of polymer wastes and their mixtures with oil shale, it can be assumed that the value of the activation energy during co-pyrolysis can be influenced by the

structure of the polymer molecule. Thus, for a mixture of oil shale with PE-LD and PP, which have a branched structure, the activation energy value increases by 1.5 times compared to the calculated value for pure components, which indicates a more active course of the decomposition process. This is in good agreement with the above data on the yield of liquid pyrolysis products, where the highest oil yield from the calculated one was obtained also for a mixture of oil shale with PE-LD and PP. In turn, for a mixture of oil shale with tires and PE-HD, the activation energy value is slightly reduced, which indicates a positive effect when these materials are processed together. This decrease can be explained by the influence of the mineral part of oil shale, which can have a catalytic effect on the thermal degradation of these polymers.

5. CONCLUSIONS

The article presents the results of studying the kinetic parameters of pyrolysis of oil shale from Estonia deposits and mixtures of these oil shales with polymer wastes in a ratio of 50% oil shale, 12.5% PE-HD, 12.5% PE-LD, 12.5% PP, and 12.5% used car tires by the TGA method. The values of the activation energy and the pre-exponential factor were obtained using the Coats–Redfern integral method. It is shown that the activation energy in the temperature range near the maximum decomposition rate of organic matter differs for oil shale and for mixtures of oil shale with polymer wastes. For a mixtures of oil shale with PE-LD and PP, which have a branched structure, the value of the activation energy increases by 1.5 times, which indicates a more active course of the decomposition process. This is in good agreement with the above data on the yield of liquid pyrolysis products, where the highest oil yield from the calculated one was also obtained for a mixture of oil shale with PE-LD and PP. For a mixture of oil shale with tires and PE-HD, the activation energy is slightly reduced, which indicates a positive effect when these materials are processed together.

The nature of decomposition of the organic part of the oil shale sample with the mixture (50% oil shale, 12.5% PE-HD, 12.5% PE-LD, 12.5% PP, and 12.5% tires) becomes the same as for PE-HD and PE-LD because their thermal degradation behavior is similar and their total organic matter in the test mixture predominates. On the basis of the data obtained, it can be concluded that in the co-pyrolysis of oil shale and polymer wastes in equal proportions, the kinetic parameters characteristic of the thermal destruction of polymer wastes will play a predominant role. The kinetics of co-pyrolysis depends mainly on plastics and tires, as they make up about 80% of all organic matter.

Also presented are data on the effect of each component of the plastic components separately on the process of weight loss of the sample during co-pyrolysis. It is shown that when plastics are added to oil shale, the experimental and calculated data coincide according to the principle of additivity contribution of each component. Thus, the data obtained can be used in the future for mathematical modeling of the pyrolysis process of multi-component mixtures and in the design of pyrolysis installations for determining the residual amount of the solid phase.

The work shows a synergistic effect in the co-pyrolysis of oil shale with plastics. The difference in oil yield from the calculated one was 8.6, 10.0, and 11.0% for PE-LD, PE-HD, and PP, respectively. For tires, this relationship was not observed. According to experimental data, the yield of oil is less than calculated. Despite the negative contribution to the yield of liquid products from tires, the total oil yield for a mixture of all

polymer components with oil shale remains positive and amounts to 6.5% wt above the calculated indicators.

This series of experiments gives ground to the statement that co-pyrolysis is a promising way for the oil shale industry to enter the waste management market. In the course of further development of the process of co-pyrolysis of polymer wastes, it is possible that oil shale will be replaced with another mineral component that provides a catalytic effect.

AUTHOR INFORMATION

Corresponding Author

Olga Pihl – Oil Shale Competence Centre, TalTech Virumaa College, School of Engineering, Tallinn University of Technology, 19086 Tallinn, Estonia; orcid.org/0000-0002-7411-8437; Email: olga.pihl@taltech.ee

Authors

Vladimir Khaskhachikh – Oil Shale Competence Centre, TalTech Virumaa College, School of Engineering, Tallinn University of Technology, 19086 Tallinn, Estonia

Julia Kravetskaja – Oil Shale Competence Centre, TalTech Virumaa College, School of Engineering, Tallinn University of Technology, 19086 Tallinn, Estonia

Allan Niidu – Oil Shale Competence Centre, TalTech Virumaa College, School of Engineering, Tallinn University of Technology, 19086 Tallinn, Estonia; orcid.org/0000-0003-3406-9869

Andres Siirde – Department of Energy Technology, School of Engineering, Tallinn University of Technology, 19086 Tallinn, Estonia

Complete contact information is available at:

<https://pubs.acs.org/10.1021/acsomega.1c04188>

Notes

The authors declare no competing financial interest.

ACKNOWLEDGMENTS

The authors gratefully acknowledge the financial support from the European Regional Development Fund and Project “Increasing the value of oil shale (products) and expanding the scope of activities of the Oil Shale Competence Center” (2014-2020.5.04.19-0376).

ABBREVIATIONS

EOS, Estonian oil shale
PE-HD, high-density polyethylene
PE-LD, low-density polyethylene
PP, polypropylene
PET, polyethylene terephthalate
Mix, 50% oil shale, 12.5% PE-HD, 12.5% PE-LD, 12.5% PP, 12.5% tires
TGA, thermogravimetric analysis
ETRMMA, European tire and rubber manufacturers’
ELTs, end of life tyres
ISO, International Organization for Standardization
EVS-ISO, Standard of the republic of Estonia-International Organization for Standardization
TG, weight loss curve
DTG, differential weight loss curve

■ REFERENCES

- (1) Production of plastics worldwide from 1950 to 2019 (in million metric tons). <https://www.statista.com/statistics/282732/global-production-of-plastics-since-1950/>. (accessed Aug 12, 2020).
- (2) Plastic—the Facts 2020. <https://www.plasticseurope.org/en/resources/publications/4312-plastics-facts-2020>. (accessed Nov 27, 2020).
- (3) Europe—91% of all End of Life Tyres collected and treated in 2018. <https://www.etrma.org/library/europe-91-of-all-end-of-life-tyres-collected-and-treated-in-2018/>. (accessed Dec 28, 2020).
- (4) Estonian national energy and climate plan (NECP 2030). https://ec.europa.eu/energy/sites/ener/files/documents/ec_courtesy_translation_ee_necp.pdf. (accessed May 28, 2021).
- (5) Velghe, I.; Carleer, R.; Yperman, J.; Schreurs, S. Study of the pyrolysis of municipal solid waste for the production of valuable products. *J. Anal. Appl. Pyrol.* **2011**, *92*, 366–375.
- (6) Cunliffe, A. M.; Williams, P. T. Composition of oils derived from the batch pyrolysis of tyres. *J. Anal. Appl. Pyrol.* **1998**, *44*, 131–152.
- (7) Williams, P. T.; Besler, S.; Taylor, D. T. The pyrolysis of scrap automotive tyres: The influence of temperature and heating rate on product composition. *Fuel* **1990**, *69*, 1474–1482.
- (8) Scheirs, J.; Kaminsky, W. *Feedstock recycling and pyrolysis of waste plastics*; John Wiley & Sons: Academic Press: New-York, 2006; pp 383–434.
- (9) Onwudili, J. A.; Insura, N.; Williams, P. T. Composition of products from the pyrolysis of polyethylene and polystyrene in a closed batch reactor: Effects of temperature and residence time. *J. Anal. Appl. Pyrol.* **2009**, *86*, 293–303.
- (10) Al-Salem, S. M.; Lettieri, P.; Baeyens, J. Kinetics and product distribution of end of life tyres (ELTs) pyrolysis: A novel approach in polyisoprene and SBR thermal cracking. *J. Hazard. Mater.* **2009**, *172*, 1690–1694.
- (11) Anene, A.; Fredriksen, S.; Sætre, K.; Tokheim, L.-A. Experimental Study of Thermal and Catalytic Pyrolysis of Plastic Waste Components. *Sustainability* **2018**, *10*, 3979.
- (12) Al-Salem, S. M.; Lettieri, P. Kinetic study of high density polyethylene (HDPE) pyrolysis. *Chem. Eng. Res. Des.* **2010**, *88*, 1599–1606.
- (13) Sharuddin, S. D. A.; Abnisa, F.; Daud, W. M. A. W.; Aroua, M. K. Pyrolysis of plastic waste for liquid fuel production as prospective energy resource. *IOP Conf. Ser.: Mater. Sci. Eng.* **2018**, *334*, 012001.
- (14) Aydin, H.; İlkılıç, C. Optimization of fuel production from waste vehicle tires by pyrolysis and resembling to diesel fuel by various desulfurization methods. *Fuel* **2012**, *102*, 605–612.
- (15) Tiikma, L.; Luik, H.; Pryadka, N. Co-Pyrolysis of Estonian Shales With Low-Density Polyethylene. *Oil Shale* **2004**, *21*, 75–85.
- (16) Senchugov, K.; Kaidalov, A.; Shaparenko, L.; Popov, A.; Kindorkin, B.; Lushnyak, V.; Chikil, V.; Elenurm, A.; Marguste, M. Utilization of rubber waste in mixture with oil shale in destructive thermal processing using the method of solid heat carrier. *Oil Shale* **1997**, *14*, 59–66.
- (17) Abnisa, F.; Wan Daud, W. M. A.; Ramalingam, S.; Azemi, M. N. B. M.; Sahu, J. N. Co-pyrolysis of palm shell and polystyrene waste mixtures to synthesis liquid fuel. *Fuel* **2013**, *108*, 311–318.
- (18) Assumpção, L. C. F. N.; Carbonell, M. M.; Marques, M. R. C. Co-pyrolysis of polypropylene waste with Brazilian heavy oil. *J. Environ. Sci. Health, Part A: Toxic/Hazard. Subst. Environ. Eng.* **2011**, *46*, 461–464.
- (19) Bernardo, M.; Lapa, N.; Gonçalves, M.; Mendes, B.; Pinto, F.; Fonseca, I.; Lopes, H. Physico-chemical properties of chars obtained in the co-pyrolysis of waste mixtures. *J. Hazard. Mater.* **2012**, *219*–220, 196–202.
- (20) Ding, K.; Zhong, Z.; Wang, J.; Zhang, B.; Fan, L.; Liu, S.; Wang, Y.; Liu, Y.; Zhong, D.; Chen, P.; Ruan, R. Improving hydrocarbon yield from catalytic fast co-pyrolysis of hemicellulose and plastic in the dual-catalyst bed of CaO and HZSM-5. *Bioresour. Technol.* **2018**, *261*, 86–92.
- (21) Hayashi, J.; Mizuta, H.; Kusakabe, K.; Morooka, S. Flash Copyrolysis of Coal and Polyolefin. *Energy Fuels* **1994**, *8*, 1353–1359.
- (22) Johannes, I.; Tiikma, L.; Luik, H. Synergy in co-pyrolysis of oil shale and pine sawdust in autoclaves. *J. Anal. Appl. Pyrol.* **2013**, *104*, 341–352.
- (23) Melendi-Espina, S.; Alvarez, R.; Diez, M. A.; Casal, M. D. Coal and plastic waste co-pyrolysis by thermal analysis mass spectrometry. *Fuel Process. Technol.* **2015**, *137*, 351–358.
- (24) Onay, O.; Koca, H. Determination of synergetic effect in co-pyrolysis of lignite and waste tyre. *Fuel* **2015**, *150*, 169–174.
- (25) Ro, K. S.; Hunt, P. G.; Jackson, M. A.; Compton, D. L.; Yates, S. R.; Cantrell, K.; Chang, S. Co-pyrolysis of swine manure with agricultural plastic waste: Laboratory-scale study. *Waste Manag.* **2014**, *34*, 1520–1528.
- (26) Zhou, L.; Luo, T.; Huang, Q. Co-pyrolysis characteristics and kinetics of coal and plastic blends. *Energy Convers. Manage.* **2008**, *50*, 705–710.
- (27) Wu, X.; Wu, Y.; Wu, K.; Chen, Y.; Hu, H.; Yang, M. Study on pyrolytic kinetics and behavior: The co-pyrolysis of microalgae and polypropylene. *Bioresour. Technol.* **2015**, *192*, 522–528.
- (28) Çepelioğulları, Ö.; Pütün, A. E. Thermal and kinetic behaviors of biomass and plastic wastes in co-pyrolysis. *Energy Convers. Manage.* **2013**, *75*, 63–270.
- (29) Tang, Y.; Huang, Q.; Sun, K.; Chi, Y.; Yan, J. Co-pyrolysis characteristics and kinetic analysis of organic food waste and plastic. *Bioresour. Technol.* **2018**, *249*, 16–23.
- (30) Aboulkas, A.; El Harfi, K.; El Bouadili, A.; Benchanaa, M.; Mokhlisse, A.; Outzourit, A. Kinetics of co-pyrolysis of tarfaya (morocco) oil shale with high-density polyethylene. *Oil Shale* **2007**, *24*, 15–33.
- (31) Aboulkas, A.; El Harfi, K.; El Bouadili, A.; Nadifiyine, M. Study on the pyrolysis of Moroccan oil shale with poly (ethylene terephthalate). *J. Therm. Anal. Calorim.* **2010**, *100*, 323–330.
- (32) Chi, M.; Xu, X.; Cui, D.; Zhang, H.; Wang, Q. A Tg-Ftir Investigation and Kinetic Analysis of Oil Shale Kerogen Pyrolysis Using the Distributed Activation Energy Model. *Oil Shale* **2016**, *33*, 228–247.
- (33) Foltin, J. P.; Prado, G. N.; Lisboa, A. C. L. Kinetic analysis of the oil shale pyrolysis using thermogravimetry and differential scanning calorimetry. *Chem. Eng. Trans.* **2017**, *61*, 559–564.
- (34) Syed, S.; Qudaih, R.; Talab, I.; Janajreh, I. Kinetics of pyrolysis and combustion of oil shale sample from thermogravimetric data. *Fuel* **2011**, *90*, 1631–1637.
- (35) Koptelov, A. A.; Koptelov, I. A.; Rogozina, A. A.; Yushkov, E. S. Potential of thermal analysis as applied to studying the kinetics of thermal degradation of polymers. *Russ. J. Appl. Chem.* **2016**, *89*, 1454–1460.
- (36) Tiwari, P.; Deo, M. Detailed kinetic analysis of oil shale pyrolysis TGA data. *AIChE J.* **2012**, *58*, 505–515.
- (37) Coats, A. W.; Redfern, J. P. Kinetic Parameters from Thermogravimetric Data. *Nature* **1964**, *201*, 68–69.
- (38) Pihl, O.; Tshepelevitsh, M.; Burko, M.; Siirde, A. Applying The Correction For Undecomposed Carbonates To Gross Calorific Values Of Oil Shales From Different Deposits. *Oil Shale* **2019**, *36*, 250–256.
- (39) ASTM D 5373:2021, Standard Test Methods for Determination of Carbon, Hydrogen and Nitrogen in Analysis Samples of Coal and Carbon in Analysis Samples of Coal and Coke.
- (40) ISO 1171:2010, Solid mineral fuels—Determination of ash.
- (41) ISO 647:2017, Brown coals and lignites—Determination of the yields of tar, water, gas and coke residue by low temperature distillation.
- (42) EVS-EN ISO 11358-1:2014, Plastics. Thermogravimetric analysis of polymers.
- (43) Rudina, M.; Serebryannikov, N. *Handbook of Oil Shale Processing*; Publishing house Chemistry: Leningrad, 1988; p 29.
- (44) Bozkurt, P. A.; Kutlu, N. M.; Canel, M. Co-Pyrolysis of Göynük Oil Shale with Polypropylene and Structural Characterization of Pyrolysis Liquid. *J. Turk. Chem. Soc., Sect. A* **2016**, *3*, 247–264.
- (45) Li, Y.; He, J. G.; Liu, Y. H. Preparation of shale oil from copyrolysis of oil shale/plastics mixtures. *Adv. Mater. Res.* **2012**, *512*–515, 2162–2165.
- (46) Sinag, A.; Sungur, M.; Canel, M. Effect of Experimental Conditions on the Yields during the Copyrolysis of Mustafa Kemal Paşa

(MKP) Lignite (Turkey) with Low-Density Polyethylene. *Energy Fuels* **2006**, *20*, 1609–1613.

(47) Maaten, B.; Loo, L.; Konist, A.; Nešumajev, D.; Pihu, T.; Külaots, I. Decomposition kinetics of American, Chinese and Estonian Oil Shales Kerogen. *Oil Shale* **2016**, *33*, 167–183.

Curriculum vitae

Personal data

Name Olga Pihl
Date of birth 02.05.1972
Citizenship Estonian

Contact data

E-mail olga.pihl@taltech.ee

Education

2015–... Tallinn University of Technology, Faculty of Chemical and Materials Technology, PhD studies
2012–2014 Tallinn University of Technology, Fuel Chemistry and Technology, MSc in tech, *CUM LAUDE*
2006–2010 Tallinn University of Technology, Fuel Technology, *CUM LAUDE*
1979-1989 Kohtla-Järve High school no. 13

Professional employment

01.01.2015–... Tallinn University of Technology, School of Engineering, Virumaa College, Head of Laboratory
01.09.2014–31.12.2014 Tallinn University of Technology, Virumaa college of TUT, Laboratory of Fuels Technology, Development Manager
11.05.2009–01.09.2014 Tallinn University of Technology, Virumaa college of TUT, Laboratory of Fuels Technology, Chemical engineer

Projects in progress

F19044 "Valuing oil shale (products) and expanding the field of activity of the Oil Shale Competence Centre" (1.01.2020–31.08.2023); Principal Investigator: Mare Roosileht; Tallinn University of Technology, School of Engineering, Virumaa College; Financier: The State Shared Service Center; Financing: 860 000 EUR.

Industrial property

Invention: Method for reduction of sulphur in shale oil and shale oil fractions; Owners: Tallinna Tehnikaülikool; Authors: Olga Pihl, Mihhail Fomitšov, Dmitri Suštšik; Priority number: P202000011; Priority date: 9.07.2020.

Utility model: Method for determination of shale oil group composition; Owners: Tallinna Tehnikaülikool; Authors: Olga Pihl, Julia Kapralova, Maria Tšepelevitš, Hella Riisalu; Priority number: U201800031; Priority date: 21.12.2018.

Utility model: Method of co-pyrolysis of plastic waste; Owners: Tallinna Tehnikaülikool; Authors: Hella Riisalu, Olga Pihl, Dmitri Suštšik, Julia Kapralova; Priority number: U201800018; Priority date: 19.07.2018.

Elulookirjeldus

Isikuandmed

Nimi Olga Pihl
Sünniaeg 02.05.1972
Kodakonsus Eesti

Kontaktandmed

E-post olga.pihl@taltech.ee

Hariduskäik

2015–... Tallinna Tehnikaülikool, Keemia- ja materjalitehnoloogia teaduskond, doktoriõpe
2012–2014 Tallinna Tehnikaülikool, Kütuste keemia tehnoloogia, magistriõpe, *CUM LAUDE*
2006–2010 Tallinna Tehnikaülikool, Kütuste tehnoloogia, *CUM LAUDE*
1979-1989 Kohtla-Järve keskkool nr. 13

Teenistuskäik

01.01.2015–... Tallinna Tehnikaülikool, Inseneriteaduskond, Virumaa kolledž, Labori juhataja
01.09.2014–31.12.2014 Tallinna Tehnikaülikool, TTÜ Virumaa Kolledž, Kütuste tehnoloogia teadus- ja katselaboratoorium, Arendusjuht
11.05.2009–01.09.2014 Tallinna Tehnikaülikool, TTÜ Virumaa Kolledž, Kütuste tehnoloogia teadus- ja katselaboratoorium, Keemia insener

Jooksvad projektid

F19044 "Põlevkivi (produktide) väärimine ja Põlevkivi kompetentsikeskuse tegevusvaldkonna laiendamine" (1.01.2020–31.08.2023); Vastutav täitja: Mare Roosileht; Tallinna Tehnikaülikool, Inseneriteaduskond, Virumaa kolledž; Finantseerija: Riigi Tugiteenuste Keskus; Eraldatud summa: 860 000 EUR.

Tööstusomand

Patentne leiutis: Meetod väävli vähendamiseks põlevkiviõlis ja põlevkiviõlifraktsioonides; Omanikud: Tallinna Tehnikaülikool; Autorid: Olga Pihl, Mihhail Fomitšov, Dmitri Suštšik; Prioriteedi number: P202000011; Prioriteedi kuupäev: 9.07.2020.

Kasulik mudel: Põlevkiviõli grupikoostise määramise meetod; Omanikud: Tallinna Tehnikaülikool; Autorid: Olga Pihl, Julia Kapralova, Maria Tšepelevitš, Hella Riisalu; Prioriteedi number: U201800031; Prioriteedi kuupäev: 21.12.2018.

Kasulik mudel: Plastjätmete koospürolüüsi meetod; Omanikud: Tallinna Tehnikaülikool; Autorid: Hella Riisalu, Olga Pihl, Dmitri Suštšik, Julia Kapralova; Prioriteedi number: U201800018; Prioriteedi kuupäev: 19.07.2018.

ISSN 2585-6901 (PDF)
ISBN 978-9949-83-854-7 (PDF)